The Thesis Committee for Sriram Solairaj
Certifies that this is the approved version of the following thesis:

New Method of Predicting Optimum Surfactant Structure for EOR

APPROVED BY

SUPERVISING COMMITTEE:

Supervisor:
_____
Gary A. Pope

_____
Upali Weerasooriya

New Method of Predicting Optimum Surfactant Structure for EOR

by

Sriram Solairaj, B.Tech

Thesis

Presented to the Faculty of the Graduate School of

The University of Texas at Austin

in Partial Fulfillment

of the Requirements

for the Degree of

Master of Science in Engineering

The University of Texas at Austin

December 2011

Acknowledgements

Abstract

New Method of Predicting Optimum Surfactant Structure for EOR

Sriram Solairaj, M.S.E.

The University of Texas at Austin, 2011

Supervisor: Gary A. Pope

Chemical enhanced oil recovery (CEOR) has gained a rapid momentum in the recent past due to depleting reserves of "easy-oil" and soaring oil prices. Hence, CEOR is now being considered for numerous oil fields including many fields with more difficult reservoir conditions such as high temperature. Surfactants with unusually large hydrophobes (carbon numbers 24 and higher) are needed for some of the crude oils, especially at high temperature. A new class of thermally and chemically stable large hydrophobe surfactant, Guerbet alkoxy carboxylates (GAC) has been tested. Unlike Guerbet alkoxy sulfates, these new GAC surfactants do not require the use of alkali for stability since they are stable over a wide range of pH including the range of pH typical of oil reservoirs. . They also exhibit synergistic behavior when mixed with internal olefin sulfonates (IOS) and alkyl benzene sulfonates (ABS). Furthermore, in an attempt to diversify the raw material base for manufacturing EOR surfactants, another new class of large hydrophobe, viz. tristyrylphenol (TSP) has also been developed in the chemical EOR group. Given the fact that there are hundreds of surfactants that could be tested for a particular oil reservoir and thousands of combinations of surfactants, co-solvents, alkali

and brine that could be tested, it is essential to use prior knowledge, experience and understanding in the initial selection of surfactants that are most likely to work well with each particular crude oil. In an attempt to simplify that process, a new correlation to predict the optimum surfactant structure has been developed. This new correlation relates the optimum surfactant structure including parameters such as the number of POs and EOs to variables such as the equivalent alkane carbon number (EACN) of the oil, salinity and temperature. The correlation can serve as a guideline in choosing the optimum surfactant and will help in improving our understanding of the relationship among variables affecting the optimum surfactant structure. Surfactant retention is another important factor affecting the economics of chemical flooding and has to be studied carefully. Using an extensive database obtained from core flood studies in the chemical EOR group at UT, a new correlation for predicting surfactant retention including the variables pH, total acid number (TAN), salinity, mobility ratio, temperature, co-solvent, and surfactant molecular weight has been developed. Both of these correlations will reduce the time and cost required to develop a good surfactant formulation. At the same time, they also help improve its performance.

Table of Contents

List of Tables

List of Figures

xiv

Chapter 1: Introduction

1.1 MOTIVATION

The scope of chemical enhanced oil recovery (CEOR) has vastly increased due to the recent technological advancements and a significant reduction in chemical cost relative to crude oil prices. Surfactant structures have been greatly improved and that has allowed us to find good solutions over a much wider range of reservoir conditions and oil properties. With increasingly harsh conditions (temperature, salinity, oil properties), there is an increasing need for large hydrophobe surfactants for achieving ultra-low interfacial tension (IFT) as well as other performance characteristics needed for efficient oil recovery. The objective of this research was therefore (1) to identify and evaluate large hydrophobe surfactants for chemical EOR; (2) to identify the key variables determining the optimum surfactant structure for a given oil and reservoir conditions; and (3) to better understand the mechanism and factors affecting surfactant retention and to identify the variables controlling the same.

1.2 BACKGROUND

The world oil production in 2010 was roughly 80 million barrels per day, with nearly 60 million barrels coming from currently producing fields, and the rest provided by unconventional oil and natural gas liquids (world energy outlook, 2010). Nearly two-thirds of the current production comes from sandstones (Sheng, 2011), and the proven reserves in sandstones has about 20 years of production time left (at current production rate) and that of carbonates have around 80 years of production time left. The worldwide cumulative production of oil so far is approximately 1 trillion barrels. Proven oil reserves are estimated to be about 1.4 trillion barrels of light oil. The recovery efficiency with the current conventional primary and secondary technology is 30-40%, which implies that a

1

very large target for advanced technology still exists. In addition 5-8 trillion barrels are available as unconventional resources (heavy oil, shale oil).

Two thirds of the oil remains in many oil reservoirs after conventional recovery methods have been applied because of capillary forces that trap the oil droplets in the pores of the rock (residual oil), because of poor sweep efficiency due to reservoir heterogeneity and other factors and because of unfavorable geological charateristics such as poor continuity that result in poor drainage or bypassing. Enhanced oil recovery (EOR) focuses on recovering this remaining oil, in other words, converting the "resources" to "reserves". The primary EOR techniques include thermal recovery, miscible flooding, and chemical flooding with other methods such as microbial EOR and low salinity waterflooding of much less significance to date. This thesis focuses on improving the oil recovery by chemical flooding. Chemical EOR is the method of recovering oil with the application of chemicals such as alkali, surfactants, polymers and co-solvents. Often a combination of chemicals is used and such chemicals can also be combined with gas injection to create in-situ foams, with cross linkers to make gels for conformance control, or with thermal methods. Chemicals can also be used to coat nanoparticles or mixed with coated nanoparticles for EOR to create foams and emulsions among other possibilities. .

Polymer flooding (P) is the simplest and most widely used chemical EOR process with commercial applications on a large scale approaching that of thermal and miscible methods currently. It improves the sweep efficiency by decreasing the mobility ratio between the displaced fluid and displacing fluid. Interestingly, for polymer flooding, the benefit increases as the reservoir heterogeneity increases. The economic success depends mainly on the oil saturation when the polymer flood is started. It is observed that tertiary

polymer flood did not mobilize the residual oil, whereas as a secondary flood displaced oil below the water flood residual oil saturation (Huh and Pope, 2008).

The addition of surfactant lowers the interfacial tension between oil and water, thus increasing the capillary number (ratio of viscous to capillary forces). This type of flood is referred to as surfactant-polymer (SP) flooding. The addition of alkali significantly decreases the surfactant required (by less surfactant adsorption), thus making it more attractive. Alkali is also added in some cases to generate in-situ soap with active oils. The soap acts as a primary surfactant. This type of flooding is called alkali-surfactant-polymer (ASP) flooding. It should be noted that all three process involves the application of polymer, indicating the importance of mobility control. The focus of this research was on the SP and ASP methods.

1.3 DESCRIPTION OF CHAPTERS

The theory and literature review is given in Chapter 2. Chapter 3 discusses the application of large hydrophobe surfactants. It covers the phase behavior and core flood experiments conducted with Guerbet alkoxy sulfates, Guerbet alkoxy carboxylates, and tristyrylphenol (TSP) alkoxy sulfate. Chapter 4 discusses the new correlation developed to predict the optimum surfactant structure. Chapter 5 discusses the different factors and mechanism affecting the surfactant retention. It also discusses the new correlation developed to predict the surfactant retention. The summary and conclusions are then discussed in Chapter 6.

Chapter 2: Theory & Literature Review

The surfactant technology has improved dramatically in the last 5 years, both in terms of efficiency and reduction in cost. Highly branched surfactants with much larger hydrophobes having almost 10 times higher molecular weight than before are available now. This literature review covers the theory on surfactant chemistry, different structures of surfactant, and the selection methodology of surfactant formulations. This will form a background study for the main thesis and more specific pertinent literature will be discussed in the relevant sections.

2.1 SURFACTANT STRUCTURES

A surfactant (surface active agent), is a substance that lowers the energy barrier between two immiscible phases. It is an amphiphile containing a hydrophilic (water-soluble) part and a lipophilic (oil-soluble) part. For an amphiphile to classify as surfactant, the hydrophobe should contain at least 8 carbon atoms. The surfactants are mainly classified based on their dissociation in water.

- Anionic surfactants – dissociate into an amphiphilic anion, and a cation, which is in general an alkaline metal ion (Na^+, K^+) or a quaternary ammonium ion. Examples include carboxylates (soap), sulfates (mostly ethoxylated), sulfonates (alkyl benzene sulfonate, olefin sulfonate), etc. They account for more than 50% of the world production. They are also the most successful surfactants for chemical EOR, as they have low adsorption on sandstones and carbonates (at high pH).

- Nonionic surfactants – do not ionize in aqueous solution, as their hydrophilic group is of non-dissociable type. Examples include ethoxylated alcohol, phenol, ether, ester, or amide. They are not applied as a primary surfactant,

rather as a co-surfactant. Sahni (2009) discusses the beneficial effects of using non-ionic surfactants as an alternative to more expensive alcohol co-solvents.

- Cationic surfactants – dissociate into an amphiphilic cation and an anion, most often of the halogen type. They are more expensive than anionic surfactants, and are not commonly used for chemical EOR. They are sometimes used for wettability alteration in oil-wet carbonate systems

- In addition, there are amphoteric (or zwitterionic) surfactants which exhibit both anionic and cationic dissociations.

Since anionic surfactants are widely used in chemical EOR they will be discussed in detail.

2.1.1 Sulfonates

Sulfonates are very important class of surfactant for chemical EOR. The carbon in the hydrophobic back bone varies from about 9 to 24. They are chemically and thermally stable at elevated temperatures and the range of pH of interest to EOR.

Alkyl Benzene Sulfonate (ABS)

Alkyl benzene sulfonates are one of the types of classical surfactants, commonly used in the detergent industry. They are mostly available in linear alkyl chains and are referred as linear alkyl benzene sulfonate (LABS, or simply LAS). The LAS molecule contains an aromatic ring sulfonated at the *para* position and attached to a linear alkyl chain attached at any position except the terminal carbon. The alkyl chain typically has 10-14 carbon atoms. The LAS surfactants are sensitive to water hardness; hence they typically need some water softening, alcohol co-solvents or chelating agents. Some ABS surfactants are slightly branched, which improves their tolerance to divalent cations.

Alpha Olefin Sulfonate (AOS)

AOS are produced by sulfonation of linear alfa-olefins. Although the production method appears simpler, the processing steps after sulfonation makes it a more complex process than that of ABS. It also results in a mixture of several components apart from alpha olefin sulfonates. The sulfonation generally results in 60-70% of alpha olefin sulfonate, 20% of hydroxyalkane sulfonate, and even traces of beta olefin sulfonate, and sulfate of hydroxyalkane sulfonate. Figure 2.1 shows the different compounds resulting in sulfonation of alpha olefin. Due to the presence of hydroxyl group generally on the third carbon, the calcium tolerance of the AOS is higher than the corresponding LAS.

$$R\text{-}CH=CH \quad\quad R\text{-}C=CH_2 \quad\quad R\text{-}CH\text{-}CH_2\text{-}SO_3^-Na^+ \quad\quad R\text{-}CH\text{-}CH_2\text{-}SO_3^-Na^+$$
$$\hspace{0.3cm} SO_3^-Na^+ \hspace{1.2cm} SO_3^-Na^+ \hspace{1.2cm} OH \hspace{3.2cm} O\text{-}SO_3^-Na^+$$

alpha olefin sulfonate   beta olefin sulfonate   hydroxy alkane sulfonate   sulfate of hydroxy alkane sulfonate
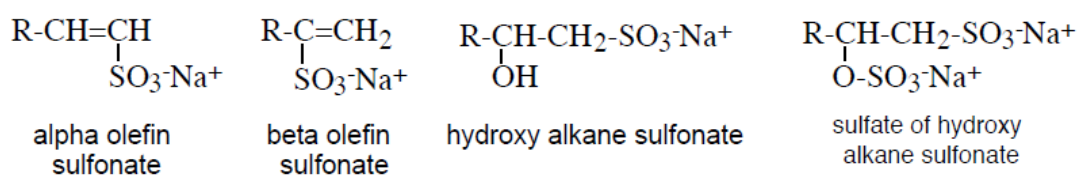
Figure 2.1: Different compounds resulting in sulfonation of alpha olefin (source: *Salager, 2002*)

Internal Olefin Sulfonates (IOS)

Unlike the sulfonation of alpha olefin, where the double bond is in the terminal carbon position, SO_3 reacts with internal olefin at any position along the chain where the double bond is randomly positioned (Barnes et al., 2010). This results in a variety of *twin-tailed* isomers of alkene sulfonate and hydroxyalkane sulfonate. Traces of di-sulfonated products are also formed. This complex mixture of different species has advantages in surfactant EOR through minimizing the formation of ordered structures that would result in liquid crystals and gels in oil-brine-surfactant mixtures. These surfactants have been proven to show excellent performance in dolomite and sandstone cores (Levitt, 2006; Jackson, 2006; Flaaten, 2007).

6

The IOS surfactants are available with the four different carbon cuts as C_{15-18}, C_{19-23}, C_{20-24}, and C_{24-28}, with C_{19-23} being the latest product. They have different salinity tolerance with C_{24-28} being the most hydrophobic having high solubilization parameters at low salinities, and C_{15-18} the most hydrophilic with low solubilization parameters at very high salinities. The general trend is decreasing solubilization ratio with increasing salinity, with C_{19-23} being an exception. Barnes et al. (2010) observed that C_{19-23} IOS showed unusual characteristic of high solubilization ratio at relatively high optimum salinity, making this surfactant more suitable for moderately high reservoir salinities (sea water salinity).

Ether Sulfonates

Ether sulfonates contain both nonionic character, provided by the ethylene oxide (EO) repeating units, and anionic character, provided by the sulfonate group. Because of this, they have very high tolerance to salinity and divalent cations. They can be used in reservoir conditions where the salinity is very high (~100,000 ppm). But, the drawback is that they are very expensive and they are not commercially available except in limited quantities for a few particular structures with relatively small hydrophobes, and because of those reasons the usage of this surfactant is currently limited and likely to remain so due to the difficulties in manufacturing it on a scale needed for commercial EOR.

2.1.2 Sulfates

The sulfate surfactants are produced by sulfation of alcohols or ethoxylated alcohols. They form one of the important classes of surfactant for chemical EOR. Traditionally they were considered only for reservoir temperatures below 65 °C, as they hydrolyze at elevated temperatures (Talley, 1988). Recently, Adkins et al. (2010) showed that the sulfates can be stabilized at high temperatures at optimal pH conditions (~10).

It's important to maintain the pH at these optimal conditions, as some base catalyzed hydrolysis occurs at very high pH (>11).

Alcohol Propoxy/Ethoxy Sulfates

Alcohol propoxy sulfates (APS) and alcohol ethoxy sulfates (AES) are prepared from commercially available branched (small, usually methyl) alcohols. As explained before, the branching is very beneficial and it minimizes the formation of viscous macroemulsions, gels and liquid crystals and promotes formation of low viscosity microemulsions. The addition of propylene oxide (PO) groups extends the hydrophobicity of the surfactant. The ethylene oxide (EO) group increases the hydrophilicity of the surfactant and it increases the optimum salinity. The addition of PO and EO also increases the tolerance to divalent cations (Maerker and Gale, 1992; Aoudia et al., 1995; Austad and Milter, 1998; Bourrel and Schechter, 1988, Jayanti et al., 2002; Levitt, 2006; Flaaten, 2007; Levitt et al., 2009). The increased tolerance to divalent cations is because of the additional intramolecular complexation between the oxygen (in EO and PO) and the divalent cations.

Guerbet alkoxy sulfates (GAS)

When the equivalent alkane carbon number (EACN) of the crude oil increases, the surfactant hydrophobe required for optimum performance also increases. The surfactant structure also depends on the reservoir temperature, salinity, hardness and the oil reactivity (Nelson and Pope, 1977; Nelson, 1984; Lake, 1989; Falls et al., 1994; Sanz and Pope, 1995; Austad and Milter, 1998; Green and Willhite, 1998; Zhang and Hirasaki, 2006).

The Guerbet reaction is a commercially viable reaction scheme for producing very large hydrophobes. A near mid branched dimer (from C_{24} to C_{32}) is formed from

alcohol monomers (from C_{12} to C_{16}). Because of this near mid branch with two long tails, they exhibit exaggerated hydrophobicity (O'Lenick Jr., 2001). Because of this twin tail structure, Guerbet ether sulfates are very efficient emulsifiers for oil and emulsify three to five times more oil than the sulfates made from linear hydrophobes. But, these Guerbet alcohols (GA) tend to be more expensive when produced in high purity for various cosmetic applications. Adkins et al. (2010) proposed a relatively inexpensive methodology by using a blend of 85-95% of GA and 5-15% of alcohol monomer, and through the use of this new Guerbet process, these surfactants can be made at low cost. The alcohol monomer subsequently becomes co-surfactant in the manufacturing process with the mixture of surfactants giving beneficial effects to surfactant EOR. By changing the number of propylene oxide (PO) and ethylene oxide (EO) groups in the surfactant it can be tailored for specific EOR needs.

2.1.3 Carboxylates

Soaps are one of the oldest known anionic surfactants. They are nothing but sodium or potassium salts of fatty acid (carboxylic acid). The primary surfactant produced when alkali reacts with organic acids in the crude oil is also a carboxylate. As sulfonates, carboxylates are also thermally and chemically stable surfactants. Just like Guerbet alkoxy sulfates (GAS), Guerbet alkoxy carboxylates (GAC) with varying numbers of BO (butylene oxide), PO, and EO can be made at low-cost. Unlike GAS surfactants, which are stable only at high pH, the GAC surfactants are stable both at neutral and high pH. Therefore, they are extremely useful in cases where alkali usage in prohibitive. GAC surfactants are evaluated in this research and the results suggest that the surfactants are capable of producing ultra-low IFT and good oil recovery performance.

9

More details on the structure and beneficial effects of these surfactants will be discussed in the experimental results.

To summarize, the performance of a surfactant at any given condition (temperature, salinity, hardness, crude oil characteristics), depends on;

- Surfactant hydrophobe length – it gives the needed hydrophobicity to the surfactant to provide the required HLB.

- Hydrophobe branching – it gives surfactant a different molecular arrangement, which helps in minimizing the formation of ordered structures that would result in unwanted macroemulsions, liquid crystals and gels.

- Presence of BO, PO, and EO – the extenders like BO, PO, and EO help in giving their individual characteristics to the surfactant. For example, the BO and PO groups extend the hydrophobicity of the surfactant, while the EO adds more hydrophilicity, thus changing the hydrophilic-lipophilic balance (HLB) of the surfactant. These groups also provide a gradual change from the hydrophobic to the hydrophilic part of the surfactant and tend to increase the interfacial area of the surfactant. The BO and PO also add to the branching of the surfactant and its oil compatibility. Because EO and PO are inexpensive relative to the hydrophobe, they also decrease the cost of the surfactant.

- Type of polar head group – even within the anionic class, the sulfate, sulfonate, and carboxylate polar head groups behave very differently with respect to the pH, salinity and hardness of the brine and temperature. They also have different thermal and chemical stability.

- Position of polar head group (positional isomers) – also makes a significant change in the property of the surfactant. For example, in an alkyl benzene sulfonate, the position of sulfonate group is in *para* position and the position

of the benzene ring on the alkane chain creates a significant difference, and the same can be observed for the position of sulfonate in internal olefin or alpha olefin hydrophobes. Most of the time the heterogeneity because of different species can be advantageous as they help in minimizing ordered structures of the surfactant.

2.2 SURFACTANT SELECTION

Recent research including this work indicates surfactant formulations consisting of a mixture of two or three surfactants show better performance than any single surfactant by itself. When two or more different but compatible surfactants are mixed together, they don't exhibit an "average characteristic", but rather they often exhibit a completely different behavior due to the formation of mixed micelles. When the mixture has improved performance over the individual surfactants, then it is said to be a *synergistic* mixture. When the reverse happens, the effect is called *anti-synergism* or *antagonism*.

In addition to the mixture of surfactants, other chemicals like co-solvent, alkali, polymers and sequestering agents are added for variety of reasons. This mixture of chemicals is usually referred to as a *surfactant formulation* or simply *formulation*.

The addition of co-solvent (e.g. alcohols) in a surfactant formulation has many advantages such as reduced microemulsion viscosity, fast equilibration, improved aqueous stability, etc. But, they also increase the cost. The usage of co-solvents can be eliminated or minimized by using surfactants with more branching or by elevating the temperature. The effect of using co-solvents to improve microemulsion phase behavior is discussed in Sahni (2009).

Before discussing the methodology and criteria required for selecting optimum surfactant structure, it's important to discuss the microemulsion phase behavior classification. Microemulsions are thermodynamically stable liquid mixtures of oil, water, and surfactant and sometimes other chemicals as well. In contrast, macromemulsions are differentiated from microemulsions from the droplet size (several orders of magnitude larger than the size of microemulsion drops (Bourrel and Schechter, 1988) and as a result they are thermodynamically unstable.

Winsor (1954) classified the microemulsions as Type I, Type II, and Type III. Type I microemulsion is an *oil-in-water* microemulsion with the oil solubilized in the micelle and the water the external phase. This is also referred as lower-phase microemulsion, water external microemulsion, or type II (-) microemulsion. Type II microemulsion is *water in oil* microemulsion with the oil solubilized in a reverse micelle and the oil the external phase. This is also referred as upper phase microemulsion, oil external microemulsion, or type II (+) microemulsion. Type III microemulsion is a bicontinuous microemulsion with the oil and water both external and internal to the micelles. The type III or middle phase microemulsions exhibit the lowest interfacial tension when in equilibrium with either oil or water excess phases and are thus desirable for enhanced oil recovery.

The transition from type I to type III to type II can be brought about by changing the electrolyte concentration (salinity), temperature, surfactant concentration, alcohol (co-solvent) concentration, oil EACN, water-oil ratio (for reactive crudes), surfactant tail length (carbon number) and branching, and the ratio of two surfactants with different HLB values. Typically for given oil, temperature, surfactant structure or structures and water-oil ratio, the electrolyte concentration (salinity) is increased, and this is referred as a salinity scan. At low salinity, the type I microemulsion forms, and oil solubilization

ratio (σ_o) is calculated as V_o/V_s (V_o is volume of oil solubilized and V_s is the volume of surfactant in the microemulsion, which is usually assumed to be the same as the volume added to the water before mixing with the oil to form the microemulsion, but this is not always a good approximation). At high salinity, type II microemulsion forms, and water solubilization ratio (σ_w) is calculated as V_w/V_s (V_w is volume of water solubilized). At intermediate salinity, both oil and water gets solubilized in the microemulsion, and the salinity at which V_o is equal to V_s (or σ_o is equal to σ_w) is called *optimum salinity,* S*, and the solubilization ratio at the optimum salinity is called *optimum solubilization ratio*, σ*. These solubilization parameters are converted to interfacial tension by Huh's equation (1979). It's given by

$$\gamma = C/\sigma^2 \qquad \text{----------- (1.1)}$$

For most crude oils, C=0.3 dynes/cm is a good approximation, which implies that if the solubilization ratio is 10, then the IFT is 0.003 dynes/cm. This solubilization ratio of 10 cc/cc is often used as a lower limit in choosing the best formulation.

The surfactant formulations are screened by conducting phase behavior experiments in sealed pipettes and aqueous stability in sealed ampoules (without oil). As mentioned above, one of the key screening criteria is that the solubilization ratio at the optimum salinity be at least 10 cc/cc. However, there are several other equally important criteria for a suitable formulation that can be easily observed from the fluids in the pipettes used to study the phase behavior. The most important of these criterion is the formation of an equilibrium microemulsion with low viscosity. It is useful and practical to make visual observations of hundreds of pipettes daily or weekly to get a qualitative indication of viscosity and interfacial tension at reservoir temperature. For these reasons, it's important not to just measure the interfacial tension, but to observe the phase changes over time. Conducting phase behavior experiments in pipettes is by far the easiest and

13

most effective way to screen up to hundreds of formulation and thousands of compositions at different salinities and so forth. It is not practical to measure so many values of IFT. Furthermore, the IFT measurements are subject to very large uncertainty unless it has already been established that the solutions are at equilibrium and chemically stable, which can only be done with the phase behavior observations over at least days to weeks. Additional compelling reasons for preferring the phase behavior approach is that it provides much more information than just IFT and these other data such as viscosity are as important to success as IFT. Phase behavior data and associated fluid properties are also needed for modeling purposes.

The chemicals in the formulation should also be studied without the presence of oil to check for surfactant solubility, and stability. These are called aqueous stability experiments. They are studied across the salinity range at which the phase behavior was studied. Typically the formulations are initially tested without polymer and later polymer is included for the final formulations. Like phase behavior pipettes, the sealed ampoules at reservoir temperature are also observed for several days or weeks or in some cases even months for the stability of the chemicals used.

Given the fact that there are hundreds of surfactants, the difficulty often lies in choosing a particular surfactant type for a given condition and crude oil. To start with, the surfactant is selected mainly based on the following:

- Oil characteristics – EACN, reactivity, other components such as paraffin content, asphaltene content, etc.
- Surfactant stability/solubility – which depends on the temperature, salinity, hardness ions
- Brine composition
- Mineralogy of geological formation

14

- Cost and available supply or potential supply from available feedstock– the most important criteria

It's well known that a surfactant has to match up the oil property for optimum performance. Crude oils are typically characterized based on API gravity, TAN, viscosity, and sometimes molecular weight. But these properties are highly variable, for instance, oils with same API gravity and TAN may behave completely different in terms of microemulsion phase behavior. The reason is that crude oils are made up of hundreds of components, and it is the distribution of these components that determines the identity of the crude oil. This property of the crude oil can be matched by comparing its phase behavior with that of a pure hydrocarbon (with known ACN). Hence the crude oil can be given an *equivalent alkane carbon number* (EACN), based on comparing the optimal salinity (with the same surfactant formulation) for the crude oil and that of the pure hydrocarbons. Cayias et al. (1976) first introduced the concept of EACN for crude oils and mixture of hydrocarbons by using a correlation between IFT behavior for homologous oils and alkane carbon number. They concluded saying that crude oils can be modeled by a unique temperature-independent equivalent alkane carbon number. Salager et al. (1979) extended the concept of EACN, and proposed a relation between the alkane carbon number (ACN) and the optimal salinity of the surfactant/brine/oil systems. They suggested that the logarithm of optimal salinity is a linear function of ACN. Similar observation was also made by Glinsmann (1979), and he concluded that live crude oil phase behavior can be simulated by adding less volatile, low-EACN hydrocarbons to the dead crude oil. Another more complex method to characterize crude oil was introduced by Puerto and Reed (1983). They suggested replacing EACN with the concept of *equivalent oils* (Eqo's), by including the oil molar volume and solubilization parameters, in addition to the optimal salinity.

At any given condition, the optimal salinity increases with an increase in EACN, often accompanied by a decrease in solubilization ratio, which implies that more hydrophobicity in the surfactant formulation is needed as the EACN of the crude oil increases. This effect is aggravated by an increase in temperature and/or salinity. The effect of these variables in determining the optimum surfactant structure is very complex and not easy to predict despite decades of research. Thus, a new correlation was developed (chapter 4) that can be used as a tool in predicting the optimum surfactant structure.

The understanding of EACN is extremely useful in modeling the live crude oil. Recent study by Roshanfekr (2010) clearly explains the effect of solution gas and pressure in microemulsion phase behavior. Solution gas (mostly methane) changes the microemulsion phase behavior from type I to type III to type II (as the EACN decreases), while an increase in pressure does the reverse. But conducting these high pressure experiments is often difficult and expensive and is therefore typically done only as a final test of the phase behavior. An alternative would be to conduct the experiments with "surrogate crude", which is a blend of dead crude and a less volatile, low-EACN hydrocarbon to match the EACN of the live crude. If hydrocarbons other than the pure alkanes are used as diluent (such as cyclohexane and decalin), the EACN can be calculated by using the following empirical correlation:

EACN = No. of carbon – 2(no. of cyclic rings) – 4/3(no. of double bonds) ---- (1.2)
For example, using this correlation, the EACN of decalin ($C_{10}H_{18}$) will be 6 (10 - 2*2 - 4/3*0).

A simplified schematic of the experimental methodology that captures some of these many criteria used to develop a formulation is given in Figure 2.2. However, the iterative nature of the process is very difficult to fully capture in any simple flow chart or

algorithm, so this and similar charts must be used with caution and judgment based on experience. The process is further complicated by the uncertainty in the TAN measurements and similar data and the variability in the impact of these characteristics.
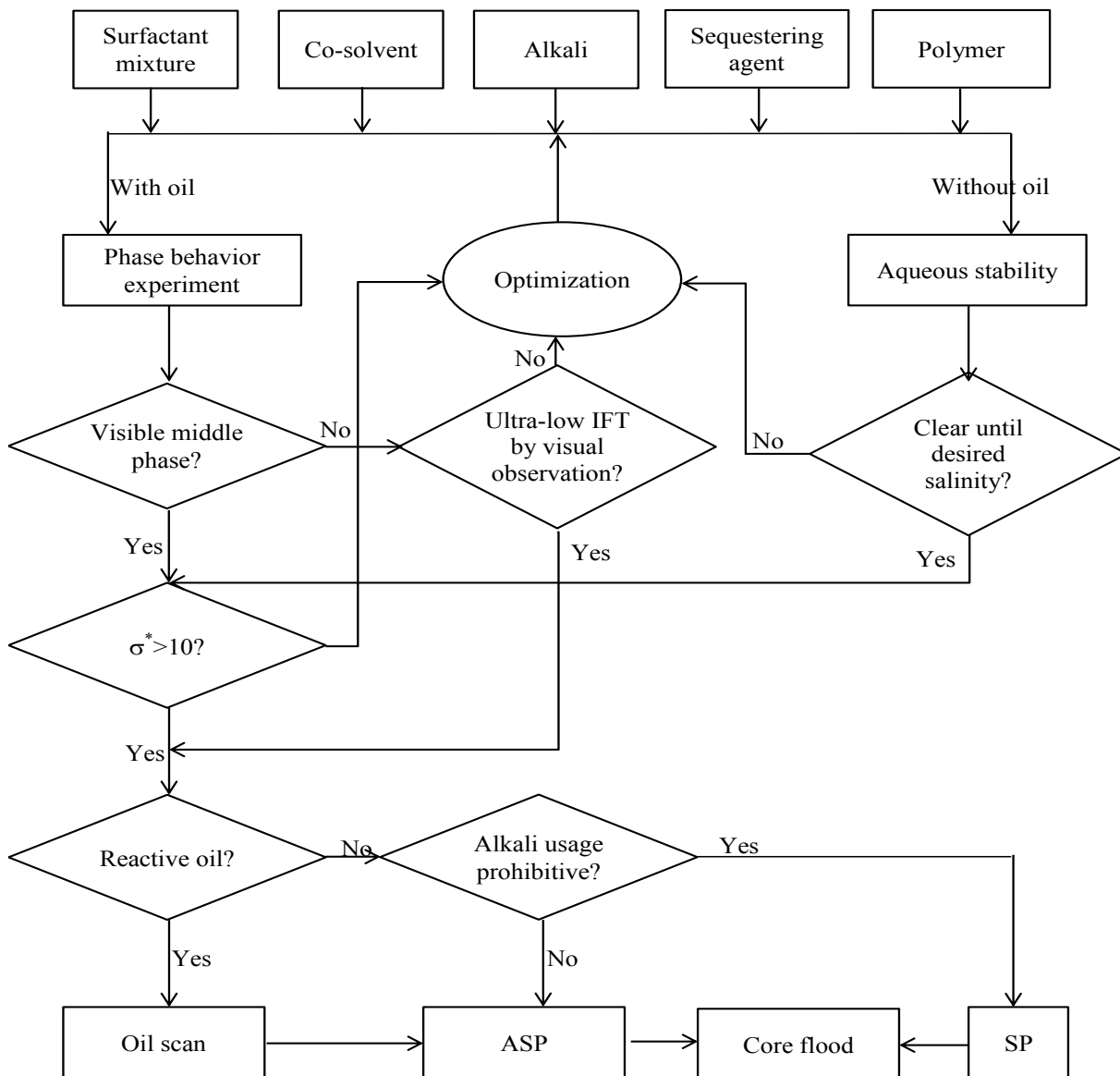
Figure 2.2: Simplified flowchart for microemulsion phase behavior methodology

.Chapter 3: Large Hydrophobe Surfactants

The need for large hydrophobe surfactants is ever increasing as chemical EOR is being expanded to more difficult reservoirs (high temperature, high salinity, and high viscosity oil). As discussed before, Guerbet reaction is the commercially viable method to produce very large branched hydrophobes. The Guerbet reaction dimerizes a linear alcohol using base catalysis at high temperature (~230 °C) to produce near mid-point branching (O'Lenick Jr., 2001). These Guerbet alcohols (GA) can then be used in the production of corresponding anionic surfactants (sulfates, carboxylates or sulfonates). Extenders like butylene oxide (BO), propylene oxide (PO), ethylene oxide (EO) are added to the alcohol before the final reaction to produce the anionic surfactant. The carboxylation and sulfation reactions are simple single step processes (Pinnawala-Arachchilage, 2010), whereas the sulfonation in a two-step complex process. Therefore, carboxylates and sulfates are less costly than sulfonates. This chapter will discuss experimental results with Guerbet alkoxy sulfates (GAS) and Guerbet alkoxy carboxylates (GAC). As an alternative to Guerbet hydrophobes, Tristyrylphenol (TSP), a new class of hydrophobes based on petrochemical feed stocks has also been introduced.

3.1 GUERBET ALKOXY SULFATES (GAS)

The Guerbet alkoxylates are sulfated via standard sulfamic acid procedure. The structure and reaction scheme is given in Pinnawala-Arachchilage, 2010. This section will cover the surfactant-brine-oil phase behavior and core flood experiments conducted using Guerbet alkoxy sulfates as a primary component in the surfactant formulation. All surfactant compositions are given in weight percent, unless otherwise mentioned.

3.2.1 Phase Behavior Experiments

The experimental methodology for using microemulsion phase behavior and aqueous stability experiments to find the optimum surfactant formulation, and the criteria to select the best formulations, is described in this thesis and some additional elements of it can also be found in the theses of Jackson, 2006; Levitt, 2006; Flaaten, 2007; Sahni, 2009; Yang, 2010; Dean, 2011 and Walker, 2011 among other places in the literature.

The target reservoir in this study is a carbonate with the lithology consisting mostly of calcite and dolomite. The temperature of the reservoir is around 100 °C (212 °F). All experiments were conducted at this temperature.

The connate brine of the reservoir is at very high salinity of 213,000 ppm with approximately 21,500 ppm of Ca^{2+} and Mg^{2+} ions. However, for the purpose of this study only the produced brine (~67,000 ppm) and injection sea brine (57,670 ppm) were used. The synthetic brine of the injection brine is referred as SUTIB, and the bicarbonate (120 ppm) from the original composition was removed due to precipitation issues in lab conditions. Similarly the synthetic produced brine is referred to as SUTPB and it has 50% of the original sulfate concentration (1299 ppm); the bicarbonate (585 ppm) was also removed. The composition of synthetic injection sea brine (SUTIB) and produced brine (SUTPB) is given in Tables 3.1 and 3.2, respectively.

In some experiments, softened injection sea brine was used. Calcium and magnesium ions were replaced by equivalent amounts of sodium ions. The synthetic softened brine is referred to as SSUTIB. The composition of SSUTIB is given in Table 3.3.

	Injection Water (ppm)
Na	18,300
Ca	650
Mg	2,110
K	n/a
SO4	4,290
Cl	32,200
CO3	0
HCO3	0
TDS	**57,670**

Table 3.1: SUTIB composition (notice no bicarbonate ions)

	Current Production Water (ppm)
Na	19,249
Ca	4,360
Mg	938
K	n/a
SO4	650
Cl	41,524
CO3	0
HCO3	0
TDS	**67,135**

Table 3.2: SUTPB composition (notice reduced sulfate ion conc. and no bicarbonate ions)

	Softened Injection Water (ppm)
Na	23,092
Ca	-
Mg	-
K	n/a
SO4	4,290
Cl	32,200
CO3	0
HCO3	120
TDS	**59,702**

Table 3.3: SSUTIB composition

Oil Properties and Characteristics

The oil in the target reservoir is a light, non-reactive oil. The dead oil has an API gravity of 32.6°, and a viscosity of around 14-16 cP at room temperature and ~2 cP at 100 °C.

Initial Screenings

As with many other candidates, depending on oil characteristics, temperature and salinity, alkyl/aryl sulfonates were one of the very first surfactants chosen for screening. At the start of this study, sulfates were applied only to low to moderate temperatures (< 65 °C), because of the poor hydrolytic stability at elevated temperatures. Because of this limitation, initial surfactant screenings were done primarily with mixtures of internal olefin sulfonates (IOS), alpha olefin sulfonates (AOS) and alkyl benzene sulfonate (ABS). The experiments were conducted more on the basis of available technology at that time and subsequent changes/enhancements were done to make the technology more attractive and feasible for field applications.

The list of experiments conducted on this particular candidate is given in Appendix 1. U-01 to U-72 includes phase behavior and aqueous stability experiments conducted using the above mentioned surfactants. Among these experiments most of the formulations consisted mixtures of C_{15-18} IOS, C_{20-24} IOS, C_{24-28} IOS, and C_{15-18} ABS. Other surfactants such as C_{12-15} AOS, C_{14-30} ABS, and C_{14-24} ABS including relatively expensive ether sulfonates were also tested. The formulations were also tested with and without the co-solvents such as triethyl glycol monobutyl ether (TEGBE), butanol-2.2 EO, and sodium dihexyl sulfosuccinate (MA-80), which acts as a temporary solubilizer before hydrolyzing to an alcohol, which then serves as a co-solvent.

The general inference from these experiments was that the high molecular weight IOS (C_{20-24} and C_{24-28}) helped in solubilizing more oil (when compared to the C_{15-18}

molecules) and thereby reducing the IFT, but they suffered from poor aqueous stability at the experimental conditions.

U-68 was one such formulation consisting of 0.5% C_{24-28} IOS, 0.2% C_{15-18} IOS and 0.3% TDA-30EO. The salinity scan was done by different dilutions of injection brine (SUTIB) and DI from 30% brine concentration (17,300 ppm) to 100% brine salinity (57,700 ppm). The solubilization ratio was 10 cc/cc at an optimum salinity of 40,000 ppm. However, the formulation didn't have aqueous stability (clear single phase) close to the optimum salinity at the experimental conditions. The solutions were clear only for couple of hours at 100 °C. Figure 3.1 shows the solubilization ratio vs. salinity plot for U-68.

After many trials (U-01 to U-72) with the combination of the surfactants mentioned above, it was realized that when the microemulsion phase behavior was good, the surfactant was too hydrophobic to be aqueous soluble, or whenever the aqueous solution was clear, the microemulsion phase behavior was poor. Achieving both the conditions for this particular candidate was very difficult. Moreover, because of the high temperature (100 °C), the selection of surfactants was basically restricted to sulfonates. Coincidentally, a new method of stabilizing sulfate surfactants at elevated temperature was identified (Adkins et al., 2010), and that gave the impetus to test Guerbet alkoxy sulfates for this particular candidate. As discussed earlier, because of the twin tail structure of the Guerbet hydrophobes, they exhibit exaggerated hydrophobicity. The ethylene oxide (EO) and propylene oxide (PO) can be tailored to fit the HLB needed for the oil and brine. The EO group helps in increasing the HLB, while the PO group does the reverse.

Experiments with EDTA.4Na

The sulfate surfactants can be stabilized at elevated temperatures, only at optimal pH conditions (usually between 9.5 and 11). Therefore, an alkaline condition has to be maintained in order to evaluate the GAS. The injection sea brine has approximately 2700 ppm of Ca^{2+} and Mg^{2+} ions. Hence, conventional alkali such as sodium carbonate or sodium hydroxide cannot be used. Because of cost considerations, water softening was not chosen as a possible solution, rather an "alkali/sequestering" agent that is compatible with the hard brine itself was attempted. Tetrasodium salt of ethylene diamine tetraacetate (EDTA.4Na) was one such sequestering agent tested in this study.

EDTA.4Na has the ability to sequester multivalent cations through its two amine groups and four carboxyl groups (Yang et al., 2010). Also, the pH is sufficiently high to stabilize the sulfates, apart from many other uses like reduction in surfactant adsorption, in-situ generation of soap, etc.

Experiments U-73 to U-79 were done to find the minimum EDTA.4Na required to sequester Ca^{2+} and Mg^{2+} in the brine. Theoritically, 10 to 1 weight ratio of EDTA.4Na is required for each ppm of divalent cations. In this case, the injection brine has approximately 2700 ppm divalent cations, and so the theoritical EDTA neeeded would be ~27,000 ppm. An EDTA.4Na scan (from 0.5% to 5%) in SUTIB was done (see U-73), and it was observed that at room temperature, samples 3% EDTA.4Na and above were clear, but at 100 °C, the entire scan turned cloudy. U-75 was a salinity scan (28,000 to 57,700 ppm) of SUTIB, fixing the EDTA.4Na concentration at 3%. Still, the cloudiness was observed in the entire scan. The same was even repeated with 6% EDTA.4Na (U-77), and still the same was observed This was almost double the theoritical EDTA required, and still a clear solution was not observed. . Consequently, it was recognized that this cloudiness was due to Ca and Mg hydroxide being formed at pH>11 where the

23

high pH overpowers the chelating ability of EDTA-4Na. It was then decided to adjust the pH of the solution after adding EDTA.4Na. A pH of at least 10.5 was desired to stabilize the sulfate surfactants to high temperatures (> 65 °C), so any solutions with a pH of more than 10.5 were lowered to 10.5 using dilute hydrochloric acid. U-79 is same as U-75, except the solution pH was adjusted down to 10.5 after adding EDTA.4Na. The results were completely different, and as expected, a clear solution was observed from 3.5% EDTA.4Na. Therefore, the minimum EDTA required to sequester the divalent cations in SUTIB was determined to be 3.5%. In fact, 3.5% EDTA.4Na was slightly on the border line, and so the concentration was subsequently increased to 3.75% in the later experiments.

Experiments with GAS in Hard Brine

Experiments U-80 to U-156 include phase behavior and aqueous stability studies using Guerbet alkoxy sulfates (GAS) in hard sea brine. One of the very first ether sulfate formulations (U-80) consisted C_{32}-7PO-32EO-sulfate and C_{20-24} IOS with 1% TEGBE, and 3.5% EDTA.4Na. The formulation turned out to be more hydrophobic, and only type II microemulsion system was observed in the salinity range tested. The same Guerbet ether sulfate was also tested along with C_{24-28} IOS and C_{24}.22EO non-ionic in separate experiments and still the formulation was more hydrophobic than expected.

The first promising phase behavior was observed when the formulation (U-83) consisted of C_{16-17}-7PO-sulfate and C_{15-18} IOS. A good transistion of type I microemulsion to type II microemulsion was observed in the desired salinity range. Also, the oil solubilization in the upper type I region was pretty close to 10. U-86 was then conducted by replacing C_{16-17}-7PO-sulfate in the formulation by a similar Guerbet type molecule (C_{16}-7PO-Sulfate). The inferences were similar to U-83, but still a sizeable

middle phase microemulsion was not observed. Then again C_{16-17}-7PO-sulfate was chosen and several experiments were conducted by changing the ratio two surfactants, with and witout the co-solvent (TEGBE) without much success.

From these experiments a better understanding was obtained for this particular oil interaction with surfactants, and it was decided to use a three component surfactant formulation, covering a hydrophobe size of high, low and intermediate carbon numbers. It was speculated that this particular approach would help in solubilizing more components in the oil. U-100 was one of such first formulations with three surfactant components. The formulation consisted of 0.5% C_{32}-7PO-18EO-Sulfate, 0.5% C_{16-17}-7PO-sulfate, 0.5% C_{15-18} IOS and 3.5% EDTA.4Na. As expected, the phase behavior was better than the previous GAS formulations, and a type III region was observed. The optimum salinity was 52,000 ppm with a solubization ratio of close to 10 at the optimum. But, it was failing in aquoeous stability at the optimum salinity.

In an attempt to improve the aqueous stability of the formulation, U-102 was conducted adding 0.5% TEGBE to U-100. The performance was similar to U-100, but it still failed in achieving aqueous stability close to the optimum salinity. U-105 was conducted with the same formualtion as U-102 except the total surfactant concentration was reduced to 1% from 1.5%, keeping the ratio of surfactants the same. Again in an attempt to increase the optimum salinity and to improve the aqueous stability, C_{16-17}-7PO-sulfate in the U-105 formulation was replaced by C_{16-17}-7PO-xEO-sulfate. U-106 was conducted with C_{16}-7PO-2EO-Sulfate, and U-107 was conducted with C_{16}-7PO-6EO-Sulfate. Figure 3.2 shows the solubilization ratio comparison plot for U-105, 106 and 107. The formulations showed good phase behavior, but still failed in getting the aqueous solubility. As we can see, the optimum salinity increased with increasing number of EO molecules in the formulation. More importantly, the solubilization ratio has also

not decreased with increased optimum salinity. This is one of the main advantages of using these long hydrophobe surfactants compared to the conventional surfactants. The surfactants can be tailored for specific applications, by changing the number of EO and PO molecules in the surfactant apart from changing the hydrophobe size itself.

In order to see the effect of surfactant concentration on aqueous stability, U-107 was repeated at different surfactant concentrations. U-118 (a), 118 (b), 118 (c), and 118 (d) were conducted at a total surfactant concentration of 1%, 0.75%, 0.5%, and 0.3% respectively. The results were not different from U-107. The decreased surfactant concentration did not help in getting the aqueous stability in that particular case. Apart from having difficuties in attaining aqueous stability, the solubilization ratio was always less than or equal to ten. So, in order to improve the performance of the surfactant phase behavior, it was decided to improve the hydrophobicity of the formulation. Out of the three surfactant components, replacing the C_{15-18} IOS by higher molecular weight surfactants seriously affected the aqueous stability. It was decided to replace C_{32}-7PO-18EO-sulfate by C_{32}-7BO-7PO-25EO-sulfate. The addition of butylene oxide (BO) as an extender, in addition to PO and EO, gives more hydrophocity to the surfactant thereby increasing the oil soulbilization.

U-124 was one such formulation which consisted 0.33% C_{32}-7BO-7PO-25EO-sulfate, 0.33% C_{15-18} IOS, 0.33% C_{16}-7PO-6EO-sulfate, 0.25% TEGBE, 3.75% EDTA.4Na. The solubililization ratio was still 10 cc/cc at an optimum salinity of 69,000 ppm. So, the formulation was not as hydrophobic as expected. It was then decided to replace the C_{16}-7PO-6EO-sulfate with high molecular weight ether sulfate. One such experiment conducted was U-131 which consisted of 0.33% C_{32}-7BO-7PO-25EO-sulfate, 0.33% C_{15-18} IOS, 0.33% C_{32}-7PO-10EO-sulfate, 0.5% TEGBE, 3.75% EDTA.4Na. As expected, the formulation was good with a solubilization ratio of about 13 cc/cc at an

26

optimum salinity of 57,000 ppm. In an attempt, to improve the phase behavior even further, the ratio of surfactants in the U-131 formulation was changed, with more percentage given to C_{32}-7BO-7PO-25EO-sulfate. U-137 was conducted with a formualtion consisting of 0.58% C_{32}-7BO-7PO-25EO-sulfate, 0.33% C_{15-18} IOS, 0.33% C_{32}-7PO-10EO-sulfate, 0.5% TEGBE, 3.75% EDTA.4Na. The phase behavior was very good with a solubilization of ratio of more than 20 cc/cc at an optimum salinity of 43,000 ppm. Figure 3.3 shows the solubilization ratio plot for U-137. Still, the aquoeus stability for the formulation, was falling short of optimum salinity, and therefore needed some modifications.

In order to improve the aqueous stability of the U-137 formulation, it was decided to increase the EO level in C_{32}-7PO-10EO-sulfate. The formulation which first met both the conditions of good phase behavior and aqueous solubility was U-147 (F). The formulation was 0.29% C_{32}-7BO-7PO-25EO-sulfate, 0.17% C_{15-18} IOS, 0.17% C_{32}-7PO-14EO-sulfate, 0.25% TEGBE, 3.75% EDTA.4Na. Figure 3.4 shows the solubilization ratio vs. salinity plot for U-147 (F). The aqueous stability was tested at different surfactant concentrations (with proportionally increased TEGBE concentrations), and it passed even for surfactant concentrations as high as 3.75% (with 1.5% TEGBE). The formulation for U-147 (F) has a total surfactant concentration of 0.625%. However, the core flood (U-01) was conducted at a total surfactant concentration of 3.75%, the details of which will be discussed in the core flood section.

One of the objectives of the research was to find a dilute surfactant formulation to be applied in the target reservoir. Therefore, the formulation U-147 (F) was further tested at concentrations as low as 0.15%. U-150 to U-153 were conducted at 0.30% and 0.15% total surfactant concentrations both with and without the co-solvent (TEGBE). Even

though reading the interfaces at these low surfactant concentrations was difficult, visual observations indicated ultra-low IFT even at these very low concentrations.

Even though a very efficient surfactant formulation had been developed for this difficult oil at harsh conditions, the 3.75% EDTA.4Na required to sequester the divalent cations in the brine is quite high, and it was a drawback in this formulation. Hence, it was decided to work on a surfactant formulation in softened sea brine.

Experiments with GAS in softened sea brine

Experiments U-157 to U-174 includes phase behavior and aqueous stability studies done using Guerbet alkoxy sulfates (GAS) in softened sea brine. The composition of softened sea brine (SSUTIB) is given in Table 3.3. Sodium carbonate (Na_2CO_3) was chosen as alkali for providing high pH for sulfate surfactant stability at elevated temperature.

Recognizing that what EDTA-4Na was providing was in-situ softening of water, the same successful formulation in hard brine (U-147 (F)) was also tested in the softened sea brine. The scan variable was Na_2CO_3 (from 0.5% to 5%) keeping the brine salinity (~60,000 ppm) constant. Figure 3.5 shows the solubilization ratio plot for U-158. It consisted of 0.29% C_{32}-7BO-7PO-25EO-sulfate, 0.17% C_{15-18} IOS, 0.17% C_{32}-7PO-14EO-sulfate (notice no TEGBE, and no EDTA.4Na). As expected the formulation showed excellent phase behavior with a solubilzation ratio of more than 20 cc/cc at an optimum salinity of 3% Na_2CO_3 (TDS ~90,000 ppm). However, it failed to achieve aqueous stability at 100 °C. At room temperature, it was clear up to 3.5% Na_2CO_3 (TDS ~95,000 ppm). The addition of even small amounts of TEGBE (0.25%) decreased the performance of the formulation. Therefore adding TEGBE was not an option for improving the aqueous stability.

The formulation was also modified slightly by increasing the EO level in an attempt to improve the aqueous solubility. U-167 was conducted with 0.29% C_{32}-7BO-7PO-25EO-sulfate, 0.17% $C_{15\text{-}18}$ IOS, 0.17% C_{32}-7PO-18EO-sulfate. The optimum salinity increased slightly to 4% Na_2CO_3, but the aqueous solubility was still not achieved at the optimum salinity. However, it was decided to test the U-158 formulation in the core flood (U-02), the details of which will be discussed in the next section. Though this formulation didn't achieve aqueous stability at the optimum salinity at 100 °C, it was still a reasonable experiment to understand the efficacy of the surfactant formulation. The next section will discuss the core flooding experiments conducted using ether sulfate formulations.
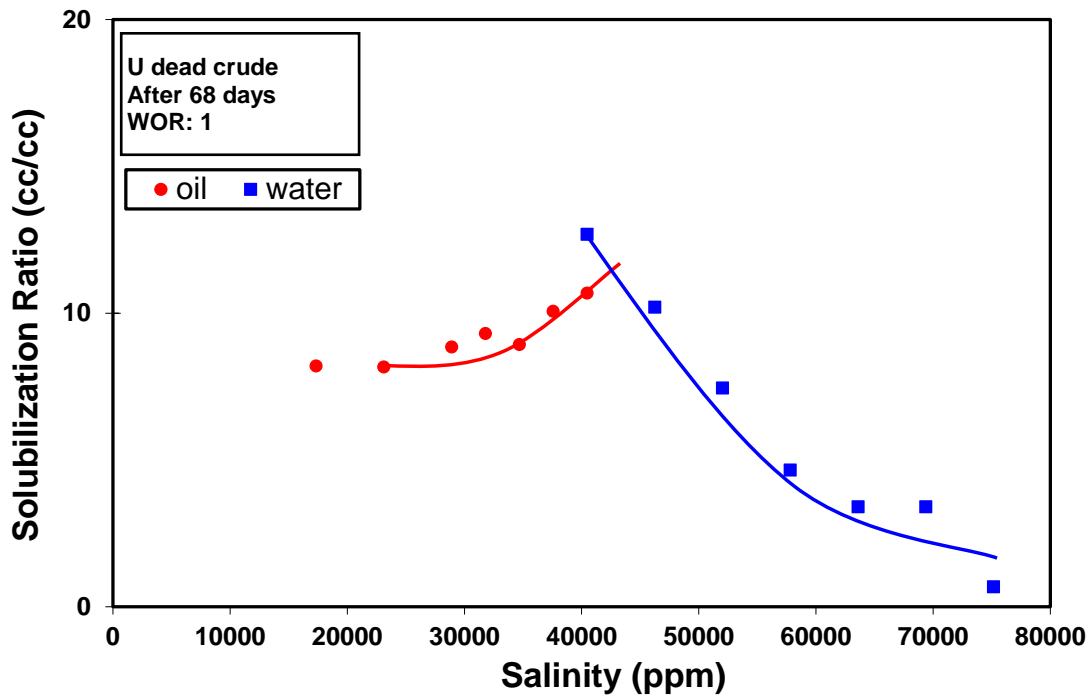
Figure 3.1: Solubilization ratio plot for U-68
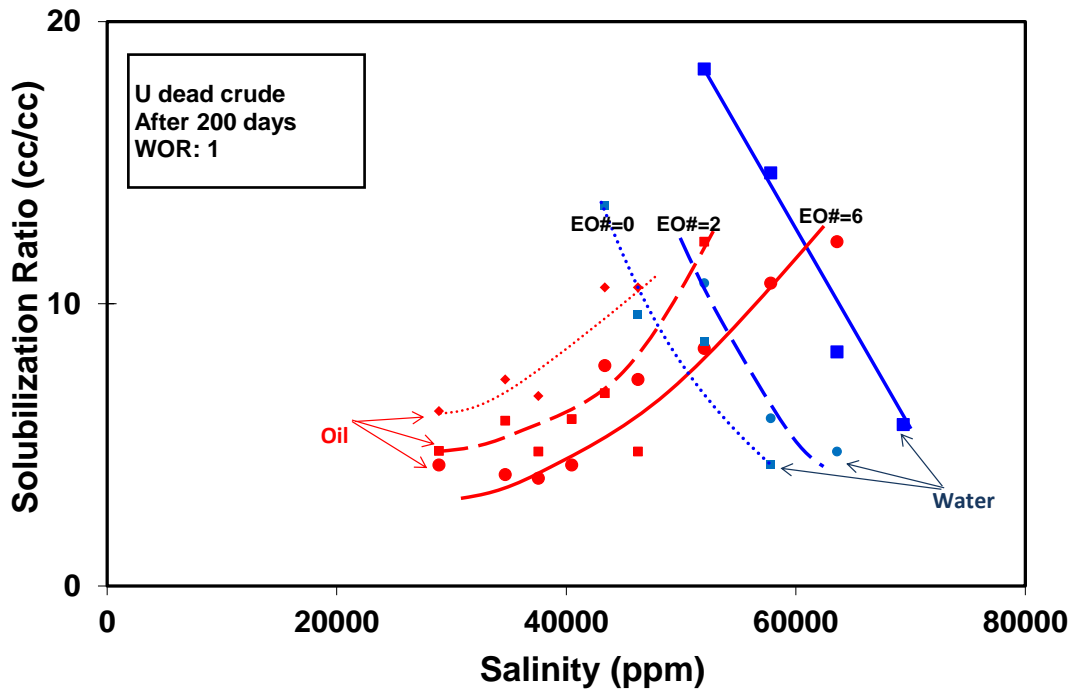
Figure 3.2: Solubilization ratio plot for U-105, 106 and 107 (0.33% C_{16}-7PO-xEO-Sulfate, 0.33% C_{15-18} IOS, 0.33% C_{32}-7PO-18EO-Sulfate, 0.5% TEGBE, 3.5% EDTA.4Na). Effect of increased EO level in the forumulation
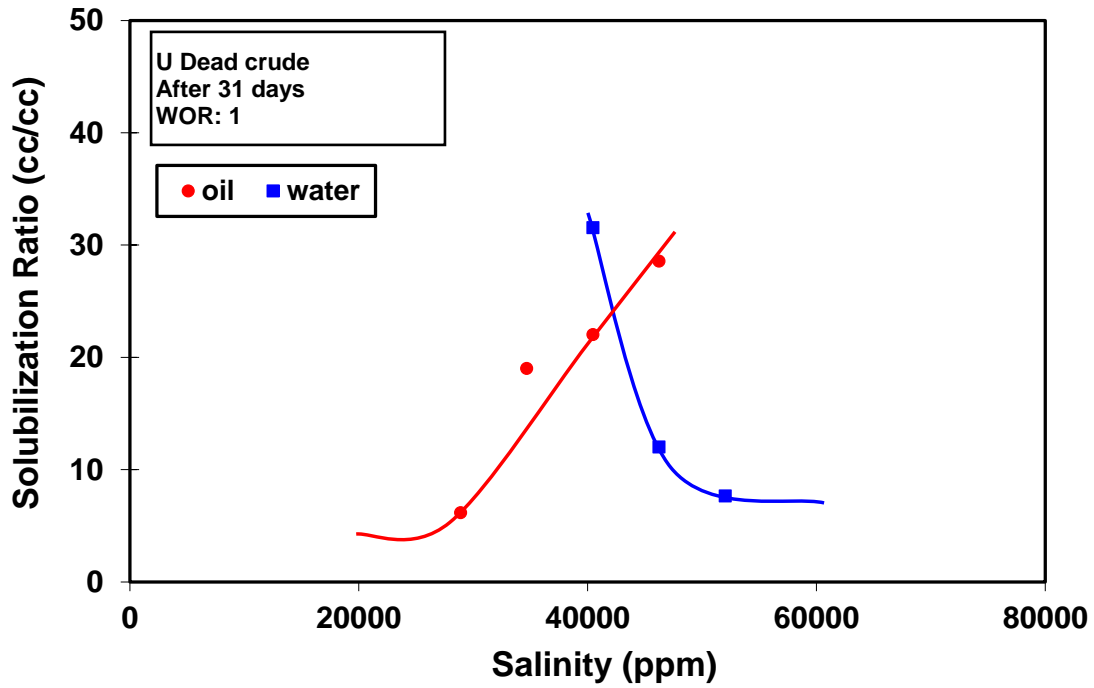
Figure 3.3: Solubilization ratio plot for U-137 (0.58% C_{32}-7BO-7PO-25EO-sulfate, 0.33% C_{15-18} IOS, 0.33% C_{32}-7PO-10EO-sulfate, 0.5% TEGBE, 3.75% EDTA.4Na)
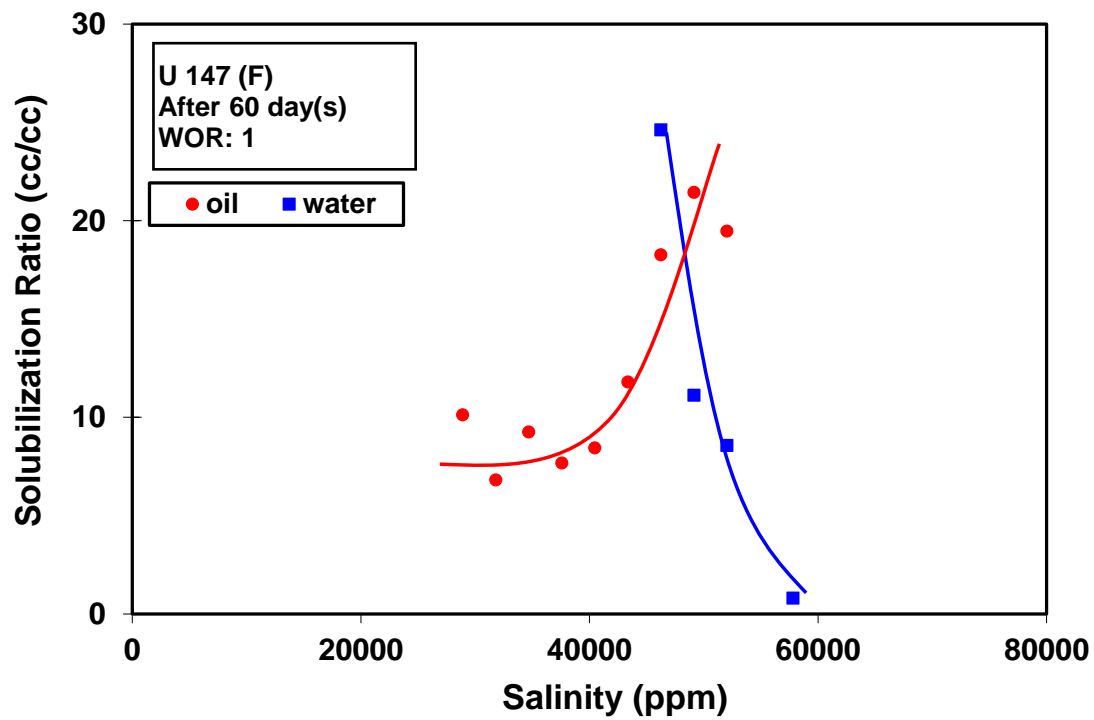
Figure 3.4: Solubilization ratio plot for U-147 (F) used in U-01 core flood (0.29% C_{32}-7BO-7PO-25EO-sulfate, 0.17% C_{15-18} IOS, 0.17% C_{32}-7PO-14EO-sulfate, 0.25% TEGBE, 3.75% EDTA.4Na)
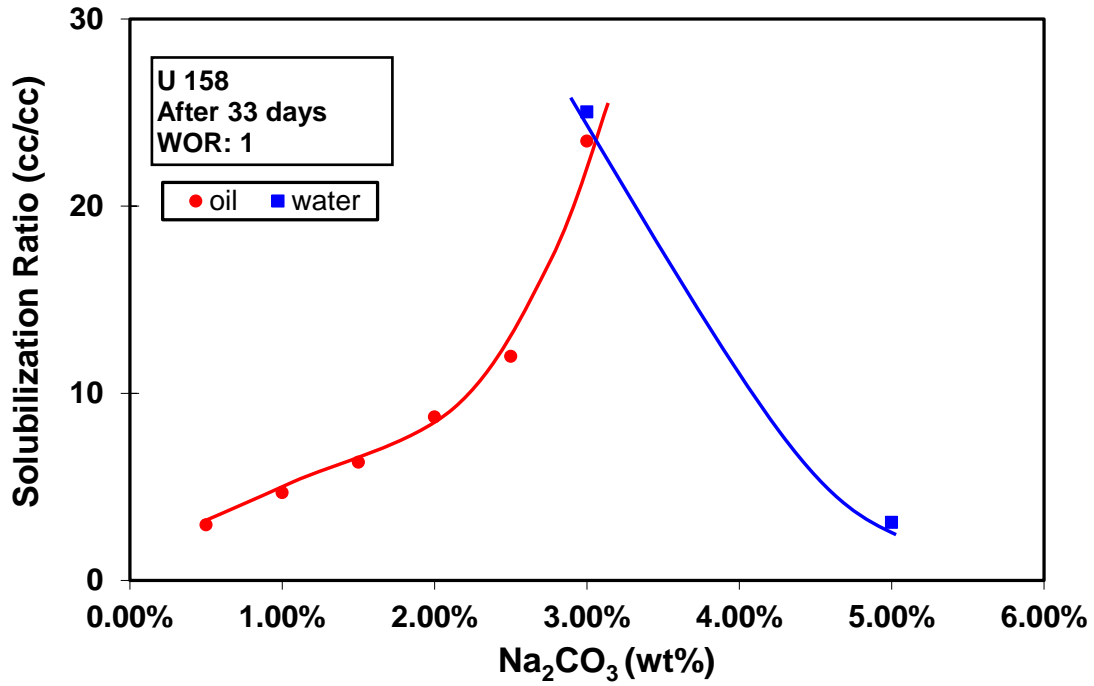
Figure 3.5: Solubilization ratio plot for U-158 used in U-02 core flood (0.29% C32-7BO-7PO-25EO-sulfate, 0.17% C15-18 IOS, 0.17% C32-7PO-14EO-sulfate)

3.2.2 Core Flood Experiments

Once a promising surfactant formulation (showing ultra-low IFT values, low microemulsion viscosities, aqueous stable) was found, it had to be tested to determine its effectiveness in recovering the oil, by conducting a core flood experiment. The experimental methodology and the materials required are well documented and can be seen elsewhere (Jackson, 2006; Levitt, 2006; Flaaten, 2007; 2008; Sahni, 2009; Yang, 2010).

Design of Core Flood

In order to test the efficacy of the surfactant formulation in tertiary flood, the core (either outcrop or reservoir) is brought close to the reservoir salinity conditions, saturations, and wettability. Then the chemical slug containing desired surfactant formulation, determined amount of polymer for mobility control at the desired salinity (usually at the optimum salinity or slightly over optimum depending on the initial salinity in the core, accounting for the effect of any dilution and dispersion) is injected followed by a polymer drive containing polymer concentration matching the viscosity of the chemical slug at the desired salinity (typically at the type I salinity). This type of phase behavior transition from type II to type III to type I during the course of the core flood is called negative salinity gradient. The importance of having a negative salinity gradient has been explained and demonstrated by Nelson and Pope (1978), Pope and Nelson (1978), Pope et al. (1979) and Hirasaki et al. (1981) among others more recently such as Levitt et al. (2006). The salinity gradient design has a surfactant formulation having an optimum salinity less than the salinity of the field brine, and a polymer drive salinity less than or at most equal to the surfactant slug salinity. The advantages of having this sort of configuration over constant salinity floods are numerous. Hirasaki et al. (1981) demonstrated the benefits of negative salinity gradient by running different experiments

34

at constant type I salinity, constant type II salinity, constant type III salinity, and finally gradient of salinity from field brine (type II) to drive salinity (type I). The authors concluded saying that the negative salinity gradient is the most beneficial, as the over optimum salinity ahead of the surfactant slug retards the surfactant (thus reducing the mobility of the surfactant), while the lesser salinity (type I) drive repartition the surfactant back from the immobile oil phase to the mobile aqueous phase, thus reducing the trapping of the surfactant. Because of this the surfactant retention is also greatly decreased. The mechanism of surfactant retention and other controlling factors will be discussed in detail in chapter 5.

Mobility control is also an equally important aspect in proper design of a core flood. The inverse of the minimum oil bank mobility is the necessary slug viscosity to have a favorable mobility ratio (Gogarty and Tosch, 1968). This oil bank mobility can be roughly estimated using Corey exponents, water and oil viscosities, and measured water flood end-point relative permeabilities. Once the viscosity needed for the slug is determined, the polymer concentration needed to have the required viscosity is determined at the desired salinity, hardness ions, temperature, and shear rate. A stepwise procedure for determining the polymer concentration is given in Dean (2011).

Core Flood Set Up

New surfactant formulations are typically first tested in an outcrop core (either sandstone or carbonate depending on the lithology) before moving to the reservoir core in final stages. The outcrop cores used were always about one foot long, with a diameter of either 1.5 or 2 inches. The core floods were done in stainless steel core holder with a confining pressure of 500 – 1000 psi. Fluids were injected by a Teledyne ISCO 5000 syringe pump. The reservoir fluids injected in to the core were contained either in a glass

column (for low pressure injection), or stainless steel column (for high pressure injections), which were displaced by an immiscible mineral oil injected from the pump. The outlet line is connected to a back pressure regulator set at 30-50 psi to prevent of fluids in the core. Pressure taps were potted across the core and connected to pressure transducers to measure the pressure drop across different sections of the core. The experimental set up is illustrated in Figure 3.6.

U-01 Core Flood

The purpose of U-01 core flood was to test the efficiency of U-147 (F) surfactant formulation in recovering the residual oil saturation in tertiary flooding. Based on the lithology, Silurian dolomite was chosen as the outcrop core to conduct this core flood. The core was 2 inches in diameter and 12 inches in length. Once the core was loaded in the core holder and confining pressure was applied, it was evacuated until it held a complete vacuum. The core was then saturated by imbibing the produced brine (SUTPB) in a measuring jar. The brine was pre-filtered by a 0.45 μm nitro cellulose filter paper. The volume of brine imbibed minus the dead volume of the core holder (in the end piece and pressure taps) gives an approximate pore volume of the core. The approximate pore volume determined in this method was 80 ml.

The pore volume was also determined using a salinity gradient tracer test, which is often a more reliable method than the volumetric measurement. A lesser salinity (or higher salinity) brine is displaced by a higher salinity (or lower salinity) brine. The effluent samples are collected and analyzed for conductivity (or salinity). For a perfectly homogeneous core, normalized conductivity (or salinity) of 0.5 corresponds to 1 PV in a plot of normalized conductivity (or salinity) vs. cumulative volume. But, the Silurian dolomites are often heterogeneous, characterized by early breakthrough and long tail. In

those cases, the pore volume is determined simply by finding the area above the curve (for lower salinity brine displaced by higher salinity) or area below the curve (for higher salinity brine displaced by lower salinity brine). The pore volume determined by this method for core used in U-01 core flood was also 80 ml.

During the brine flood, the steady state pressure drop was also monitored, and with that the permeability to brine was determined to be 242 mD. After the brine flood, the dead crude oil which was pre-filtered through a 0.45 micron filter was injected at a constant injection pressure of 130 psi. Because, of the 30 psi back pressure, the pressure drop during the oil flood was close to 100 psi. The effluent was collected in a 100 ml burette, and when no more brine is produced, the flow rate and the pressure drop were measured. The initial oil saturation was determined to be 0.90, and the permeability to oil was 118 mD, equating to an end-point oil relative permeability value, k_{ro}^{o}, of 0.48. This value of initial oil saturation is quite unusual for a Silurian dolomite, the reason of which was not understood.

Once the core was brought to its initial oil saturation, it was flooded with the produced brine (SUTPB) to bring the core to its residual state. It was conducted at 1 mL/min (~18 ft/day), and the effluent was collected in a 100 mL burette until no more oil was produced. The residual oil saturation was determined to be 0.56. The steady state pressure drop was measured, and the end point permeability to water was determined to be 10 mD, equating to an end-point water relative permeability, k_{rw}^{o}, of 0.038.

With the core at residual oil saturation, the chemical slug of following composition was injected, followed by a polymer drive with the composition shown below in Table 3.4.

ASP Slug	Polymer Drive
1.74% C_{32}-7BO-7PO-25EO-sulfate	2500 ppm AN-125
0.99% C_{32}-7PO-14EO-sulfate	34300 ppm SUTIB
0.99% C_{15-18} IOS	Frontal velocity: 1.96 ft/day
1.5% TEGBE	Viscosity ratio @ 10 s^{-1}: 12.05
2500 ppm AN-125 3.75% EDTA.4Na 48750 ppm SUTIB 0.08 PV (PV*C – 30) Frontal velocity: 1.96 ft/day Viscosity ratio @ 10 s^{-1}: 13	

Table 3.4: ASP slug and PD composition for U-01 core flood

The chemical flood was conducted at ~2 ft/day, with the surfactant slug containing a total surfactant concentration of 3.75%. The reason for choosing such a high concentration of surfactant was to minimize the usage of EDTA.4Na in the surfactant slug. Since, this was one of the first core floods conducted with this formulation, a conservative estimate of surfactant mass was chosen. The surfactant slug size was 8% PV (PV*C – 30). The oil broke through at 0.15 PV, and this quick oil breakthrough could be probably because of the high concentration of surfactant in the chemical slug. The effect of choosing dilute surfactant slug vs. concentrated surfactant slug, keeping the same mass of surfactant will be discussed in the coming sections. The oil cut during the breakthrough was as high as 80%, and dropped drastically to less than 15% within 0.7 PV. The cumulative oil recovery at the end of 3 PV was 69.5% of the water flood residual oil. The oil saturation at the end of 3 PV was 0.17.

In order to eliminate any chances of material balance calculations mistake, a second surfactant slug with the same composition as before was injected at 3 PV. As expected, more oil was produced, and at the end of 5 PV, the cumulative oil recovered was close to 91% of the water flood residual oil. The oil saturation decreased from 0.17

to less than 0.05 during the second surfactant flood. Figure 3.7 shows the oil recovery plot for U-01. The pressure drop profile is given in Figure 3.8.

The poor performance of the core flood can be pointed out to several reasons, the very first being the salinity gradient design. When designing the salinity gradient of the core flood, the salinity due to 3.75% EDTA.4Na was not considered. As per the phase behavior experiment (U-147 (F)), the optimum salinity was observed at 48,000 ppm brine salinity in addition to 3.75% EDTA.4Na (TDS ~85,500 ppm), and the type I salinity was around 35,000 ppm (TDS ~72,500 ppm). But, the polymer drive in the core flood was designed at 34,300 ppm brine salinity without 3.75% EDTA.4Na. This implies that the salinity behind the surfactant slug was far lower than the desired salinity. Another reason was the poor mobility control of the slug and the polymer drive. The effluent viscosity was 0.82 cP (@ 90 C), as compared to the injected viscosity of 4.4 cP (@ 90 C). Clearly the loss of mobility control was a major factor in the poor performance of the core flood. The reason for the viscosity loss was not clearly understood.

U-02 Core Flood

As discussed before in the phase behavior section, the high usage of EDTA.4Na in the formulation when hard brine was used was a drawback in the formulation, and so it was decided to use the softened sea water, and sodium carbonate as the alkali. An optimum surfactant formulation was identified (U-158), and it's identical to U-147 (F) without the usage of EDTA.4Na and TEGBE.

As before, the Silurian dolomite was chosen as the core, of 2" in diameter and 12" in length. The core was loaded in a stainless steel core holder with the pressure taps across different sections. The core was evacuated and saturated by 0.25X produced brine (SUTPB) by letting it imbibe under vacuum. Then the core was flooded with the same

39

brine for several pore volumes, and it was displaced by produced brine (SUTPB). The effluent samples were collected and analyzed for conductivity. The normalized conductivity was plotted against cumulative volume collected, and the pore volume was determined by finding the area above the curve. The pore volume was found to be 90 mL. The permeability to brine was determined to be 241 mD.

The core was then flooded with 0.45 micron filtered U dead crude at a constant injection pressure of 100 psi. The steady state pressure drop and flow rate was measured, and the permeability to oil was determined to be 141 mD, equating to an end-point oil relative permeability, k_{ro}^o, of 0.59. By measuring the volume of brine collected in the effluent, the initial oil saturation was determined to be 0.57.

After the oil flood, the core was flooded with the produced brine (SUTPB) at 1 mL/min (16 ft/day) until no more oil was produced. By material balance, the residual oil saturation after water flood, S_{orw}, was found to be 0.38. The permeability to water was found to be 8 mD, equating to an end-point water relative permeability, k_{rw}^o, of 0.035.

With the core in residual oil saturation, 0.6 PV of chemical slug containing 0.3% total surfactant concentration, equating to a PV*C value of 18 was injected. The ASP slug was injected at 2 ft/day followed by a polymer drive at the same velocity. The composition of the ASP slug and polymer drive is shown in Table 3.5. 500 ppm sodium dithionite was used along with the ASP slug and PD to keep the core in reduced state.

The oil recovery plot is shown in Figure 3.9. The oil broke through almost immediately after the start of the chemical flood, which indicates that the core probably didn't reach true residual oil state after the water flood. The average oil cut was about 30%, and most of the oil was produced in less than 2 PV. The cumulative oil recovered at the end of 2 PV was 82% of the water flood residual oil. The oil saturation was decreased to 0.069 at the end of 2 PV. The pressure drop profile during the chemical flood is shown

in Figure 3.10. Even though the pressure drop during the oil bank migration is quite noisy, the pressure drop towards the end of the flood is quite steady and about 4 psi/ft for 2 ft/day frontal velocity. The pH of the effluent samples was analyzed, and plotted against PV, as shown in Figure 3.11. One can see from the plot that the samples between 0.8 and 1.2 PV retained high pH, indicating that the alkali propagated along with the surfactant slug.

ASP slug	Polymer drive
Slug Size: 0.6 PV (PV*C - 18)	Slug Size ~1.5 PV
0.08% C_{32}-7PO-14EO-sulfate	4500 ppm AN-125
0.14% C_{32}-7BO-7PO-25EO-sulfate	680 ppm of sodium dithionite
0.08% C_{15-18} IOS	64000 ppm SSUTIB
3500 ppm AN-125	Frontal velocity: ~2 ft/day
680 ppm of sodium dithionite	Viscosity ratio @ $10s^{-1}$: 51
30,000 ppm Na_2CO_3 in SSUTIB (89,900 ppm TDS)	
Frontal Velocity: ~2ft/day	
Viscosity ratio @ $10s^{-1}$: 43	

Table 3.5: ASP slug and PD composition for U-02 core flood

Overall, the core flood performed as expected, but could have reduced the oil saturation even more, if sufficient surfactant mass had been injected. Typically a PV*C (pore volume injected*surfactant conc.) of 25 – 30 is considered conservative for non-reactive oils. But, in this core flood only 0.6 PV slug of 0.3% surfactant concentration (PV*C – 18) was injected. Nevertheless, it still recovered more than 80% of the water flood residual oil. The surfactant retention was not measured in this core flood, which would have otherwise given an insight on whether sufficient surfactant to satisfy adsorption was injected.
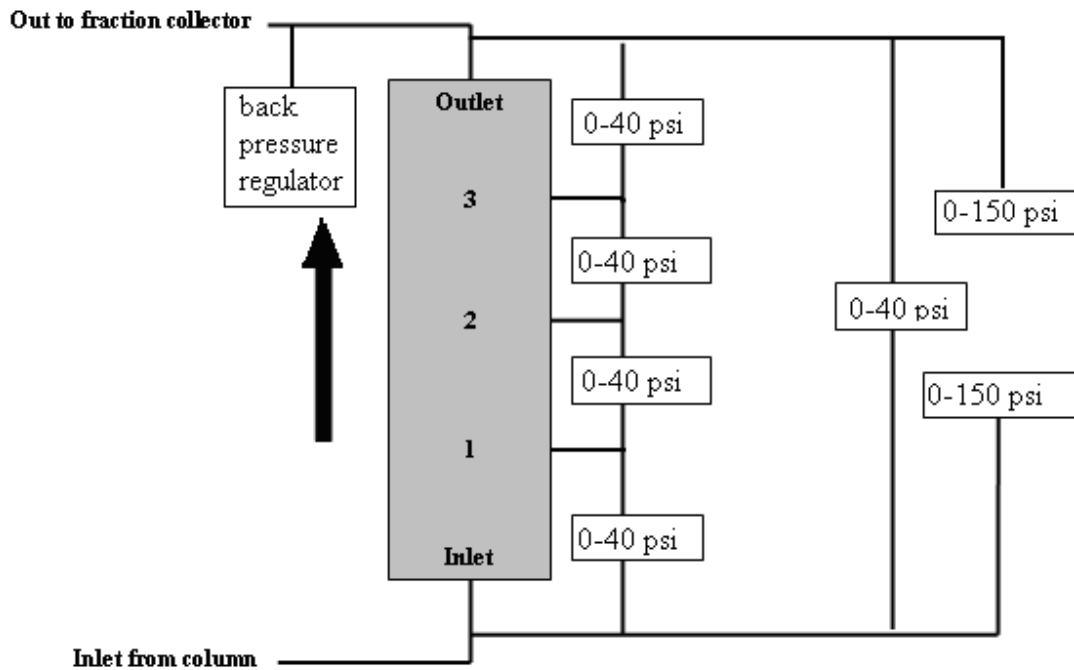
Figure 3.6: Schematic of the core flood set up
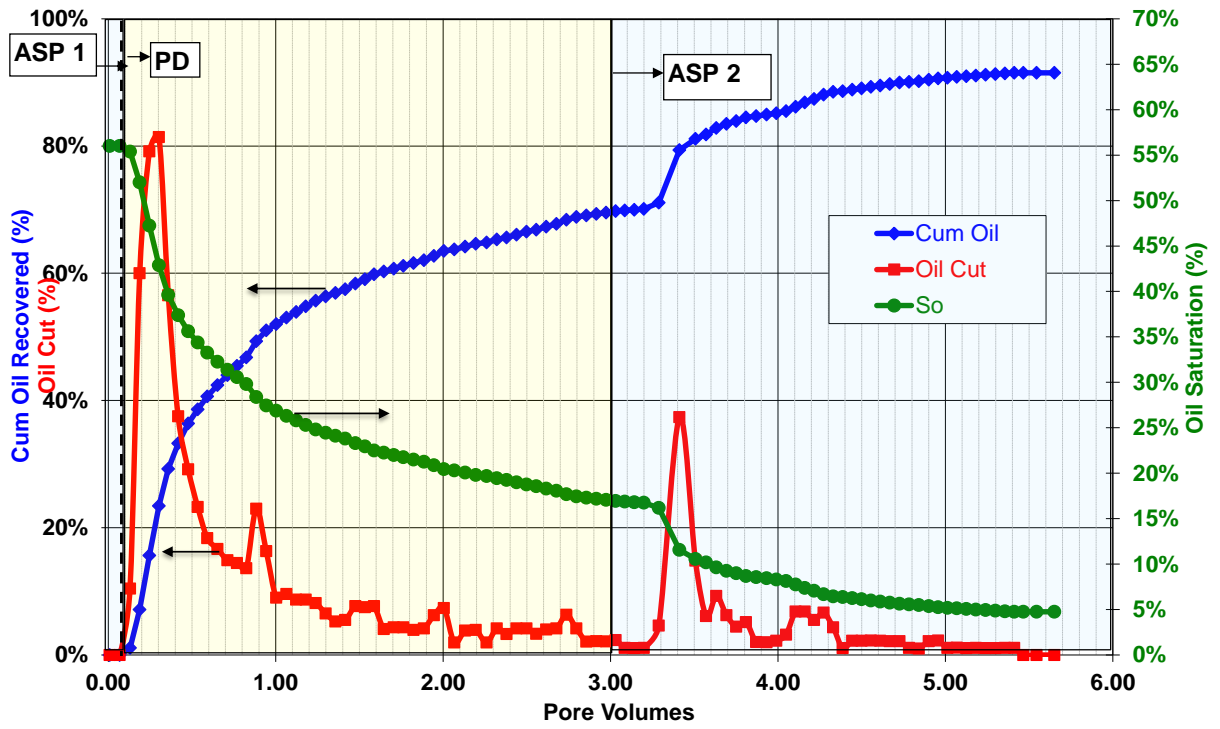
Figure 3.7: Oil recovery plot for U-01
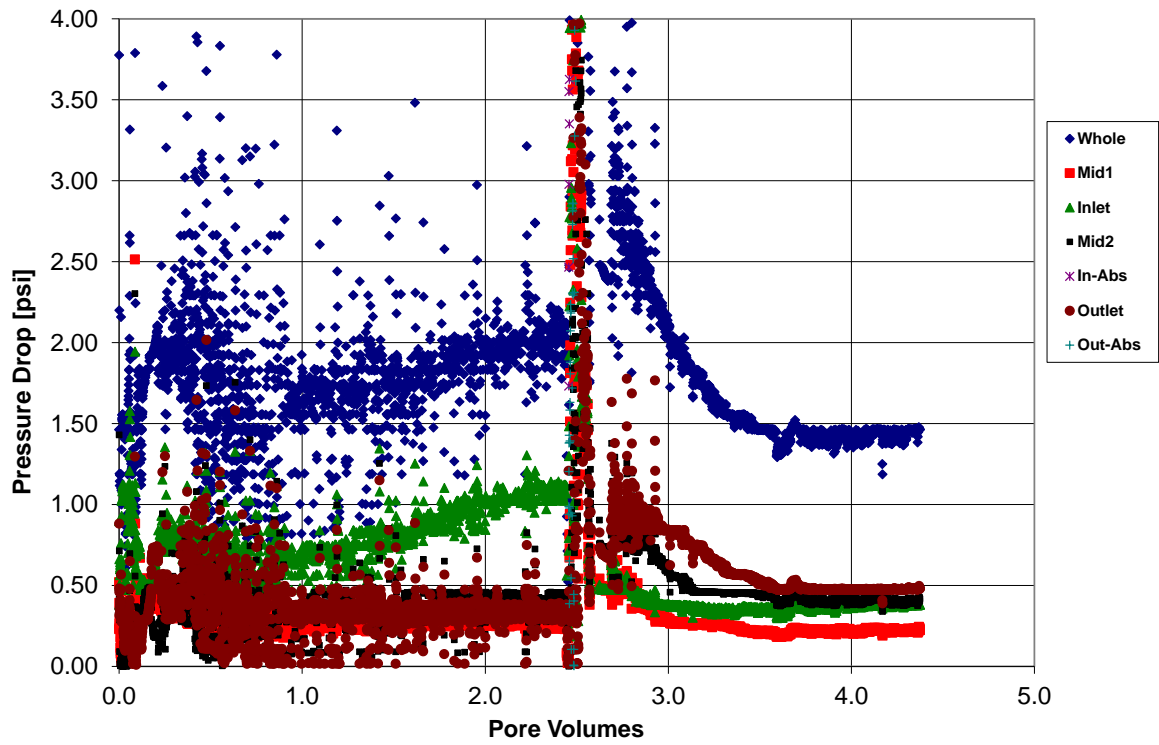
Figure 3.8: Pressure drop profile during chemical flood for U-01
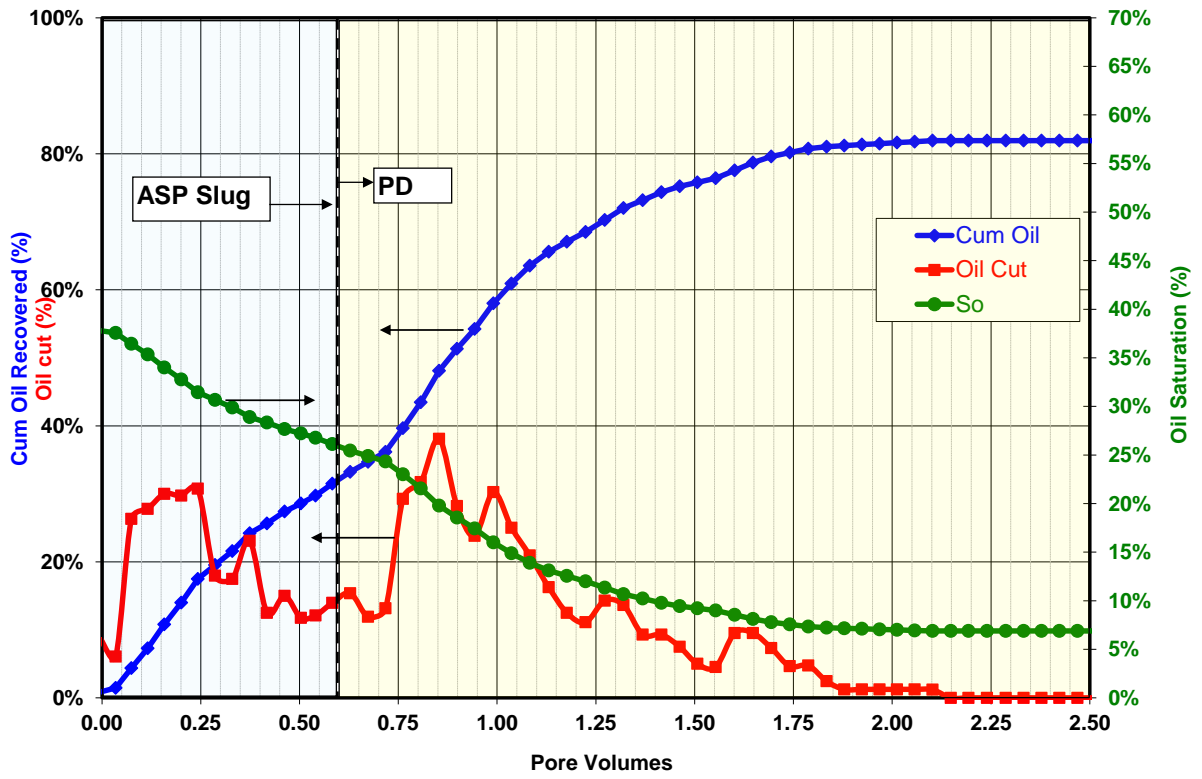
Figure 3.9: Oil recovery plot for U-02
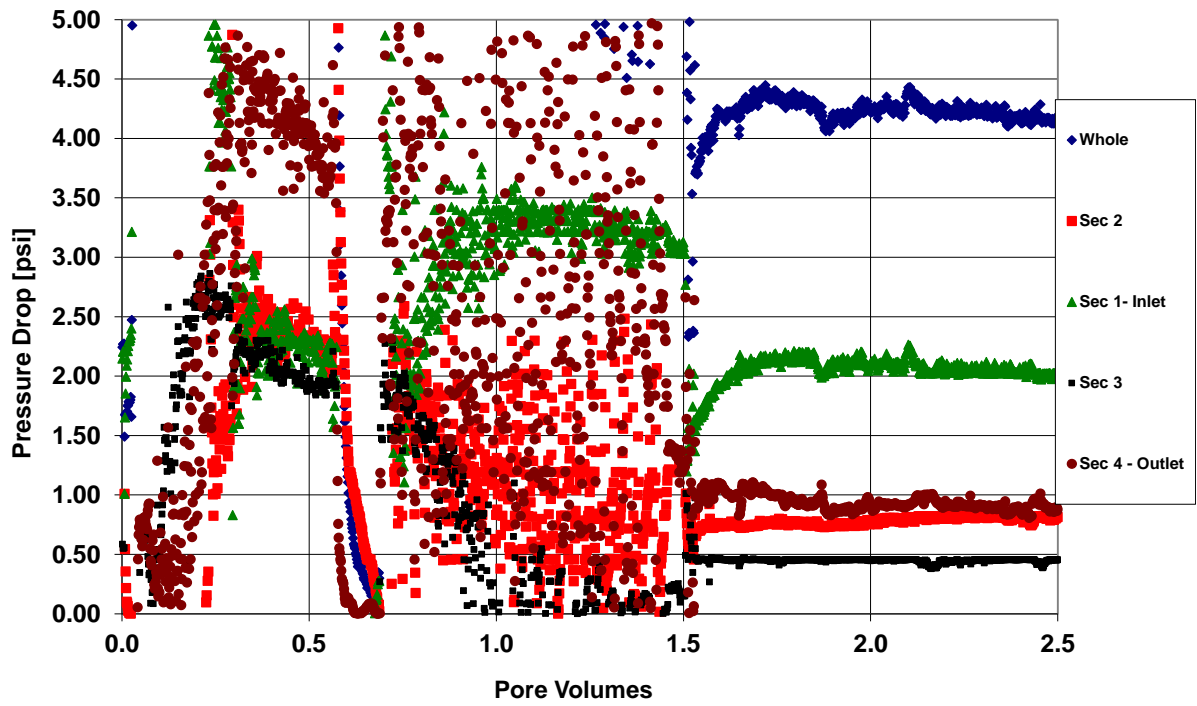
Figure 3.10: Pressure drop profile during chemical flood for U-02
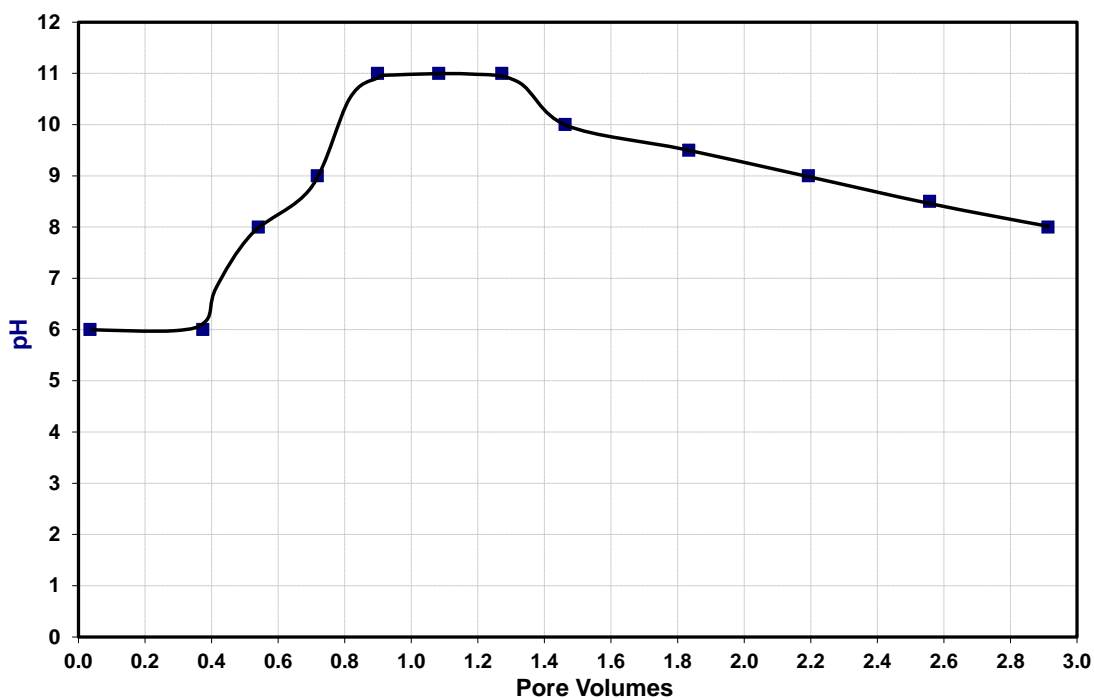
Figure 3.11: U-02 effluent pH

3.2.3 Conclusions on GAS Formulations

The advent of stabilizing ether sulfate surfactants at elevated temperatures was a significant invention, and it greatly increased the available surfactants that can be tested for a particular candidate. Even though the crude oil used in this is study has a low viscosity at the reservoir temperature of 100 C, it doesn't behave like typical light oil, but ratheran oil with high equivalent alkane carbon number. Therefore a very large hydrophobe surfactant was needed for this oil. Furthermore, the high temperature, high salinity with divalent cations severely restricted the choice of surfactants to be tested. Ether sulfonates will tolerate these harsh conditions, but the few ether sulfonates that are commercially available do not have sufficiently large hydrophobes for this oil and they are also too expensive. Guerbet alkoxy sulfates (GAS) can be manufactured at low cost

47

and satisfy the requirement for large hydrophobes, so their evaluation has opened up the opportunity to explore new reservoir candidates for chemical EOR under harsh conditions that would have otherwise not been considered.

3.3 GUERBET ALKOXY CARBOXYLATES

The introduction of large hydrophobe surfactants, Guerbet alkoxy sulfates (GAS) opened the world of chemical EOR for new reservoir candidates under harsh conditions. However, GAS require high pH (10-11) for chemical stability at high temperatures (>65 °C). Hence, alternative cost effective thermally and chemically stable anionic surfactant structures are highly desired, especially for applications under conditions where alkali usage is prohibitive. The Guerbet alkoxy carboxylates (GAC) meet these needs. The Guerbet reaction produces large, branched hydrophobes through the dimerization of linear alcohols. As with GAS, alkoxy groups like PO and EO are added as extenders. It is then followed by carboxymethylation to produce the carboxylate surfactants. Commercial Guerbet alcohols (ISOFOL) are alkoxylated at a commercial lab and then the carboxylation is done in the chemical EOR group at The University of Texas. They are both thermally and chemically stable with and without alkali. The initial evaluation of this new class of surfactants was reported in Dean (2011).

3.3.1 SP Formulations with Non-reactive Oil

Even though having sodium carbonate alkali in a surfactant formulation has many advantages such as in-situ generation of soap with active oils, reduced surfactant adsorption and stabilization of HPAM polymers and ether sulfates at elevated temperatures, there are some situations where alkali usage in the field is prohibitive. For example, when the target reservoir formation has anhydrite or gypsum in the pores of the rock, calcium dissolution occurs which results in the precipitation of calcium hydroxide

or carbonates depending on the type of alkali used and the pH. In such a case, efficient SP formulations have to be developed to meet the needs.

Phase Behavior Experiments

The experimental conditions are the same used for the GAS surfactants. The target reservoir is also the same as described in the previous section. The injection brine used was the synthetic sea water (SUTIB), and the produced brine used for core flooding experiments was SUTPB. The phase behavior scans are done at different dilutions of SUTIB and DI. The compositions of SUTIB and SUTPB are given in Table 3.1 and 3.2 respectively. Experiments were all conducted at 100 °C.

Experiments U-216 to 253 and U-266 to 321 (Appendix 1) were phase behavior and aqueous stability studies conducted using these new ether carboxylates. As understood from the previous experiments with ether sulfate surfactants, the target oil performs better when the formulations contain mixtures of C28 or C32 hydrophobes and internal olefin sulfonates (IOS).

One such high performance formulations identified was U-230, and it contained 0.5% C_{32}-7PO-32EO-carboxylate and 0.5% C_{19-23} IOS. The formulation was a simple two surfactant mixture containing no alcohol (co-solvent) or chelating agents like EDTA.4Na to sequester the divalent cations. The solubilization ratio plot for this formulation is shown in Figure 3.12. It has a solubilization ratio of 15 cc/cc at an optimal salinity around 35,000 ppm (60% SUTIB + 40% DI). The aqueous stability of the formulation was also studied, and a clear solution was observed until 42,000 ppm above which the solutions precipitated. Care should be taken that the surfactant solutions are neutralized before mixing them with the brine. The final pH of the aqueous solutions after mixing with the surfactants was close to 7.5. It has to be noted that the formulation has an optimum

solubilization ratio of 15 cc/cc even after nearly 300 days (Figure 3.12), indicating that the carboxylate surfactants are thermally and chemically stable. A picture of the phase behavior pipettes of U-230 (after 292 days) is shown in Figure 3.13. This formulation was used in U-04 core flood at 2% total surfactant concentration, the details of which will be discussed in the core flood section.

All the experiments discussed so far were conducted with U dead crude. It is well established that reservoir pressure and solution gas can significantly alter the microemulsion phase behavior, and thus cannot be ignored. However, doing these high pressure phase behavior and core flood experiments are often difficult and expensive. Therefore, the experiments are first conducted at ambient pressure by replacing the dead crude oil with "surrogate oil" accounting for the effect of solution gas.

The live oil EACN is determined by knowing the solution gas oil ratio (GOR, at current reservoir pressure), dead oil and gas molecular weight, dead oil EACN (determined experimentally by doing salinity scans with the surfactant formulation at various dilutions of dead crude oil and lighter hydrocarbon of known EACN). Once the EACN of the live oil is calculated, the surrogate crude is prepared to match the live oil EACN by mixing the dead crude oil and less volatile pure hydrocarbon of known EACN.

The procedure was carried out for U dead crude and the live oil EACN was calculated to be 6.9, which equates to 56.4 wt% U dead crude (EACN-11.4), and 45.4 wt% cyclohexane (EACN-4). Therefore, the experiments conducted with U surrogate crude contained 50 wt% dead crude and 50 wt% cyclohexane. The surrogate crude has a viscosity of ~0.5 cP at the reservoir temperature of 100 °C.

In order to match for the EACN for the surrogate crude, the formulation had to be changed to have the optimum salinity to be in the same range (35,000 to 40,000 ppm). When there is a decrease in the oil EACN, the optimal salinity also decreases (Cayias et

al., 1976; Glinsmann, 1979). Therefore, the HLB of the formulation has to be increased, to maintain the same optimal salinity window. It was decided to replace the C_{32}-7PO-32EO-carboxylate with a C_{28}-xPO-xEO-carboxylate, because of some impurity concerns in the C32 Guerbet alcohol. Also the C_{19-23} IOS was replaced by a more hydrophilic C_{15-18} IOS.

U-295 (b) was one such formulation containing 0.5% C_{28}-25PO-45EO-carboxylate, 0.5% C_{15-18} IOS which showed excellent phase behavior and aqueous stability. As mentioned before, the scan was a salinity scan at different dilutions of SUTIB and DI (from 30% SUTIB+70% DI to 100% SUTIB). Figure 3.14 shows the solubilization ratio plot for U-295 (b). The solubilization ratio was 20 cc/cc at an optimum salinity of 40,000 ppm (70% SUTIB + 30% DI). As before, the surfactant solutions are neutralized before mixing them with the brine. The aqueous pH was adjusted to 7 -7.5. This formulation had excellent aqueous stability and clear solution was observed at salinities as high as 60,000 ppm. The formulation was also tested at different surfactant concentrations to see the effect of surfactant concentration on the microemulsion phase behavior. U-298 and U-310 were conducted at 0.2% and 0.3% total surfactant concentration respectively, and visual observation of the samples (by observing the emulsion characteristics when the fluids are mixed to create an emulsion) indicated ultra-low IFT around the same salinity window (35,000 – 45,000 ppm) even at these low surfactant concentrations. The formulation at 0.3% surfactant concentration (U-310) was chosen for core floods U-06 (Estillades carbonate) and U-07 (U reservoir core composite).

Revisiting alkyl benzene sulfonates (ABS) as co-surfactants

In an attempt to find an alternative, less expensive surfactant formulation, a low molecular weight ABS surfactant (C_9-C_{12}) was tested. Some alkyl benzene sulfonates may be less expensive than some internal olefin sulfonates, and are readily available, since they are primarily detergent class surfactants. However, they may have less tolerance to salinity and divalent cations when compared to IOS. A new type of C_{11} linear ABS from Huntsman was used for evaluation in this study. Formulations were tested by replacing the IOS in the previous formulation (U-295 (b)). The ratio of carboxylate to ABS was changed to improve the aqueous stability and the phase behavior.

The formulation for U-311 contained 0.7% C_{28}-25PO-55EO-carboxylate, and 0.3% C_{11}-ABS. The solubilization ratio plot for U-311 is given in Figure 3.15. The formulation has a solubilization ratio of 20 cc/cc at an optimum salinity of 23,000 ppm (45% SUTIB + 55% DI). Clear aqueous solutions were also observed till 23,000 ppm. The aqueous stability samples were observed for more than 100 days at 100 °C, and still the same was observed, again indicating the thermal and chemical stability of alkoxy carboxylates. The aqueous stability samples picture is shown in Figure 3.16. It should be noted that the ABS by itself didn't have aqueous stability, as they have poor tolerance against divalent cations; but it's the synergy between the carboxylate and the ABS that improved the formulation.
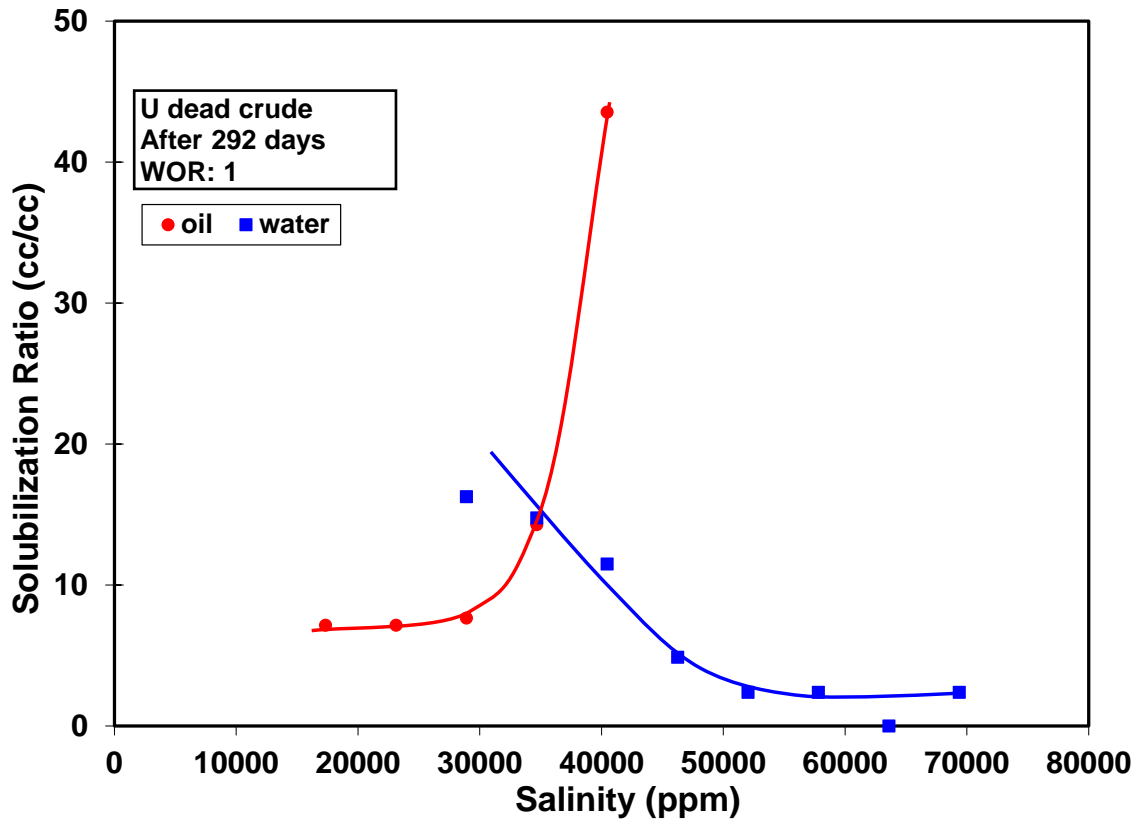
Figure 3.12: Solubilization ratio plot for U-230 (0.5% C_{32}-7PO-32EO-carboxylate, 0.5% C_{19-23} IOS, SUTIB scan) – used in U-04 core flood
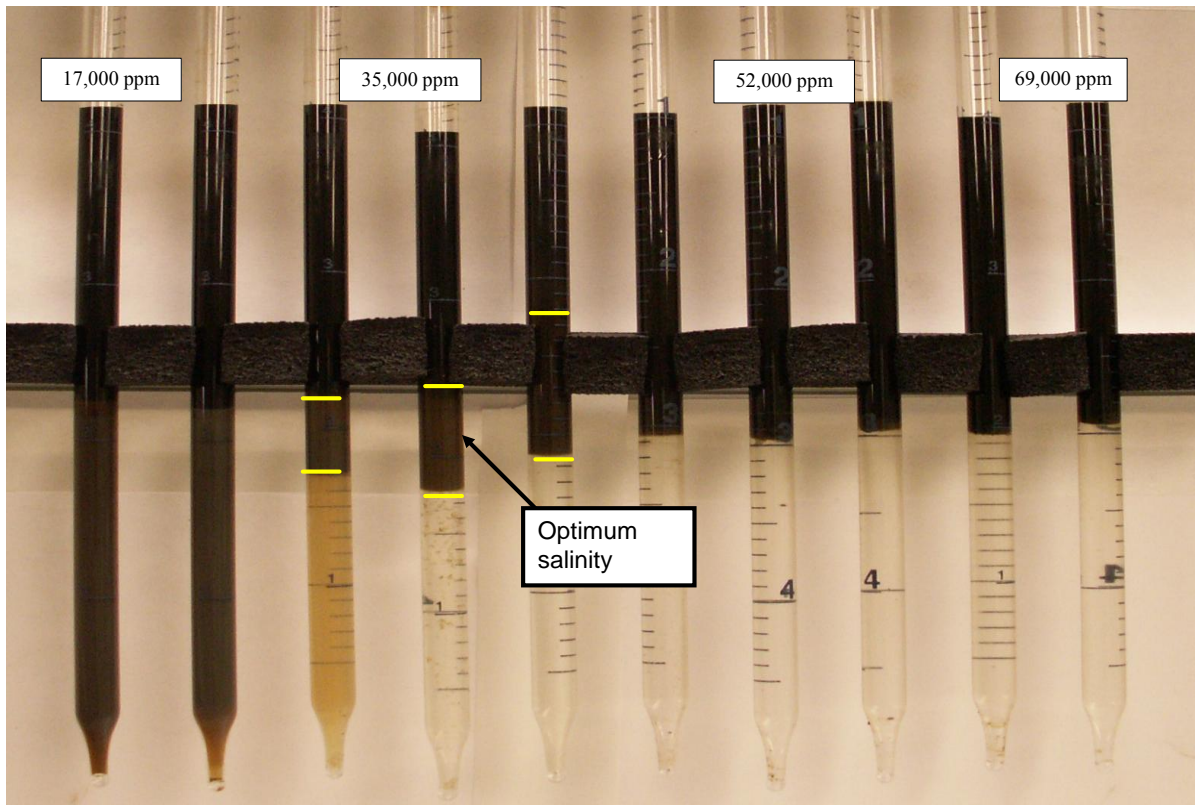
Figure 3.13: Phase behavior pipette picture of U-230 (after 292 days) – Stable microemulsion indicating the thermal and chemical stability of the surfactant formulation
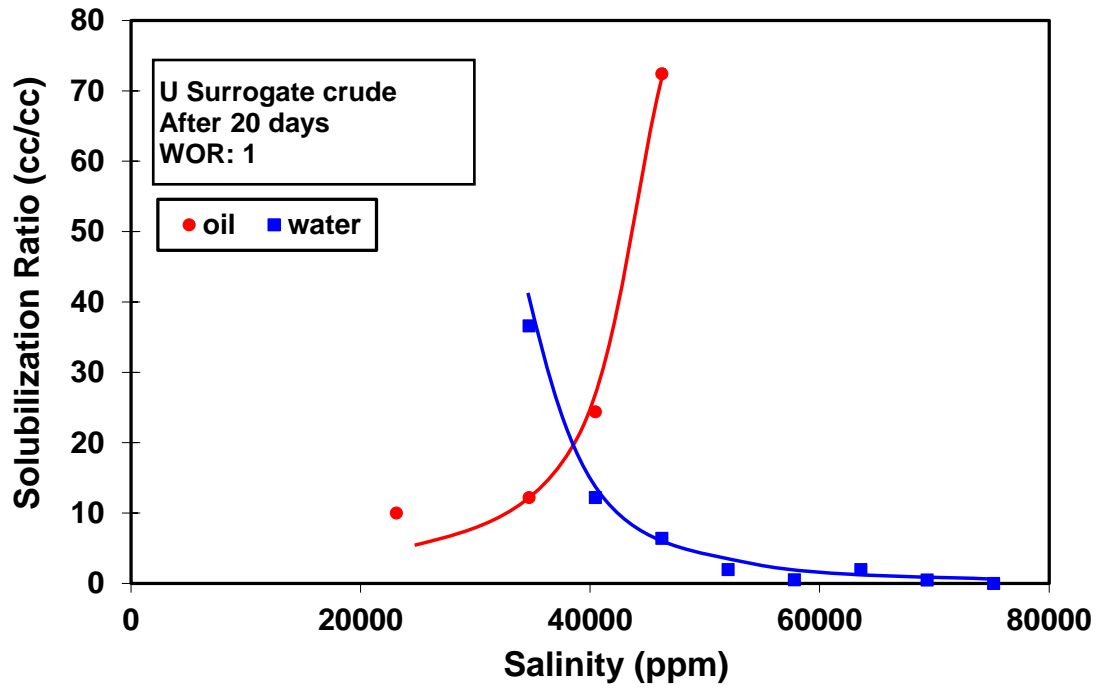
Figure 3.14: Solubilization ratio plot for U-295 (b) (0.5% C_{28}-25PO-45EO-carboxylate, 0.5% C_{15-18} IOS, SUTIB scan) – used in U-06 and 07 core floods
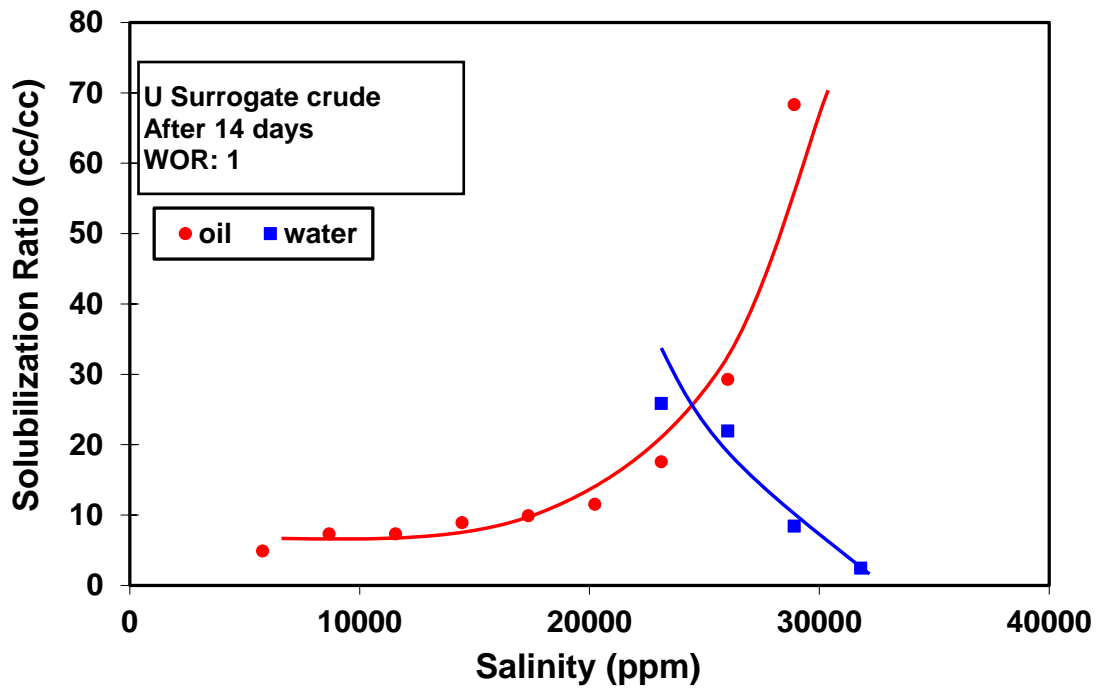
Figure 3.15: Solubilization ratio plot for U-311 (0.5% C_{28}-25PO-55EO-carboxylate, 0.5% C_{11} ABS, SUTIB scan)
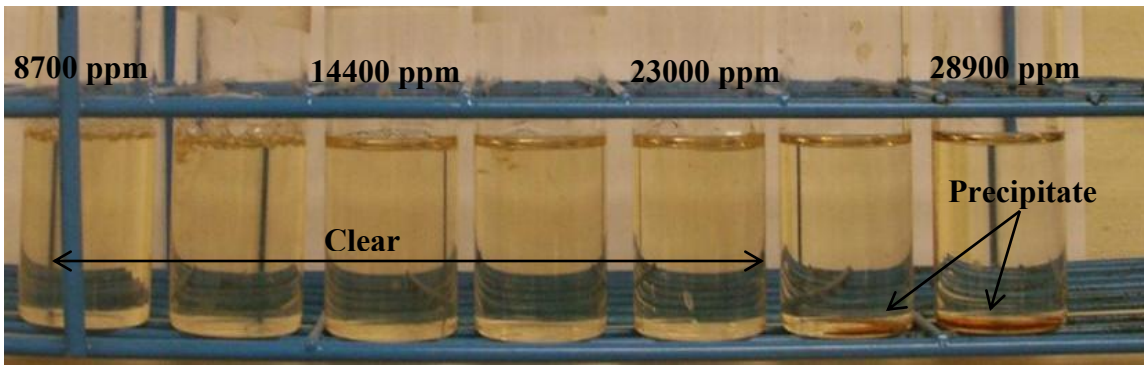
Figure 3.16: Aqueous stability samples for U-311 (0.5% C_{28}-25PO-55EO-carboxylate, 0.5% C_{11} ABS, SUTIB scan) – After 100 days at 100 °C

Core Flooding Experiments

The alkoxy carboxylates-IOS formulations performed extremely well in microemulsion phase behavior and aqueous stability studies and it was decided to test them in core flooding experiments to test the efficacy and robustness of the chemicals used. A formulation with dead oil (U-230) was tested in a Silurian dolomite outcrop (U-04), and a formulation with surrogate crude (U-310) was tested both in an Estillades carbonate (U-06) and reservoir core (U-07).

U-04 core flood

Figure 3.12 shows the solubilization ratio plot for U-230, a formulation containing C32 alkoxy carboxylate and C_{19-23} IOS. The phase behavior plot is given for 1% total surfactant concentration. However, it was decided to use more than the required amount of surfactant mass, 2% total surfactant for 0.25 PV (PV*C – 50), since it was one of the first core floods conducted with this new class of carboxylate surfactants. The core flood set up and experimental conditions are the same as explained in GAS section.

The core used was a Silurian dolomite of 2" in diameter and 12" in length. The core was loaded in a stainless steel core holder with a confining pressure of ~1000 psi. The core was then evacuated, and saturated with 0.25X SUTPB (Table 3.2). The approximate pore volume of the core was determined to be 100 mL in this step. Then the core was flooded with the same brine for several pore volumes, and it was displaced by 1X produced brine (SUTPB). The effluents were collected and analyzed for salinity. The normalized salinity was plotted against cumulative volume collected, and the pore volume was determined by finding the area above the curve. The pore volume was found to be 98 mL. The salinity gradient tracer test is shown in Figure 3.17. The long tail (nearly 3 PV) in reaching the target salinity indicates the heterogeneity (or dual porosity structure) of the core. The permeability to brine was determined to be 478 mD.

The core was then flooded with 0.45 micron filtered U dead crude at a constant injection pressure of 150 psi with a back pressure of 30 psi. The steady state pressure drop and flow rate was measured, and the permeability to oil was calculated to be 190 mD, equating to an end-point oil relative permeability, k_{ro}^o, of 0.40. By measuring the volume of brine collected in the effluent, the initial oil saturation was determined to be 0.73.

After the oil flood, the core was flooded with the produced brine (SUTPB) at 0.5 mL/min (7 ft/day) until no more oil was produced. By material balance, the residual oil saturation after water flood, S_{orw}, was found to be 0.45. The cumulative oil recovery to water flood was 37.8% of OOIP. The permeability to water was found to be 13 mD, equating to an end-point water relative permeability, k_{rw}^o, of 0.03.

With the core at residual oil saturation, the chemical flood was ready to begin. A 0.25 PV SP slug was injected at a frontal velocity of 2 ft/day followed by the PD at the same velocity. The composition of SP slug and PD is shown in Table 3.6.

SP Slug	Polymer drive
1.0% C_{32}-7PO-32EO Carboxylate	4500 ppm FP 3330s
1.0% C_{19-23} IOS	25,000 ppm (40% SUTIB + 60% DI)
4500 ppm FP 3330s	Frontal velocity: ~2 ft/day
40,000 ppm (70%SUTIB + 30% DI)	Viscosity ratio @ 10^{s-1}: 54
Frontal Velocity: ~2ft/day	
Viscosity ratio @ 10^{s-1}: 46	
PV of the slug: 0.25	
pH ~7.0	

Table 3.6: Composition of SP slug and PD used in U-04

The oil recovery during chemical flood is shown in Figure 3.18. The oil broke through at 0.3 PV at average oil cut of 50% from 0.3 PV to 0.8 PV. The core flood was successful with the cumulative oil recovery of 90.5% of the water flood residual oil saturation. The final oil saturation after the chemical flood was 0.044. This value was also verified by conducting a post chemical salinity tracer test.

The long tail in the oil production after 2 PV is probably another indication of the core heterogeneity. The pressure drop profile during the chemical flood is shown in Figure 3.19. It can be seen that the steady state pressure drop for this chemical flood was 1.5 psi/ft (at 2 ft/day frontal velocity). This low pressure drop even at this high viscosity is very favorable and is close to the reservoir pressure gradient. The effluent samples were analyzed for surfactant concentration, and the surfactant retention was calculated to be 0.33 mg/g of rock.

The purpose of U-06 core flood was to evaluate the performance of the formulation tested in U-04 core flood in dilute surfactant concentration (0.3 wt%). As explained in the phase behavior section, the dead crude oil was replaced by surrogate crude (blend of dead oil and less volatile, low molecular weight pure hydrocarbon), to match the EACN of live oil. Because of that, the formulation was changed to match the new EACN. The new formulation chosen was U-310 (0.3% total surfactant concentration) and slug size of 1 PV, equating to a PV*C value of 30.

The core used was an Estillades carbonate outcrop of 1.5" in diameter and 12" in length. The core was loaded in a stainless steel core holder with a confining pressure of 1000 psi. It was flooded with 0.25X SUTPB, followed by 1X SUTPB. As before, the pore volume was found by plotting normalized salinity against cumulative volume and it was found to be 92 mL. The salinity gradient tracer plot is shown in Figure 3.20. It can be seen that the core is much more uniform and homogeneous compared to the Silurian

dolomite used in the previous core flood. The permeability to brine was determined to be 187 mD.

The core was then flooded with 0.45 micron filtered U surrogate crude at a constant flow rate of 25 mL/min corresponding to a pressure drop of about 125 psi/ft. By measuring the volume of brine collected, the initial oil saturation was found to be only 0.43. This unusual low initial oil saturation was speculated as a reason of low viscosity of the surrogate crude (~0.5 cP @ 100 °C). It was then decided to do a second oil flood with increased pressure drop, so as to displace brine from smaller pore throats. The core was flooded again with U surrogate crude at an injection pressure of almost 250 psi. Still, negligible brine was only produced, and the oil saturation, S_{oi}, went up to 0.46 from 0.43. The permeability to brine was found to be 95 mD, equating to an end-point oil relative permeability, k_{ro}^{o}, of 0.51.

After the oil flood, the core was flooded with the produced brine (SUTPB) at 1 mL/min (15 ft/day) until no more oil was produced. The cumulative oil recovery to water flood was 62% of OOIP. The better performance of the water flood compared to the previous core floods could be because of the decreased viscosity for the surrogate crude. The permeability to water was found to be 26 mD, equating to an end-point water relative permeability, k_{rw}^{o}, of 0.14. The residual oil saturation after water flood, S_{orw}, was found to be 0.15.

With the core at residual oil saturation, the chemical flood was ready to begin. The SP slug was injected for 1 PV at a frontal velocity of 2 ft/day followed by the PD at the same velocity. The composition of SP slug and PD is shown in Table 3.7.

SP Slug	Polymer drive
0.15% C_{28}-25PO-45EO Carboxylate	4500 ppm FP 3330s
0.15% C_{15-18} IOS	20,000 ppm (35% SUTIB +65% DI)
4500 ppm FP 3330s 36,000 ppm (65% SUTIB + 35% DI) Frontal Velocity: ~2ft/day Viscosity ratio @ 10^{s-1}: 55 PV of the slug: 1.0 pH ~7.0	Frontal velocity: ~2 ft/day Viscosity ratio @ 10^{s-1}: 56

Table 3.7: Composition of SP slug and PD used in U-06

The oil recovery for U-06 is given in Figure 3.21. The oil broke thorough at ~0.5 PV with average oil cut of 30% from 0.5PV to 0.8 PV and decreased thereafter. The dilute surfactant slugs are always characterized by delayed oil breakthrough and low oil fractions. The delayed oil breakthrough could also be as a reason of low water flood residual oil to start with. The effect is explained in the next section with the help of fractional flow theory. The pressure drop profile during the chemical flood is given in Figure 3.22. The whole pressure drop was about 5.5 psi/ft at 2 ft/day frontal velocity, which is very favorable.

The core flood was very successful and it recovered nearly 95% of the water flood residual oil. The oil saturation after chemical flood, S_{orc}, was 0.008. The final oil saturation after chemical flood is a better indication of the success of the core flood than the percentage oil removed of the original oil or residual oil. From that stand point, this has been the most successful core flood despite a "dilute" surfactant slug being used.

Surfactant retention was also measured by measuring the surfactant concentrations in the effluent. Since the surfactants used in the formulation differ greatly in molecular size, the individual surfactant concentrations were also able to be identified.

The surfactant concentration was plotted against the PV, and is shown in Figure 3.23. The total surfactant retention was determined to be 0.34 mg/g-rock, with the individual contributions of 0.16 mg/g-rock (C_{15-18} IOS) and 0.18 mg/g-rock (C_{28}-25PO-45EO-carboxylate). From Figure 3.23, it can also be seen that the individual surfactants had transported together and no preferential adsorption or retention had occurred. The surfactant adsorption and retention will be discussed in detail in chapter 5.

U-07 Core Flood

The purpose of U-07 core flood was to mimic the U-06 core flood in U reservoir cores. The core composite was made from seven different cores (dia – 1.5 inches) of total length, 11.48 inches. The approximate permeability was measured using a mini permeameter, and the permeabilities of the individual core varied from 95 mD to 700 mD. The cores were arranged in such a way that we have high permeability both at the inlet and outlet and the medium permeability makes the middle section.

The core composite was loaded in a stainless steel core holder, and a confining pressure of 500 psi was applied. The core was evacuated and saturated with produced brine. As before, salinity gradient tracer test was conducted by displacing the 0.25X produced brine with 1X produced brine (SUTPB). The pore volume was found to be 61 mL. The steady state pressure drop was measured, and the permeability was determined to be 261 mD, with the permeabilities of individual sections being 292 mD, 156 mD, 292 mD, and 544 mD for sections 1, 2, 3, and 4 respectively (from inlet to outlet).

After the brine flood, the core was ready to be flooded with oil. Since the initial oil saturation in the previous core flood was low when flooded with surrogate crude oil (~0.5 cP), it was decided to displace the brine with dead crude (~2 cP), followed by surrogate crude miscibly displacing the dead crude. The first oil flood with the dead

crude was done at a constant volume of 30 mL/min corresponding to a pressure drop of about 250 psi/ft. The dead oil was then miscibly displaced with the surrogate crude. The effluent oil viscosity was measured at different times to ensure the dead oil was completely displaced. Even after following the above mentioned strategy, the initial oil saturation, S_{oi}, was measured to be only 0.46. The permeability to oil was found to be 136 mD, equating to an end-point oil relative permeability, k_{ro}^o, of 0.52.

After the oil flood, the core was flooded with the produced brine (SUTPB) at 0.5 mL/min (10 ft/day) until no more oil was produced. The cumulative oil recovery to water flood was 54% of OOIP. The permeability to water was found to be 28 mD, equating to an end-point water relative permeability, k_{rw}^o, of 0.11. The residual oil saturation after water flood, S_{orw}, was found to be 0.21.

With the core at residual oil saturation, it was ready to be injected with the chemical slug. The SP slug of 1 PV was injected at 1 ft/day, followed by polymer drive at the same velocity. The compositions of SP slug and PD are exactly the same as U-06 (the only change being the frontal velocity). Refer Table 3.7 for details.

The chemical flood oil recovery profile is shown in Figure 3.24. The oil recovery profile is similar to the U-06 chemical flood, except an earlier oil breakthrough and a longer tail, characterizing the core heterogeneity compared to the more uniform Estillades core used earlier. The cumulative oil recovery at the end of chemical flood was 72.3% of the water flood residual oil. The oil saturation after chemical flood, S_{orc}, was measured as 0.05. Since it was a reservoir core flood, the final oil saturation was again verified by conducting a salinity gradient tracer test (at the PD viscosity). The pressure drop profile during the chemical flood is shown in Figure 3.25. The pressure drop was only 1.5 psi/ft, which is very favorable and close to reservoir pressure gradient. The salinity gradient tracer test to verify the final oil saturation is shown in Figure 3.26.

As explained before, S_{orc} is a better indication of surfactant performance than percent oil recovery. A final oil saturation of 0.05 indicates the IFT was reduced to ultra-low values in the reservoir core at a low pressure gradient and thus validates the efficacy of the formulation.
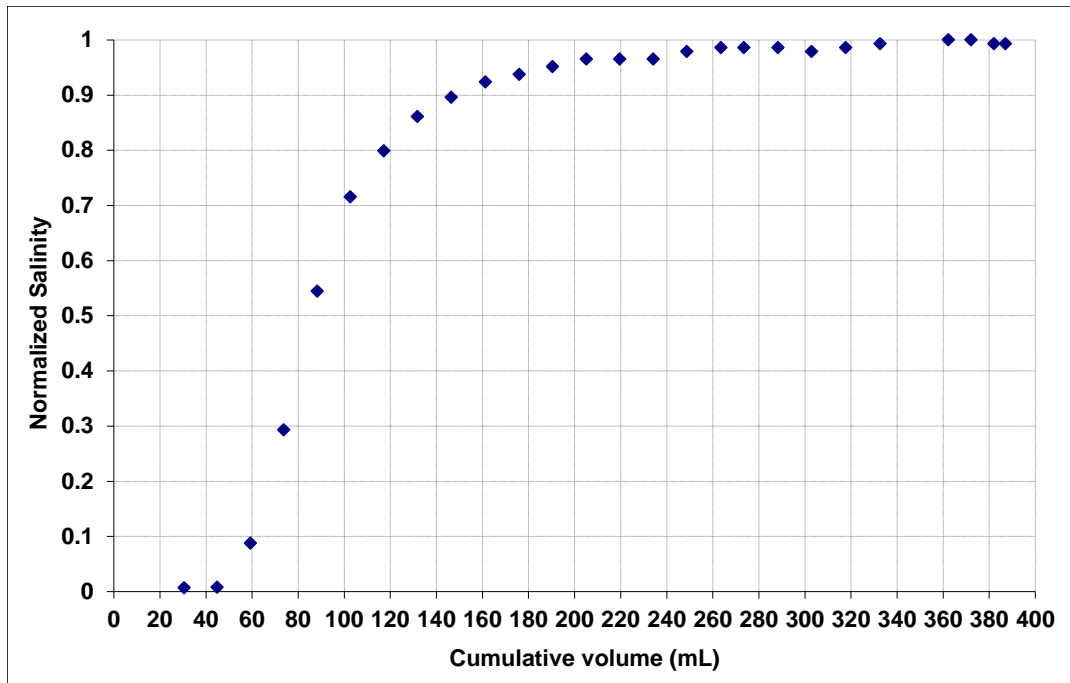
Figure 3.17: Salinity gradient tracer test for U-04 (Silurian dolomite; PV-98 mL) – Long tail indicating the heterogeneity of the core
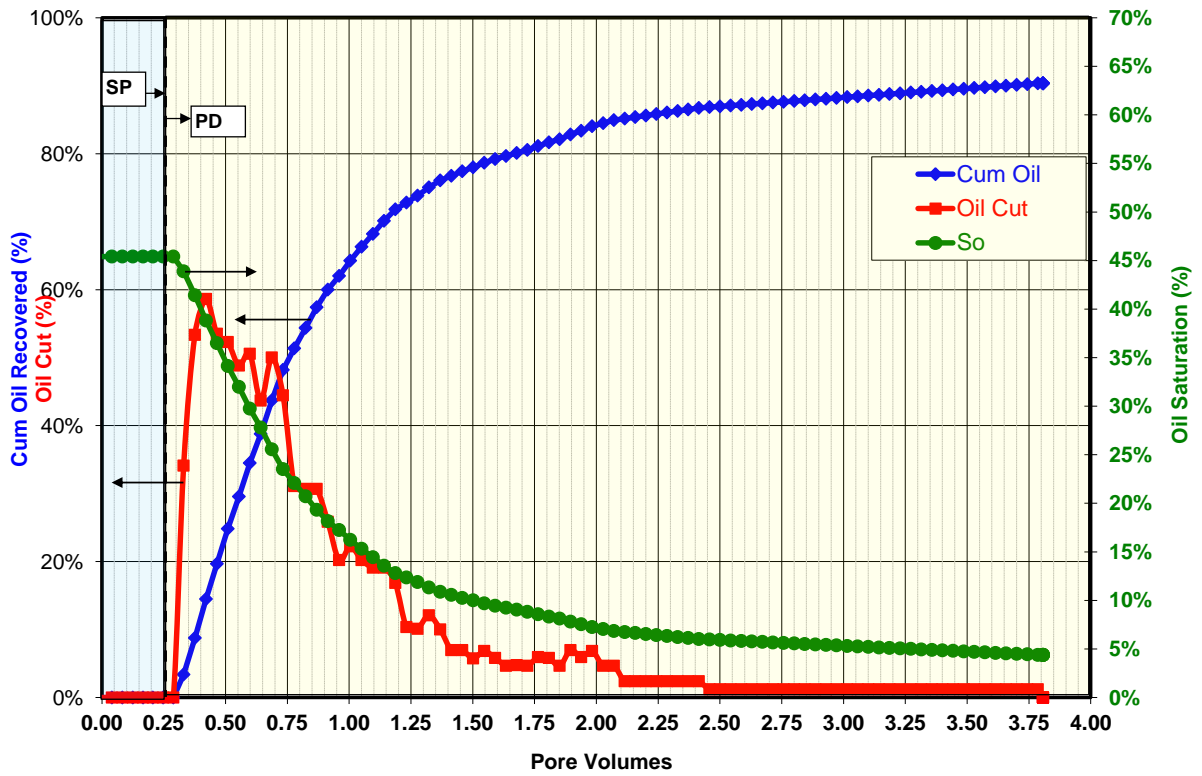
Figure 3.18: Oil recovery profile for U-04
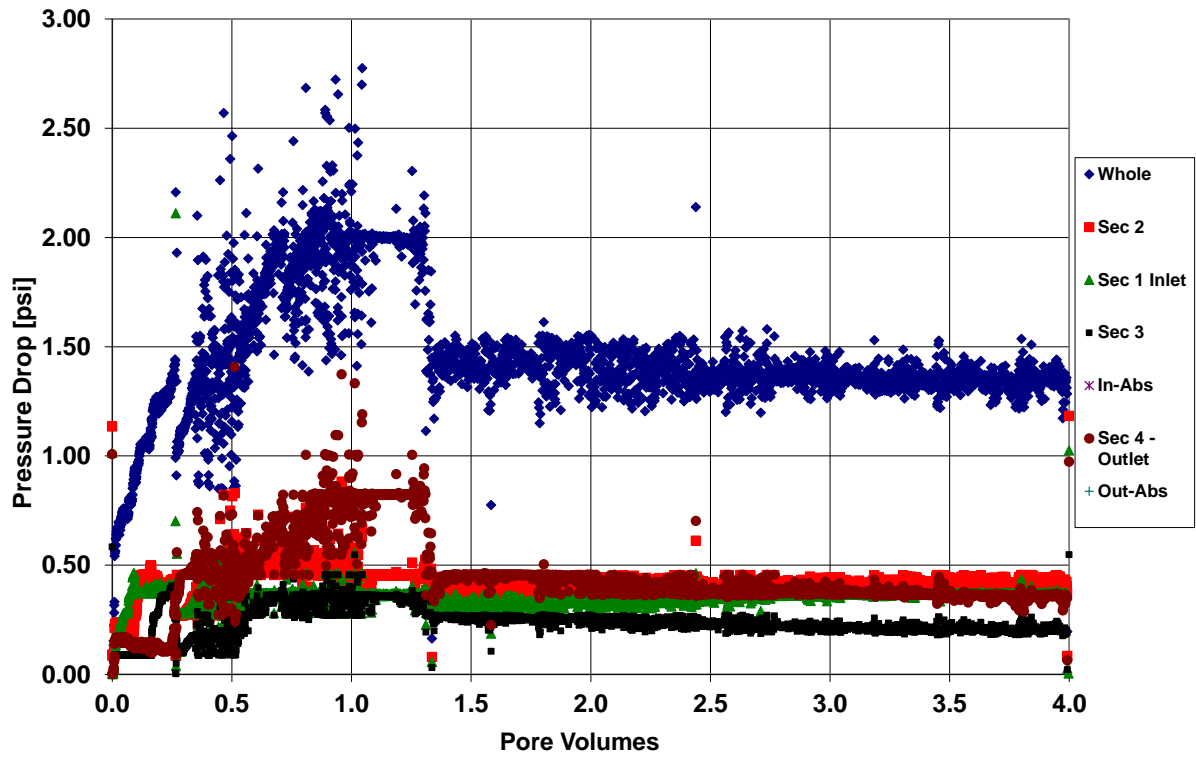
Figure 3.19: Pressure drop profile for U-04 chemical flood (2 ft/day) – pressure gradient close to the reservoir pressure gradient
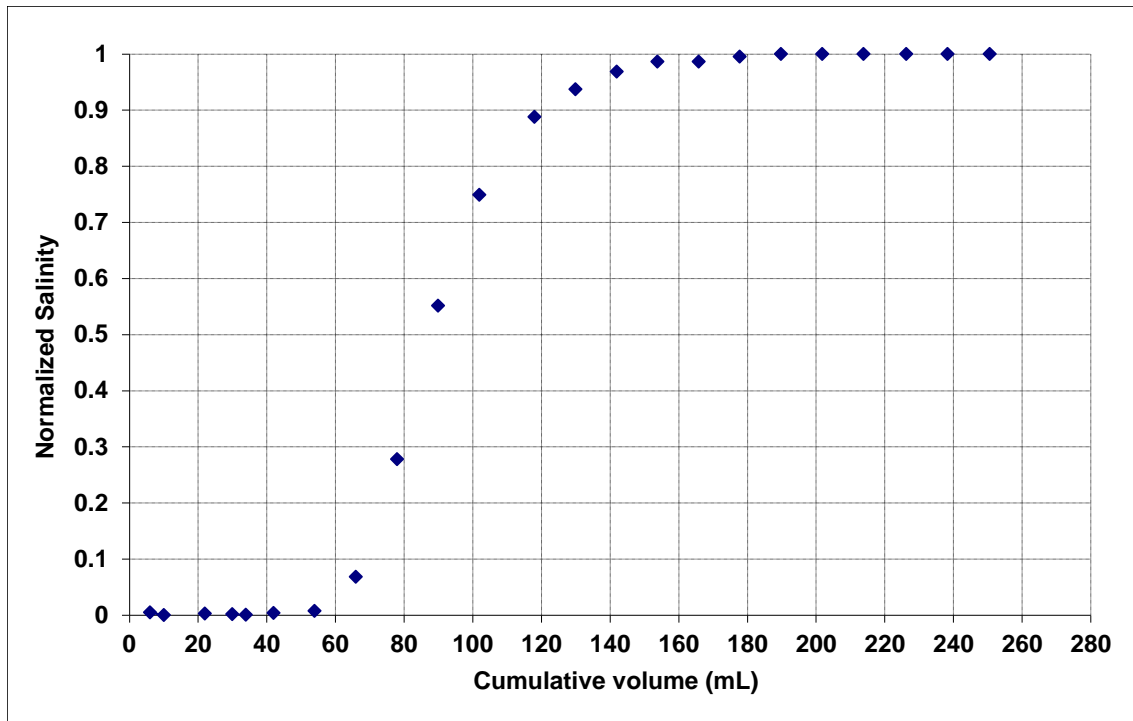
Figure 3.20: Salinity gradient tracer test for U-06 (Estillades carbonate; PV-92 mL) – More uniform and homogeneous core
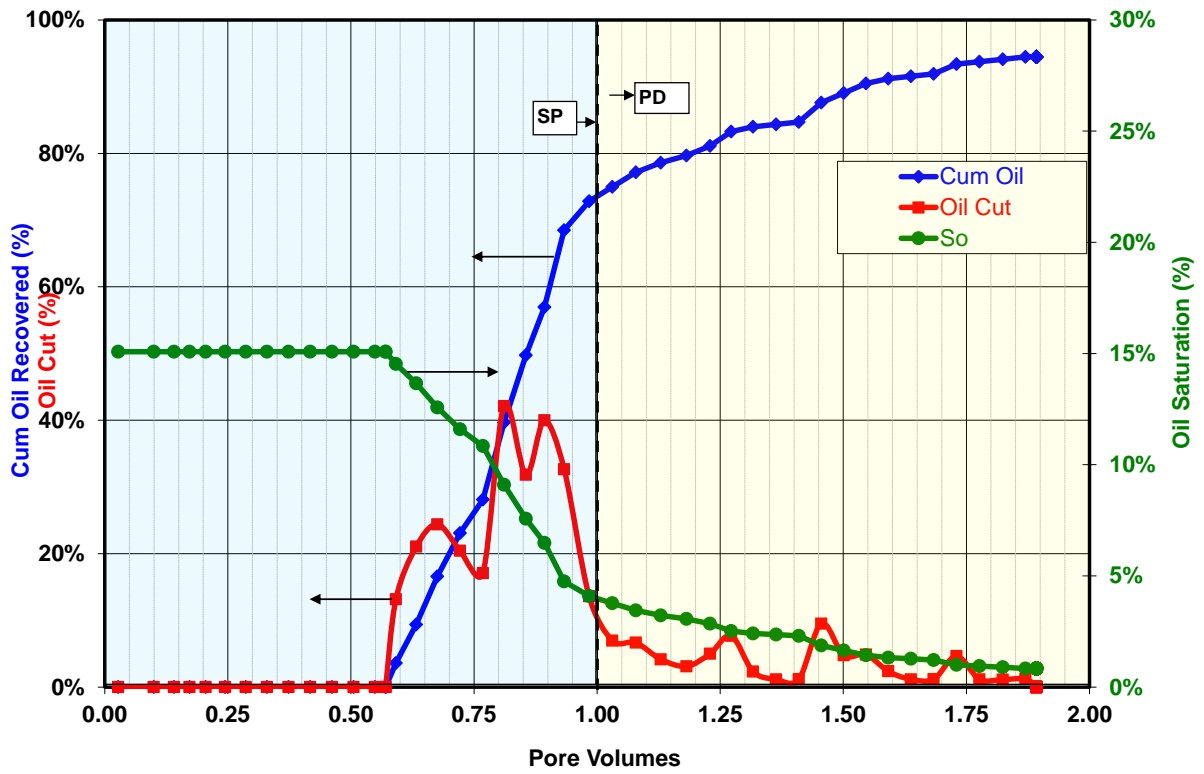
Figure 3.21: Oil recovery profile for U-06
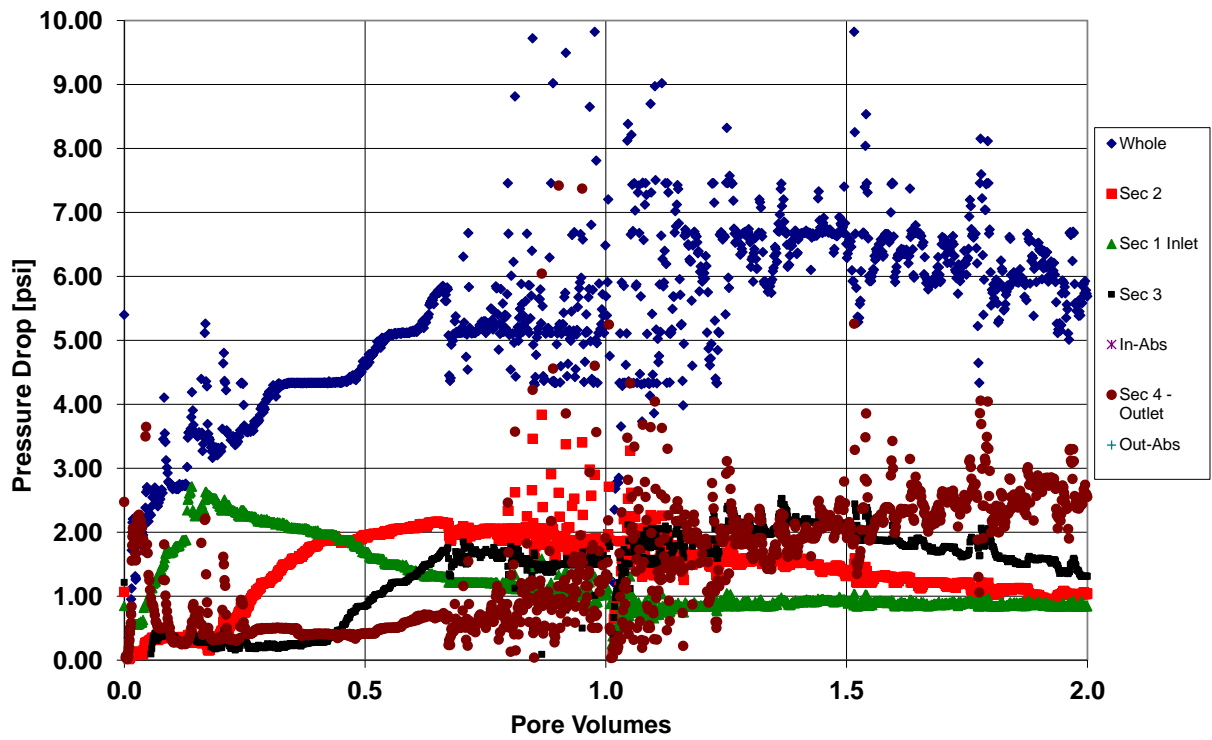
Figure 3.22: Pressure drop profile for U-06 chemical flood (2 ft/day)
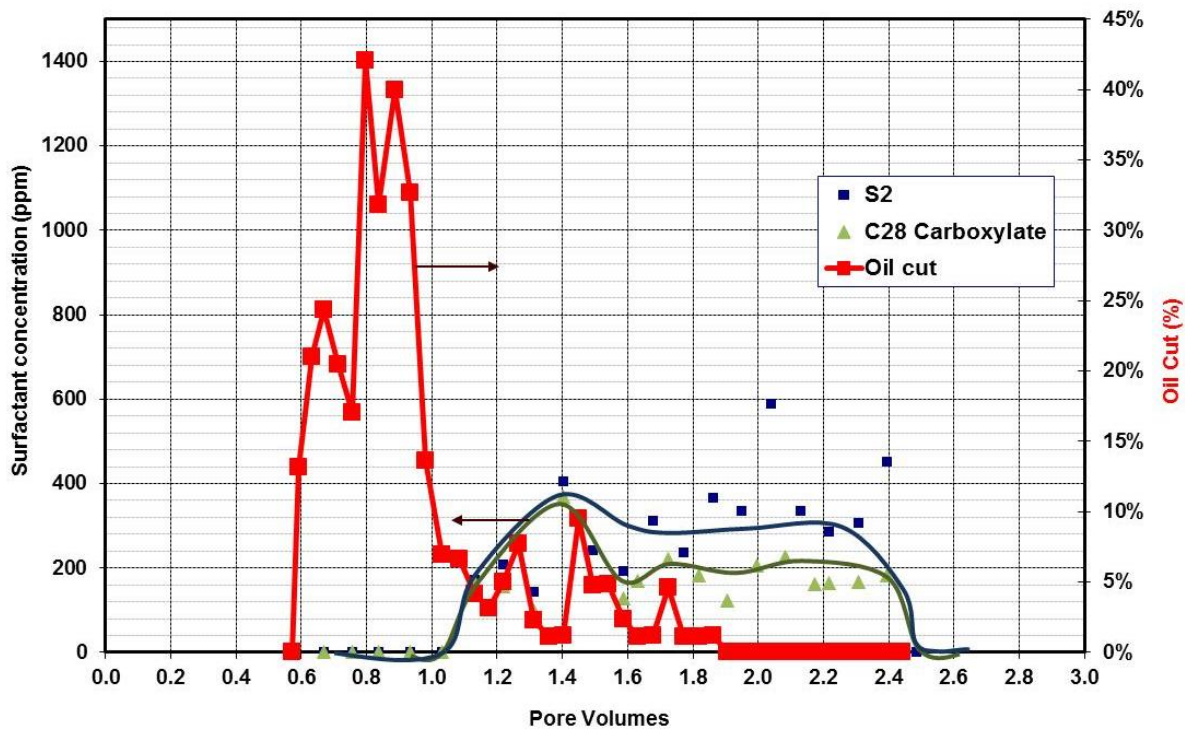
Figure 3.23: Surfactant concentration in the effluent for U-06 (surfactant retention – 0.34 mg/g-rock)
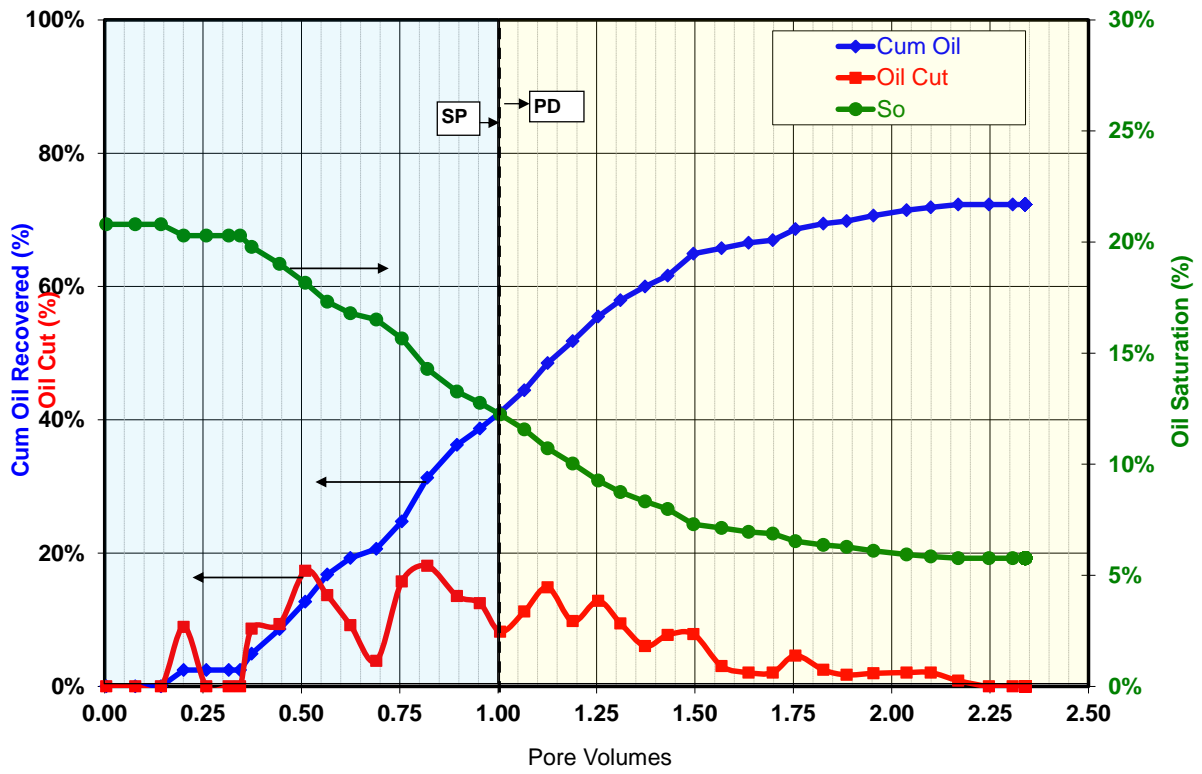
Figure 3.24: Oil recovery profile for U-07 (reservoir core flood)
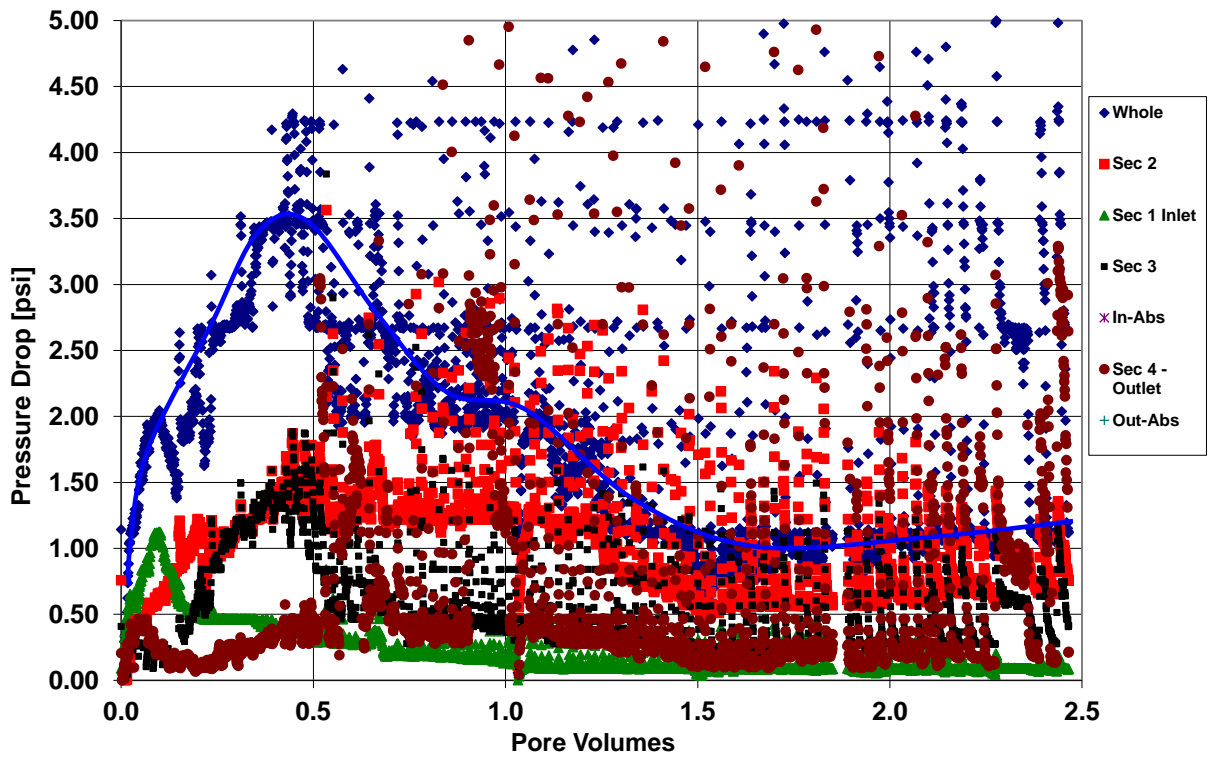
Figure 3.25: Pressure drop profile during chemical flood for U-07 (1 ft/day) – Low
pressure gradient close to reservoir pressure gradient
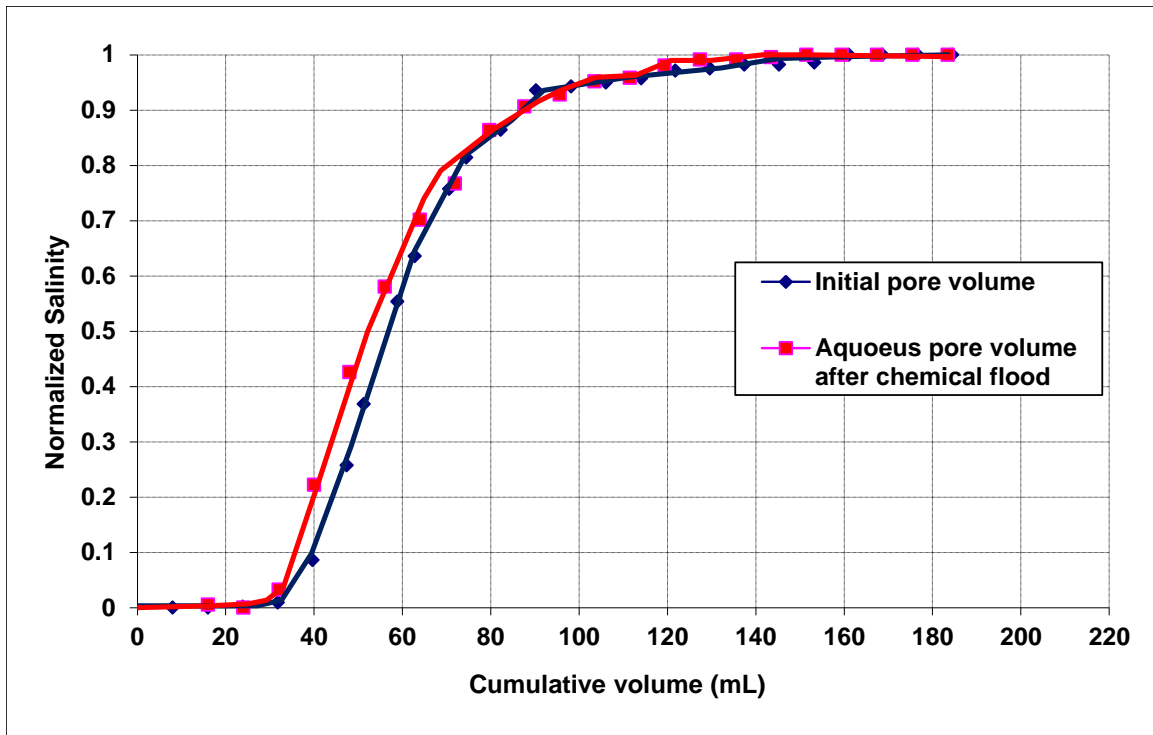
Figure 3.26: Salinity tracer test to verify residual oil saturation after chemical flood for U-07 (Actual PV – 61 mL)

Fractional Flow Analysis of Concentrated Surfactant Slug vs. Dilute Surfactant Slug (of Same Surfactant Mass)

For any chemical flood to be successful, sufficient surfactant mass in addition to satisfying surfactant adsorption has to be injected. This surfactant mass is a product of surfactant concentration (C) and the pore volumes (PV) of surfactant injected. This value of PV*C is an important parameter to compare core floods than just the surfactant concentration or the pore volume used. There has always been a debate on whether to use a smaller slug of high surfactant concentration or a larger slug of lower surfactant concentration. Even for the same value of PV*C, there are numerous advantages of using

73

a higher surfactant concentration than a dilute surfactant slug. The problem will be explained with the help of fractional flow theory.

The use of fractional flow analysis applied to enhanced oil recovery based on classical Buckley-Leverett theory was proposed by Pope (1980) among others before and since 1980. He extended the classical Buckley-Leveret theory in a unified way to polymer flooding, low-tension flooding, micellar-polymer flooding, miscible flooding and hot water flooding and first introduced solutions for three-phase immiscible flow in permeable media.

All the assumptions in extending fractional flow theory for EOR applies, and the additional assumptions considered for explaining this problem are (1) perfect surfactant (ultra-low IFT), (2) perfect mobility control.

Consider a surfactant solution of concentration, ω_s, is injected. If there is no adsorption, then the surfactant would breakthrough at exactly 1 PV, otherwise it is retarded by a factor, D_s, called the retardation factor. It is nothing but the amount of surfactant adsorption expressed in terms of pore volumes, and the surfactant front lags by this factor over what it would otherwise be. It is given by the expression,

$$D_s = \frac{(1-\varphi)\rho_g \widehat{\omega_s}}{\varphi \rho_s \omega_s} \qquad \text{--------------- (3.1)}$$

where, φ is porosity, ρ_g is the grain density (or matrix), ρ_s is density of the surfactant solution, $\widehat{\omega_s}$ is the adsorption of surfactant on stationary phase (rock) per unit mass of rock.

From the above equation it can be seen that for a fixed surfactant adsorption/retention value, as the surfactant concentration decreases the retardation factor also increases. This delayed retardation also delays the surfactant breakthrough, and thus the rate of oil production.

74

The water-oil fractional flow curve for the given parameters (Table 3.8) is shown in Figure 3.27. The oil breakthrough ($t_d^{b.t.o}$) during tertiary flood is found graphically by finding the inverse of the slope of the line drawn from S_{or} (water flood residual oil) to the point on water-oil curve (S_{ob}, f_{ob}) where the line from $-D_s$ to S_{orc} (by assumption (2) – at sufficiently high viscosity the tangent line will intersect the low-tension curve at or very close to $S_w = 1-S_{orc}$) meets. Mathematically it is given by the equation,

$$t_d^{b.t.o} = (S_{ob}-S_{or}) / (f_{ob}-0) \qquad \text{--------------- (3.2)}$$

$S_{wr} =$	0.27
$S_{or} =$	0.45
$k^\circ_{ro} =$	0.40
$k^\circ_{rw} =$	0.04
$\mu_w =$	0.3
$\mu_o =$	2.1
$m =$	2
$n =$	2

Table 3.8: Parameters used in drawing the water-oil fractional flow curve

It can be seen from Figure 3.27 that for a porosity of 0.25, grain density of 2.87 g/cc and surfactant retention of 0.3 mg/g-rock, the retardation of the surfactant for 2 wt% surfactant slug is 0.13, whereas for 0.2 wt% surfactant slug, it is 1.3. This also results in delayed oil breakthrough with lesser oil fraction in the oil bank. The cumulative oil recovery (N_{pd}) in terms of initial oil in place (OOIP) is given by the equation shown below.

$$N_{pd} = f_{ob}*(t_d-t_d^{b.t.o}); \qquad \text{for } t_d^{b.t.o}<t_d<t_d^{b.t.s} \qquad \text{------------- (3.3)}$$

The cumulative oil recovery curve for two cases is shown in Figure 3.28. It can be seen that the ultimate oil recovery for two cases are same (since same surfactant mass),

but the recovery rate is much lesser in dilute surfactant case than the concentrated surfactant of small slug size. The comparison for two cases is also given in Table 3.9.
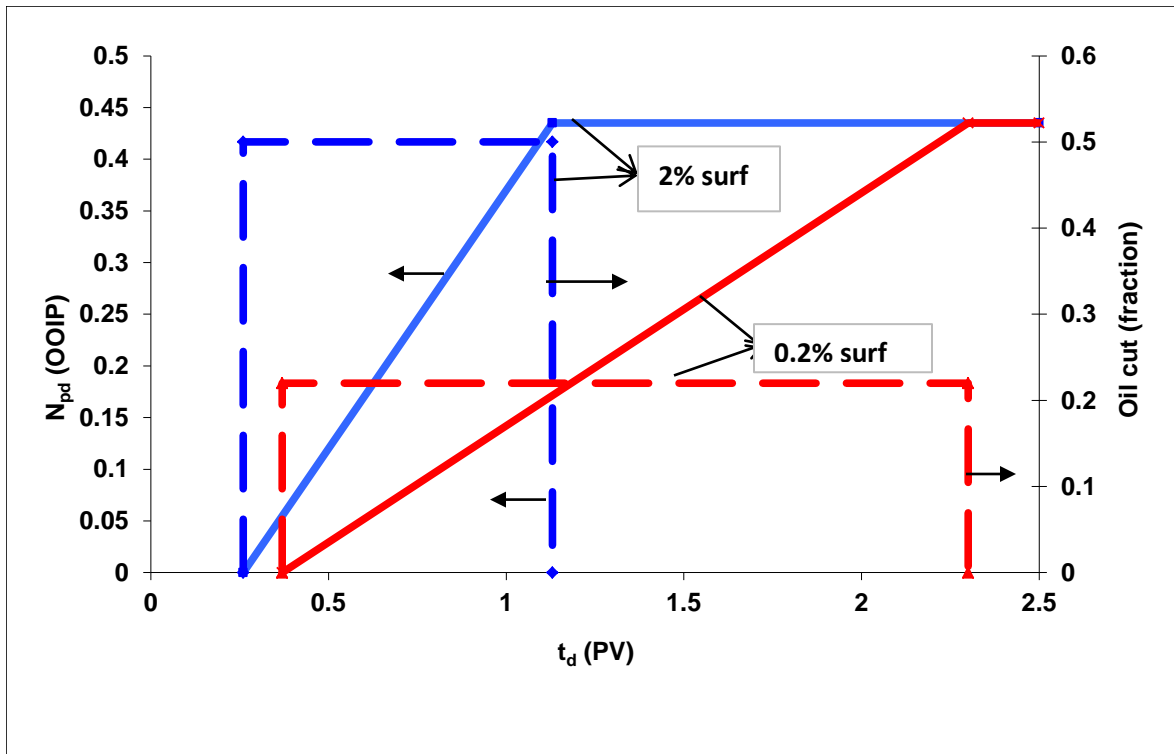
Figure 3.28: Oil recovery profile comparison for 2% surfactant slug and 0.2% surfactant slug

Experiment No.	Surfactant concentration (wt. fraction)	Surfactant retardation factor, D	Surfactant breakthrough time, 1+D	Oil cut (fraction)	Oil breakthrough time
Case (i)	0.02	0.13	1.13	0.5	0.26
Case (ii)	0.002	1.3	2.3	0.22	0.37

Table 3.9: Comparison of concentrated surfactant slug and dilute surfactant slug
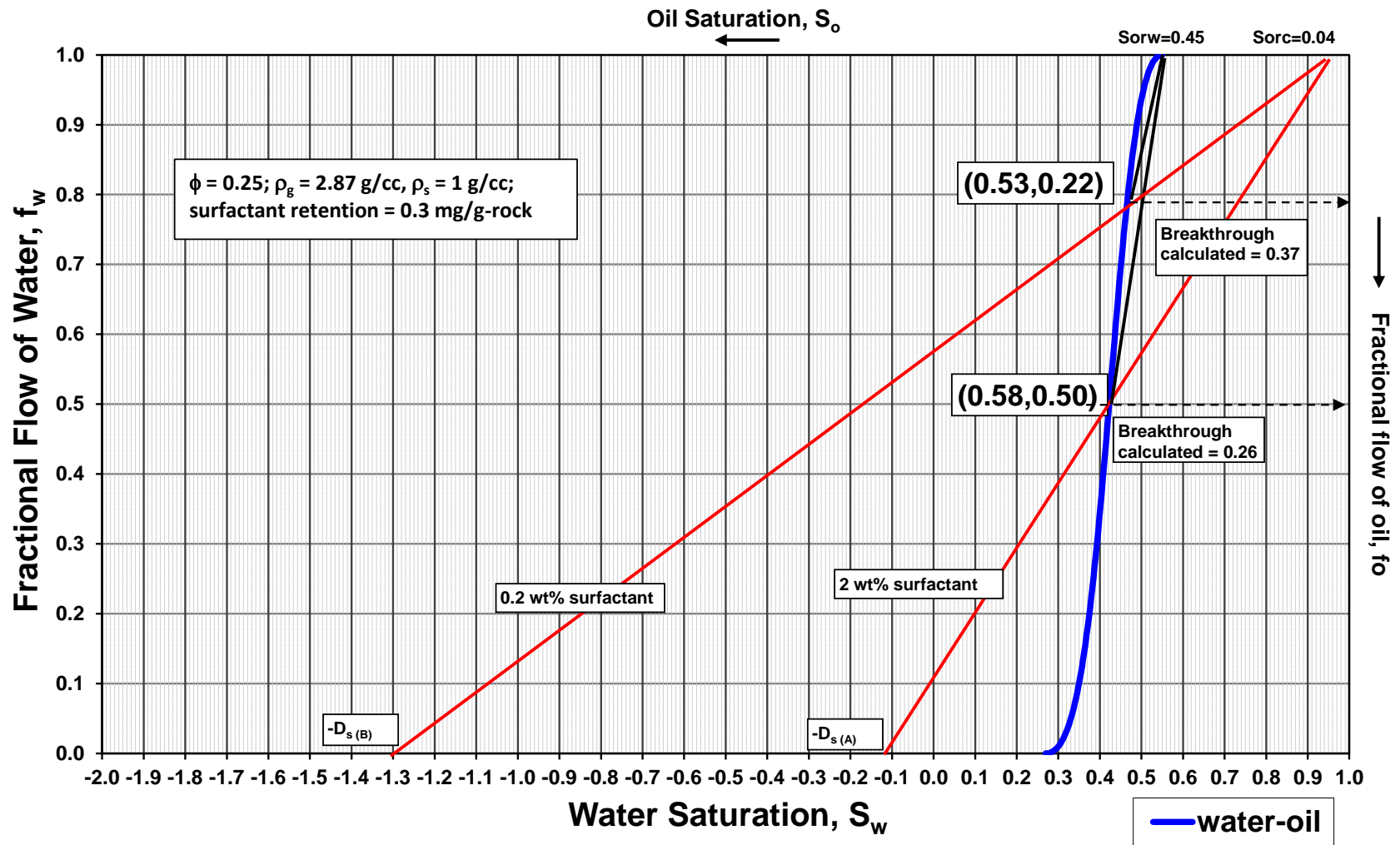
Figure 3.27: Fractional flow analysis for dilute surfactant slug vs. concentrated surfactant slug

Apart from the fact that the concentrated surfactant slug recovers oil at a much faster rate, there are other advantages to using it as against a dilute slug. As explained before, salinity gradient is an important aspect determining the success of the chemical flood. A smaller slug is easier in the design of salinity gradient, and when followed by a polymer drive of lesser salinity, the surfactant re-dissolves into the aqueous phase, thus reducing the surfactant retention also.

3.3.2 SP Formulation with Reactive Oils

The carboxylate surfactants, because of their high performance even in difficult conditions (high temperature, high salinity, divalent cations), were tested for different reservoir conditions with varied oils including some reactive oils. An interesting observation was found when these carboxylate formulations were tested for reactive oils (oils which react with alkali to produce soap). Even though the experiments were conducted at neutral pH condition, some crude oils showed reactivity (activity), i.e., change in optimal salinity with change in oil concentration (because of change in ratio of soap to surfactant). Also in some cases, even if there was not much of a change in optimal salinity with oil concentration, the microemulsion phase behavior itself changed dramatically with time, like for example shift from type I to type II with increased mixing (agitation). This suggested that there is some kind of mobilization of surfactant from oil, but as mentioned earlier there was no alkali added (neutral pH) to induce soap generation. This implies that the carboxylate surfactants help in mobilizing some organic acids (naphthenic acids) in the crude oil to the interface thereby giving more surface activity in addition to the synthetic surfactants added. This surprise finding stimulated further interest in an already exciting technology of carboxylate surfactants, and it becomes worthwhile to study the underlying mechanism and/or to develop an analytical technique

to qualitatively/quantitatively analyze the mobilization of naphthenic acids in the crude oil.

Experimental Observations

Dean (2011) reported one such carboxylate formulations with reactive oil. Field C is a low temperature (30 °C) sandstone reservoir with viscous (80 cP), reactive oil (TAN~1.8 mg KOH/g oil. The oil has an API gravity of 19. The reported formulation consisted of 0.25% C_{28}-25PO-15EO-carboxylate, 0.15% C_{15-18} IOS, and 0.10% C_{20-24} IOS mixed in synthetic brine. The total salinity of the brine is 18,000 ppm containing about 950 ppm of Ca^{2+} and Mg^{2+}. The scan variable in phase behavior experiment is NaCl. Figure 3.28 (from Dean, 2011) shows the activity plot (change in water oil ratio) for the above mentioned surfactant formulation with Field C oil. The abscissa is given as C_{oil}/C_{surf} which in other words is equivalent to the ratio of soap to surfactant. It can be seen from the figure that the optimal salinity for 50% oil (WOR-1), is 18,300 ppm, whereas for 10% oil (WOR-9), it is 73,000 ppm. This significant increase in optimal salinity with decreased oil concentration clearly indicates that a soap which is more hydrophobic than the synthetic surfactant added is being produced (notice no alkali added).

For this particular case, the low temperature combined with high viscosity, resulted in slow equilibration time for microemulsion phase behavior (in tubes). In order to increase the kinetics, the samples were moved to elevated temperature (80-100 °C) for a short period (typically overnight) and then brought back to the original temperature. The increased temperature drives the surfactant to the oleic phase (shift in phase behavior from type I to type II), resulting in rapid microemulsion formation (hypothesis presented later) in this neutral pH condition.

The second example, Field L is also a sandstone reservoir of temperature, 55 °C, with viscous (75 cP), reactive oil (TAN-2 mg KOH/g oil) of API gravity 18.8°. The surfactant formulation consisted of 0.25% C_{28}-25PO-15EO-carboxylate, 0.15% C_{15-18} IOS, and 0.10% C_{20-24} IOS. As before, the scan variable is NaCl on top of synthetic brine of 26,000 ppm TDS (~1200 ppm Ca^{2+} and Mg^{2+}). The activity plot for this formulation is shown in Figure 3.29. It can be seen that the optimal salinity for 50% oil (WOR-1) is about 55,000 ppm, and for 10% oil, the optimal salinity is 77,000 ppm. Again, the production of soap is the only way by which this phenomenon can be explained. The change in optimal salinity with soap/surfactant ratio (the slope of the optimal salinity line) is not as steep as the previous example. This could be probably because of the lesser difference in optimal salinity of the natural soap and synthetic surfactant in this particular case.

The third case, Field Y, is a moderately reactive (TAN ~0.8-1.0 mg KOH/g oil), slightly viscous (20 cP) crude oil. The reservoir temperature is 21 °C, but the experiments were conducted at 30 °C. The formulation consisted of 0.25% C_{24}-25PO-18EO-carboxylate, 0.25% C_{12} ABS, 0.25% C_{13}-13PO-sulfate, and 0.25% TEGBE. The activity map for this formulation is shown in Figure 3.30. Again it can be seen that there is a shift in optimum salinity from 44,000 ppm to 54,000 ppm for change in oil concentration from 50% (WOR-1) to 10% (WOR-9).
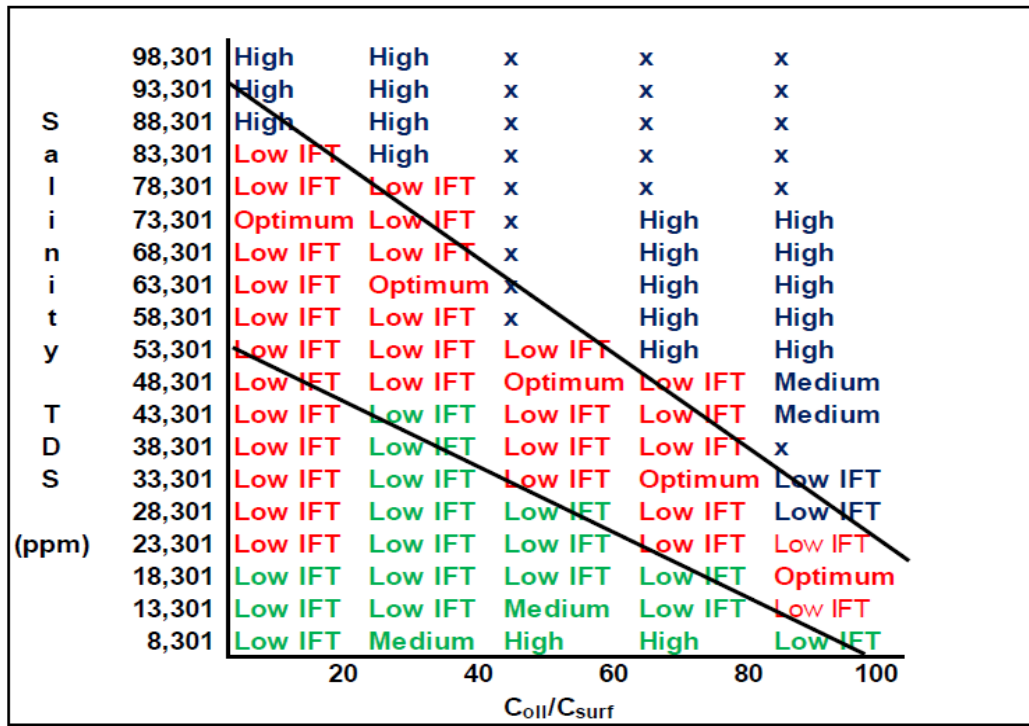
Figure 3.28: Activity plot for Field C oil with carboxylate formulation (Source: *Dean, 2011*)
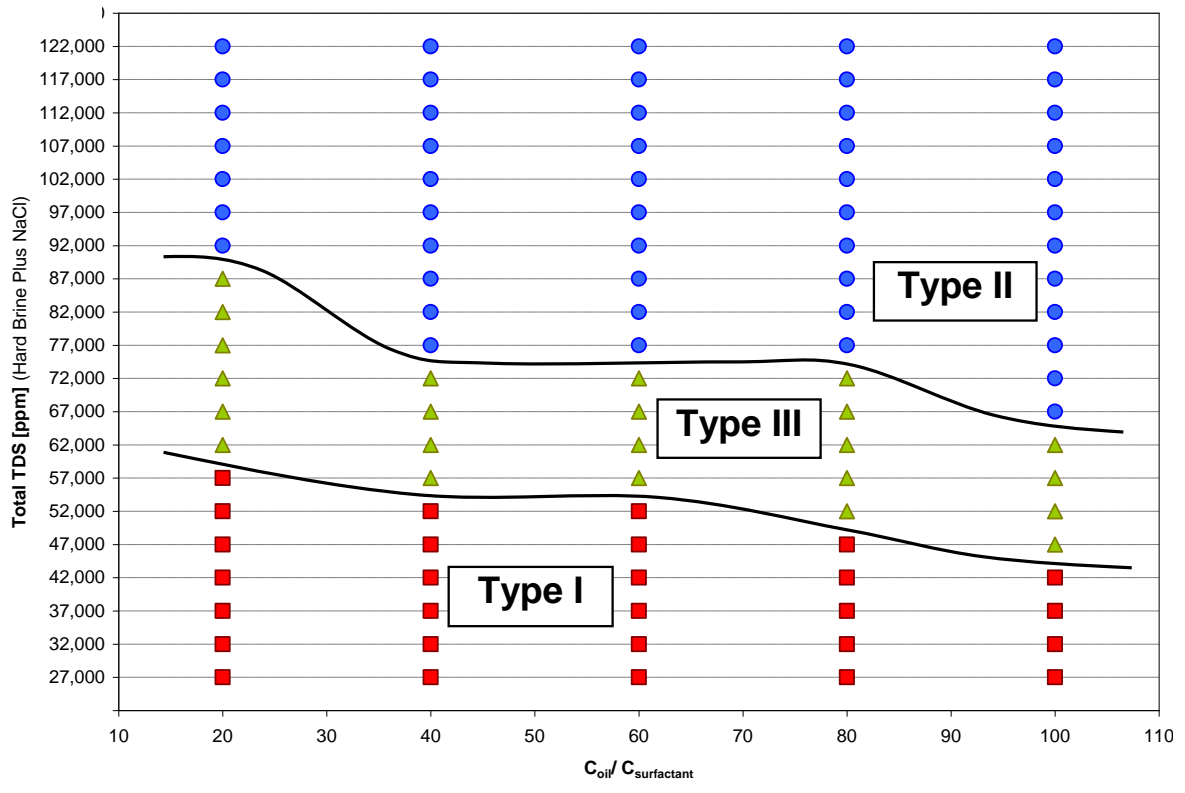
Figure 3.29: Activity plot for Field L oil with carboxylate formulation
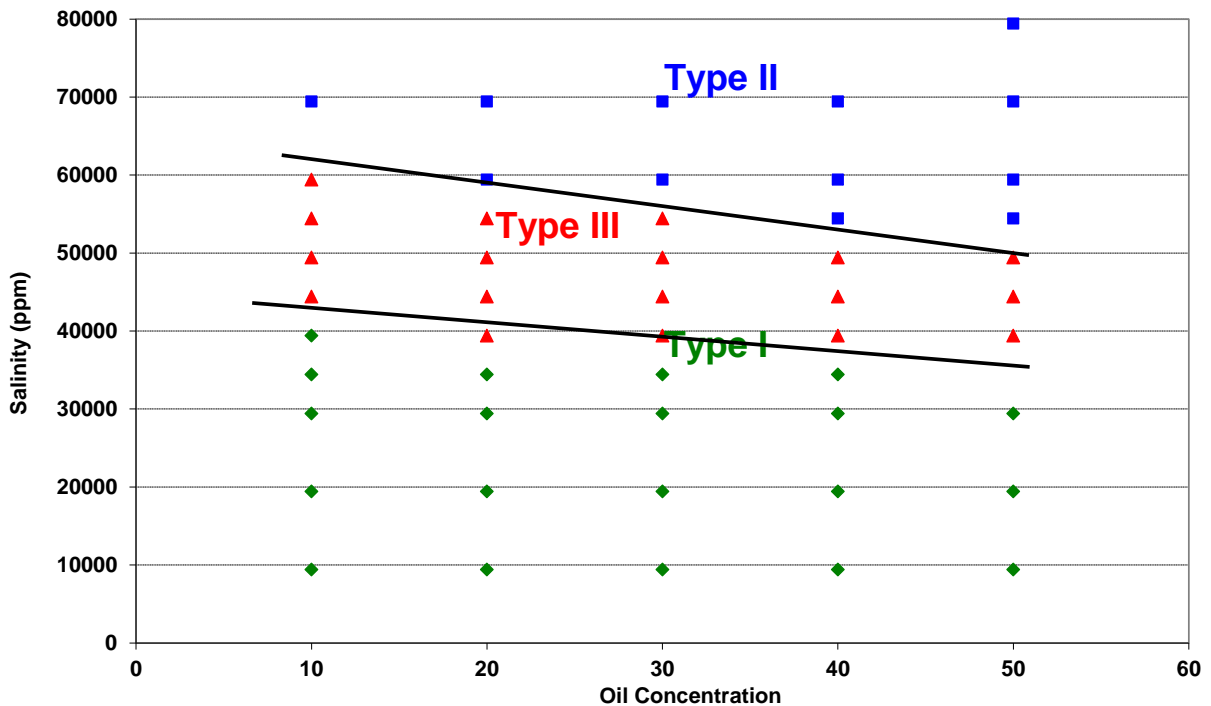
Figure 3.30: Activity plot for Field Y oil with carboxylate formulation

Hypothesis for Soap Formation

So, how do we see this effect of "soap" generation without alkali being added? What's special in these carboxylate surfactants that are not there in sulfates or sulfonates? In an attempt to answer these questions, the following hypothesis can be proposed. Figure 3.31 shows a pictorial representation of the interaction between naphthenic acids (in the oil phase) and carboxylate surfactants compared to the interaction between the naphthenic acids and sulfate or sulfonate surfactants. The carboxylate group in the carboxylate surfactant is "similar" to the carboxylic acid groups in crude oil; hence a strong interaction between the two is plausible, whereas the sulfate or sulfonate groups are "less similar".

83
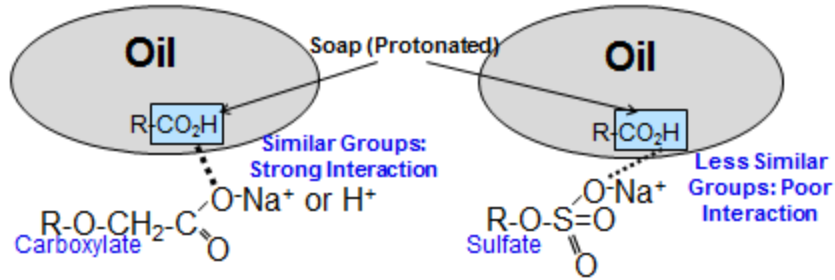
Figure 3.31: Schematic of the interaction between carboxylate group in the surfactant with the protonated soap (naphthenic acids) in crude oil

Analytical Methods

The experimental results shown above clearly indicate that the carboxylate surfactants help in formation of soap (or something that behaves like soap mixed with the synthetic surfactants), which acts in synergy with the synthetic surfactant added. Hence it was decided to develop an analytical method that can serve as a tool for validating the postulation.

TAN Approach

As per the postulation that there is a mobilization of organic acids, there should be a change in total acid concentration between the actual crude oil and the equilibrated oil phase in the phase behavior. This change in organic acid concentration would also reflect in the change in TAN (total acid number).

Even though there is a strong correlation between the concentration of carboxylic acid fraction and TAN (Meredith et al., 2000), the reader should be cautioned that TAN is an average value arising from all the acidic components in the crude oil (sulfur content, CO_2, phenols, etc.) and not just naphthenic acids, which are responsible for the soap generation. Figure 3.32 (data from Meredith et al., 2000) shows the plot of naphthenic acid concentration (obtained by various analytical techniques such as gas

chromatography and gas chromatography mass spectroscopy) against TAN values (from direct analysis of the samples and assay reports). The straight line in the graph is the expected TAN value calculated, assuming that the TAN was controlled by its carboxylic acid content alone. It can be clearly seen that the predicted TAN values are lesser than the actual reported TAN, indicating that they are more complex functions depending on various parameters like the sulfur content of the oil, degree of biodegradation, etc. As per the predicted values, the contribution of acids to TAN varies from as low as 10% to 65%. That implies, for any given oil, even if there's a change in acid concentration due to any mobilization of acids (as per the postulation), there may or may not be an equivalent change in the TAN value. Regardless of these uncertainties, the TAN approach should serve as a valuable tool in explaining the crux of the problem. Therefore, the first analytical technique tried to validate the postulation was TAN method.

The method is nothing but measuring the change in acid number between the actual crude oil (initial oil before mixing with surfactant solution for phase behavior experiment) and the equilibrated oil from phase behavior experiment (excess oil phase, typically from type III salinities, sometimes from type I). Most of the TAN measurements were potentiometric titration (commercial lab), and some of the measurements were aqueous titrations (conducted at UT Austin).

The summary of TAN results for the original oil and the excess oil for different fields is given in Table 3.10. The samples are selected to represent wide variety of oils, highly reactive, moderately reactive, less or non-reactive, and simulated reactive oil (dodecane + pure naphthenic acid). Some of the oil samples (Field L, OB) showed a significant decrease in acid number after the interaction with the aqueous solution (carboxylate surfactant solution), but, when repeated for several trials, the same trend was

not observed. In short, the results are all over the place, and even the few samples that were repeated did not yield consistent results.

One of the reasons for the discrepancy in the results could be partly due to the complex correlation between the naphthenic acid concentration and TAN for a given crude oil. Also the difficulty in getting a consistent result indicates some probable differences in the sampling procedure, assuming the measurement was correct. When the equilibrated excess oil from phase behavior was sampled, to the possible extent, care was taken not to disturb the interface (containing oil-brine-surfactant) which would otherwise create a noise in the TAN measurement. Moreover, the naphthenic acid by definition encompasses all organic acids in the crude oil containing carboxylic group, and the molecular weight of these acids varies from 200 to 1200 Dalton (Shepherd, 2008). Therefore, the structure of soap produced depends mainly on the distribution of acids in crude oil, rather than the total concentration of acids, which is an indicator of TAN. Therefore, a method that can identify the individual acids has to be developed. Electrospray ionization (ES) combined with mass spectroscopy (MS) can be a useful tool in quantifying the acids, and this has been proposed as a recommendation for future work.

3.3.3 Conclusions on GAC Formulations

Thermally and chemically stable, new class of surfactants has been identified and evaluated. Formulations containing GAC surfactants produced ultra-low interfacial tensions and core flood experiments produced high oil recoveries with residual oil saturation as low as 1%. Surfactant retention measurement for a mixture of long hydrophobe carboxylate and IOS showed no preferential retention or chromatographic separation. Additional benefits have been observed when GAC surfactants were tested

with reactive oils. For the first time, oil activity (soap generation) has been observed at neutral pH conditions also. Low-cost alkyl benzene sulfonate (ABS) has been tested as an alternative co-surfactant showing enhanced calcium tolerance, due to the synergy between the carboxylate and ABS. Thus, the advent of this new class of cost-effective surfactants greatly broadens the application of chemical EOR.
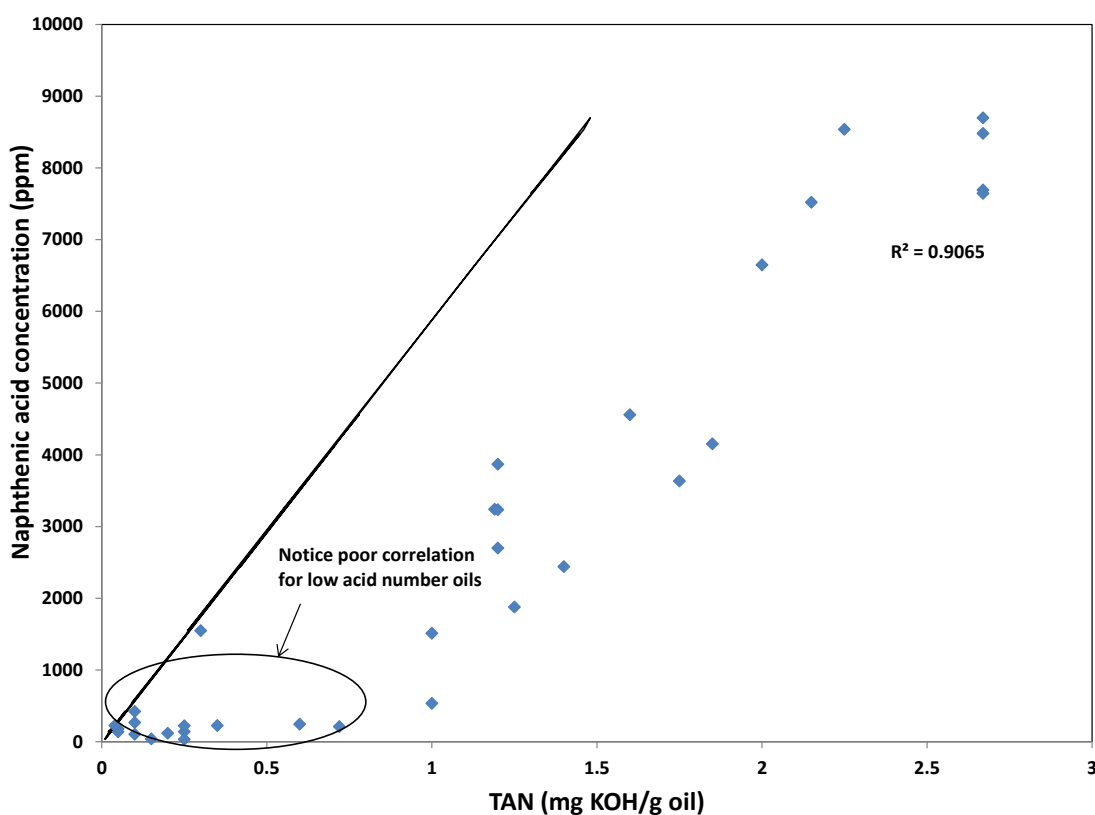
Figure 3.32: Naphthenic acid concentration as a function of TAN. Points represent samples from different geographical locations. The straight line is expected TAN value, if it were a function of naphthenic acids only – Figure reproduced from data by Meredith et al., 2000.

S.No	Description	Trial 1 TAN (mg KOH/g)	Trial 2 TAN (mg KOH/g)	Trial 3 TAN (mg KOH/g)	Trial 4 TAN (mg KOH/g)	Reported/known TAN
1	Field L Oil	2.58	1.98	2.09	2.27	
2	Excess Oil Phase from L (SP) 13 Re 1.5% to 2.5% salinity	0.64	0.58	2.02	4.05	
3	Field C oil #3	1.86				Crude oil diluted with 11.5% decalin (Reported TAN ~ 2.3)
4	Excess Oil Phase from C-103	1.74				Avg. Type I
5	R Oil #1	0.2				N/A
6	Excess oil phase from R-82 (56000ppm)	0.18				-
7	Field Y Oil	0.73				Reported TAN (literat.) - 0.8 mg KOH/g
8	Excess oil phase from Y-73 2.5% Salinity	0.47				Type I sample.
9	Field O Oil	1.33	0.39			No TAN available
10	Excess oil phase from O-88 (30000ppm, 50% oil conc.)	0.16	0.91			Good microemulsion PB, slight negative slope observed for oil scan with this SP form.
11	Excess oil phase from O-88 (25000ppm, 40% oil conc.)	-	0.28			
12	Excess oil phase from O-88 (20000ppm, 30% oil conc.)	-	0.52			
13	Naphthenic acid in dodecane (oil phase used in U-320, 320 (R)	2.25	2.24	2.27	1.99	2 mg KOH/g calculated
14	Excess oil phase from U-320 (4%, 5%)	2.59			1.87	
15	Excess oil phase from U-320 (R) (8, 9%)	2.20			1.67	

Table 3.10: Summary of TAN measurements – shaded cells indicates that they were done in UT Austin and the rest were potentiometric titration done in commercial lab.

3.3 TSP Hydrophobes

The need for EOR surfactants with large hydrophobes is compelling. . The Guerbet hydrophobes (C_{24-32}) are made from Guerbet alcohols (C_{12-16}), and in order to have a sustainable supply of chemicals, there is a need for alternative hydrophobe with diverse raw material base. Moreover, any change in the chemical structure of hydrophobe will drastically modify the overall performance of the surfactant. Hence the advantages are two fold (raw material diversification and modified performance). Tristyrylphenol (TSP) is the novel class of hydrophobe developed to satisfy the above mentioned needs at low cost. The raw materials are petrochemical based feed stock, styrene and phenol. The structure and reaction scheme of TSP hydrophobe is shown in Figure 3.33. As with Guerbet alcohols they can be made into alkoxy sulfates or carboxylates (or even sulfonates). The TSP consists of four benzene rings which could help in solubilizing heavy components in the crude oil such as asphaltene and other aromatic components.

For the purpose of demonstrating the effectiveness of the hydrophobe, formulation containing TSP alkoxy sulfate will be used. Field M is one such example where TSP alkoxy sulfate was optimum than other surfactants. Field M is a sandstone reservoir of temperature, 62 °C, with an oil of API gravity 28°. The dead oil viscosity is 28 cP (150 °F), and that of the live oil is 9.14 cP (Reservoir pressure and 150 °F). But, the oil has high paraffin content (resins – 15%, asphaltene – 10%) and it's a solid at room temperature. The oil is also reactive with an acid number of 1.0 mg KOH/g oil.

The phase behavior experiments were conducted with surrogate oil at ambient pressure. The surrogate oil was prepared by diluting the dead oil with 12.5 wt% cyclohexane (EACN-4) to match the EACN of the live oil. The formulation consisted of 0.20% TSP-7PO-12EO-sulfate, and 0.05% MA-80 (sodium dihexyl sulfosuccinate, which

is a temporary solubilizer – Yang, 2010). The scan variable is Na_2CO_3, and all the solutions were prepared in synthetic softened brine (~5000 ppm NaCl). The activity map for the formulation is given in Figure 3.34. It can be seen that the optimum salinity for 50% oil concentration to 10% oil concentration varies from 30,000 ppm TDS to more than 50,000 ppm TDS.

3.3.1 Live Oil Core Flood using TSP Alkoxy Sulfate

A high-pressure live oil core flood in Field M reservoir core was conducted using the formulation given above. A surrogate oil core flood was conducted prior to this, and following the success of that core flood, live oil core flood was decided. The saturation pressure of the reservoir is 1496 psi. As a factor of safety, 1700 psi was chosen. Therefore, the core flood was conducted with a back pressure of 1700 psi. The confining pressure of the core holder was set at 1750 psi. The composition of the live oil used in the core flood is given in Table 3.11. It contains about 30 mol% methane and 10 mol% CO_2.

Component	Mole%	Wt%
Dead Crude Oil	59.52	96.51
CO_2	9.4	1.58
CH_4	31.08	1.91

Table 3.11: Composition of the live oil used in the core flood

The core was first flooded with the synthetic hard brine, STMB (~5000 ppm NaCl with ~300 ppm Ca^{2+} and Mg^{2+}). The permeability to brine was found to be 4600 mD. Also the pore volume of the core determined by salinity gradient tracer test was found to be 94 mL. Then the core was flooded with the live oil with the composition shown in Table 3.11 with a back pressure of 1700 psi to ensure that the single phase was maintained. The steady state pressure drop was measured, and the permeability to oil was

found to be 2266 mD, equating to an end-point oil relative permeability, k_{ro}^o, of 0.48. The initial oil saturation by material balance was found to be 0.55.

After the oil flood, the core was flooded with STMB until no more oil was produced. The residual oil saturation was determined to be 0.18. From steady state pressure drop, the permeability to water at the end point was determined to be 564 mD, equating to an end-point water relative permeability, k_{rw}^o, of 0.12.

With the core at residual oil saturation, the core was ready to be flooded with the chemical slug. The ASP slug of 0.45 PV (PV*C − 9) was injected at 2 ft/day frontal velocity, followed by polymer drive at the same velocity. The composition of the ASP slug and PD is given in Table 3.12. It should be noted that the 6% TDS of the ASP slug is provided by 2.5% Na_2CO_3, 3.5% NaCl (and 5000 ppm softened synthetic brine). The reason is to extend the aqueous stability limit for the formulation. The MA-80 hydrolyzed rapidly when it was just 6% Na_2CO_3 than for Na_2CO_3 and NaCl mixture.

The chemical flood was very successful and it recovered more than 90% of the residual oil saturation, and more importantly, it reduced the oil saturation to 0.013.The pressure drop for the polymer drive was also only 2 psi/ft which is very favorable. The oil recovery profile is given in Figure 3.35, and the pressure drop profile is shown in Figure 3.36. Surfactant retention was also determined to be only 0.1 mg/g-rock. It should be noted that this live oil core flood was designed with parameters obtained from phase behavior experiments conducted at ambient pressure with surrogate crude oil. This implies that when the oil is characterized properly (matching the EACN), the live oil has little or no difference from the surrogate oil, which is very important in validating, because conducting experiments (phase behavior and core flood) at high pressures are often difficult and very expensive.

91

3.3.2 Conclusions on TSP Hydrophobe

A new class of alternative, cost-effective, petrochemical based hydrophobe was successfully developed and tested. The new structure (4 benzene rings) helps in solubilizing heavy (aromatic) components, which helps in finding optimum surfactant formulation for certain crude oils (more paraffin content, asphaltene). High-pressure (1700 psi) live oil core flood conducted with this new class of surfactant produced high oil recoveries and reduced the oil saturation to nearly 1%.

ASP Slug	PD
0.20 % TSP-7PO-12EO-sulfate	2,500 ppm FP3630S in SSTMB
0.05% MA-80	500 ppm dithionite in SSTMB
2.5 % Na_2CO_3	Viscosity: 55 cp @ $10s^{-1}$, 62 ^{o}C
3.5% NaCl	Frontal velocity: 2 ft/day
3,200 ppm FP3630S in SSTMB	
500 ppm dithionite in SSTMB	
Viscosity: 46 cp @ $10s^{-1}$, 62 ^{o}C	
Frontal velocity: 2 ft/day	

Table 3.12: ASP slug and PD composition
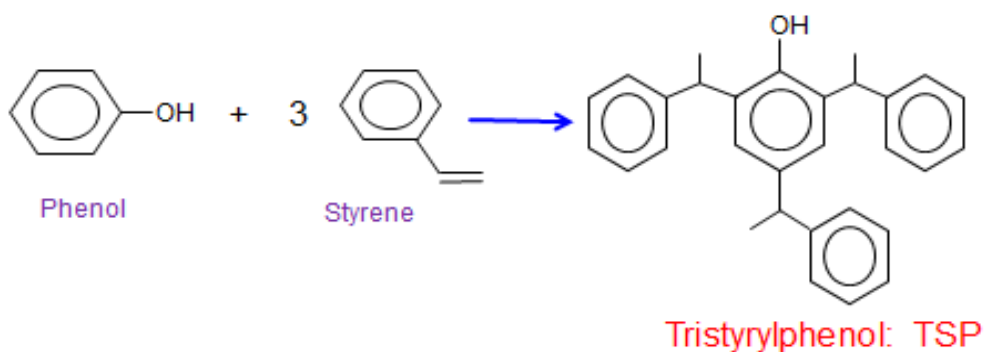
Figure 3.33: Structure and reaction scheme of TSP hydrophobe
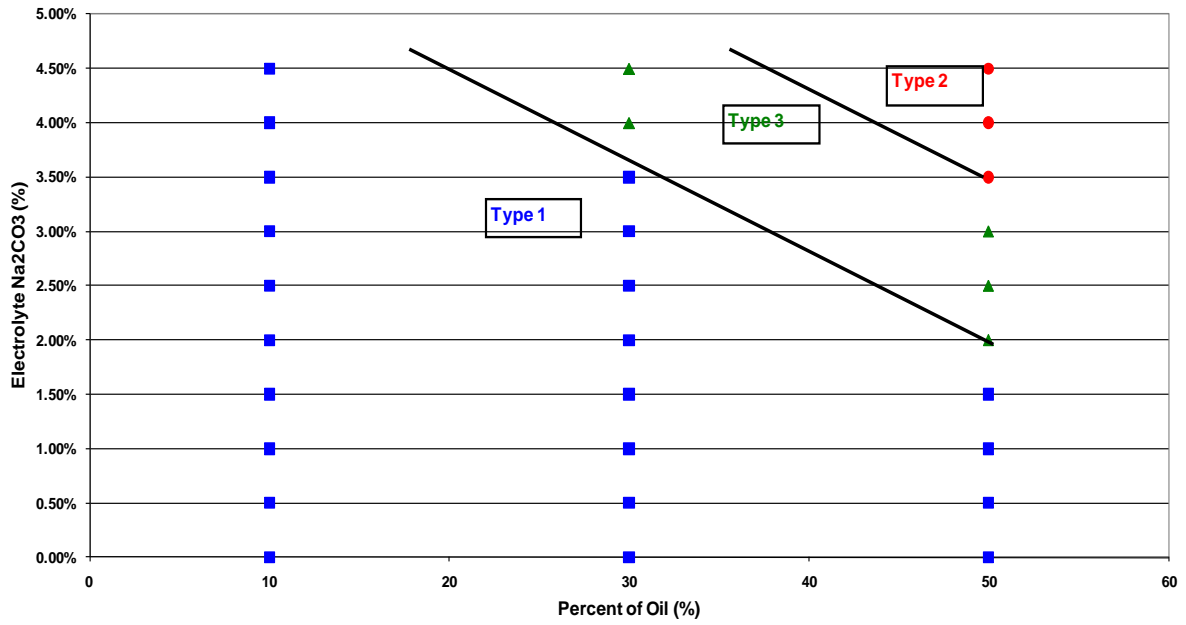
Figure 3.34: Activity plot for Field M oil with TSP formulation
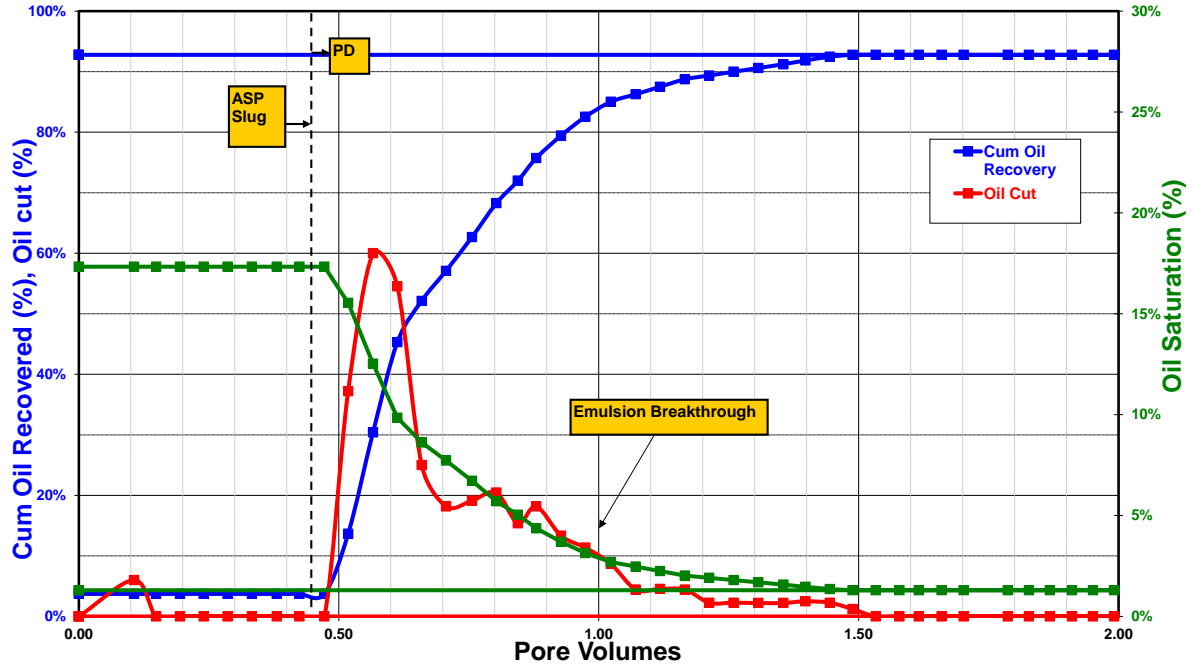
Figure 3.35: Oil recovery profile for live oil core flood with TSP formulation

93
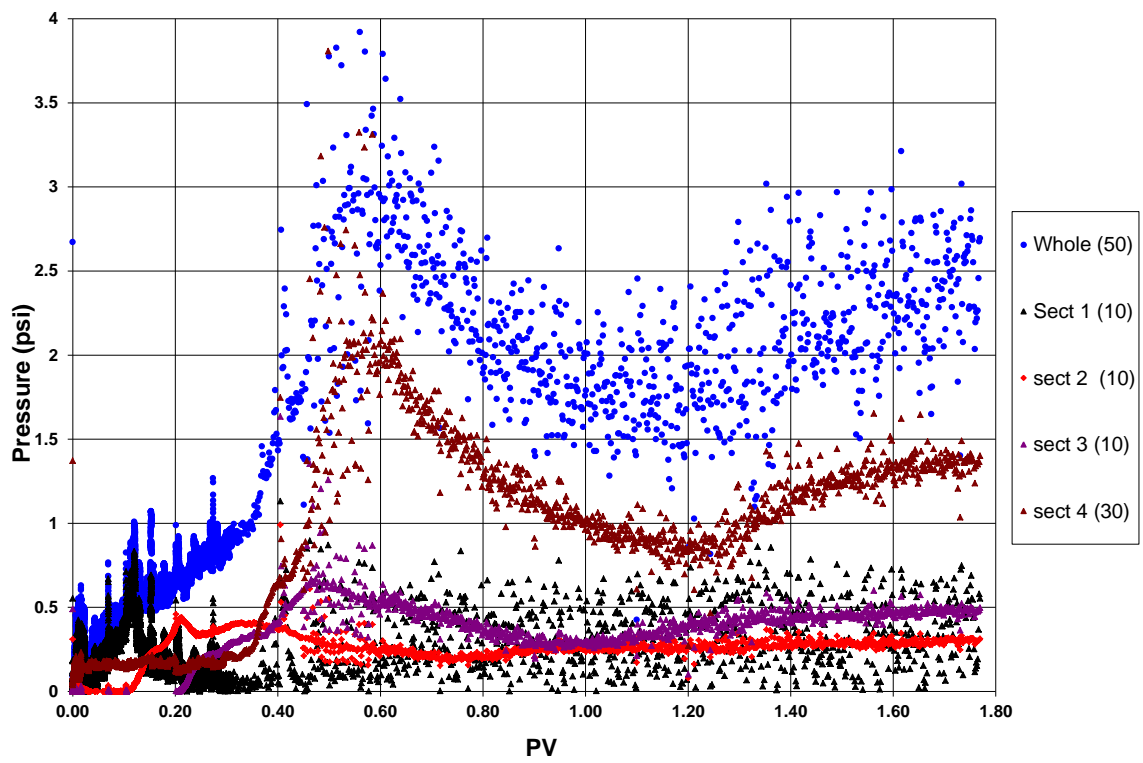
Figure 3.36: Pressure drop profile for live oil core flood

Chapter 4: New Correlation to Predict the Optimum Surfactant Structure

4.1 BACKGROUND

It's well known that the oil recovery efficiency depends on microemulsion phase behavior and interfacial tension (IFT). The surfactants needed to obtain good phase behavior and ultra-low IFT vary greatly with oil characteristics and reservoir conditions. Hence, it is often necessary to test many surfactant formulations before finding a highly effective one. Based on both sound principles and extensive experience, the optimum surfactant structure is known to be related to the oil characteristics, the brine composition, and the temperature among other variables. Griffin (1949) first introduced the concept of hydrophilic-lipophilic balance (HLB) to quantify for the relative affinity of surfactant for water and oil. According to this empirical relation, each oil is characterized by "required HLB" (HLB_{req}), corresponding to the HLB of the surfactant resulting in the most stable emulsion. However, this method doesn't take into account the effect of other formulation variables such as salinity, hardness, temperature, alkali, alcohol (co-solvent) type and concentration and co-surfactant type and concentration. In 1954, Winsor introduced the R-ratio that relates the relative energies of interaction between the surfactant adsorbed at the interface and the aqueous and oil phases surrounding it. It takes into account the molecular effects at the interface, but is still limited by the fact that energies of interaction cannot be measured experimentally. Shinoda (1964) proposed a method based on the determination of phase inversion temperature (PIT) – equivalent to cloud point phenomenon (decrease in hydrophilicity of ethylene oxide moiety of surfactants upon heating). It takes into account the effect of formulation variables (salinity, oil, additives), but in practice this technique can be applied only to ethoxylated nonionic surfactants, since ionic surfactants show opposite sensitivity to temperature.

95

A more general method of characterizing surfactant formulations for specific oil was first introduced by Salager et al. (1979, 1999, 2003, 2007, 2008). They developed an empirical correlation for classical surfactant structures including the formulation variables salinity, temperature, alcohol type and concentration and surfactant type. They expressed the correlation for anionic surfactants by Eq. (4.1) and nonionic surfactants by Eq. (4.2) separately as:

$$\ln S - K\ ACN - f(A) + \sigma - a_T\ \Delta T = 0 \qquad (4.1)$$

$$\alpha - EON + b\ S - k\ ACN - \phi(A) + c_T\ \Delta T = 0 \qquad (4.2)$$

In these expressions, S is the brine salinity in wt% NaCl, ACN is the alkane carbon number of the oil phase, f(A) and ϕ(A) are functions of alcohol type and concentration, σ and α are parameters characteristic of the surfactant structure, EON is the average number of ethylene oxide groups in the nonionic surfactant, ΔT is the temperature difference measured from a reference temperature (25 °C), b, k, K, a_T and c_T are empirical constants that depend on the type of surfactant. K is 0.16 for alkylbenzene sulfonates and about 0.10 for alkyl sulfate. The value of k is 0.16 for nonionic surfactants. The coefficient for temperature is small for anionic surfactants (0.01) and much larger for nonionic surfactants (0.06).

Later, these correlations were generalized in terms of *surfactant affinity difference* (SAD), as a variation of Gibb's free energy when a surfactant molecule passes from oil to water:

For anionics:

$$HLD = SAD/RT = \ln S - K\ ACN - f(A) + \sigma - a_T\ \Delta T \qquad (4.3)$$

For nonionics:

$$HLD = SAD/RT = \alpha - EON + b\ S - k\ ACN - \phi(A) + c_T\ \Delta T \qquad (4.4)$$

Where, HLD is the dimensionless surfactant affinity difference, called *hydrophilic-lipophilic deviation*. Whenever SAD is negative, zero, or positive, *R* is less than, equal to, or greater than 1 respectively.

Even though Salager's equation correlates some of the formulation variables related to microemulsion behavior, the correlation has been developed for just a few classical surfactants and cannot be readily used to predict the best surfactant structure. We now have many new surfactants with widely different structures and many more good formulations with a wider range of oils, temperature and so forth. Furthermore the parameters σ and K (or α and k) are characteristics of specific surfactants and hence have to be determined experimentally.

The objective of this research was to develop an explicit correlation between the optimum surfactant structure and the most important formulation variables including the parameters for new-generation surfactants both to assist with understanding the complex relationship among important formulation variables and as a guide to efficiently selecting the best surfactant structures to then be rigorously evaluated in the laboratory for specific oils and conditions. Since the objective was to determine the relationship among the variables for an optimum structure, only experimental data for optimized formulations were used in the regression analysis described below. This is a very fundamental point and needs to be clearly understood. Many measurements are made for formulations with unacceptable behavior e.g. the IFT is too high. These data were not used. Only data for "good" formulations were used and this clearly affects the outcome of the results.

4.2 HYDROPHOBE CARBON NUMBER EQUATION

The preliminary study conditions used for the correlation are:

1. Linear equation used to correlate variables

2. EACN used to characterize oil

3. Only non-reactive oils used in correlation

4. Data sets for optimized formulations at optimum salinity used in correlation (all formulations have ultra-low IFT)

5. Mole fraction averages used for surfactant mixtures

6. Co-solvent not included in correlation

7. Divalent cations not included in correlation

8. Hydrophobe branching not included in correlation

Based on these conditions mentioned above and the variables chosen for correlation, the equation used to correlate the hydrophobe carbon number is:

$$N_c = a_1E_O + a_2N_{PO} + a_3N_{EO} + a_4(T-T_{ref}) + a_5\log S^* + C \tag{4.5}$$

Where, a_1, a_2, a_3, a_4, and a_5 are regression coefficients and C is the intercept.

N_c is mole average weighted carbon number (in the hydrophobe) of the surfactant mixture ($\sum_{i=1}^{n} x_i Nc_i$, where x_i and Nc_i is the mole fraction and carbon number in the hydrophobe for surfactant i respectively)

E_o is the equivalent alkane carbon number (EACN) of the oil

N_{PO} is mole average weighted propylene oxide (PO) number in the surfactant mixture ($\sum_{i=1}^{n} x_i NPO_i$, where x_i and NPO_i is the mole fraction and number of PO number for surfactant i respectively)

N_{EO} is mole average weighted ethylene oxide (EO) number in the surfactant mixture ($\sum_{i=1}^{n} x_i NEO_i$, where x_i and NEO_i is the mole fraction and number of EO number for surfactant i respectively)

T is the temperature of interest (°C) and T_{ref} is reference temperature (21 °C)

$\log S^*$ is the common logarithm ($\log_{10}(x)$) of optimum salinity, S^* (ppm)

The formulation variables were correlated in the form of equation (4.5) by conducting a multi-variable regression. The data used in the regression study is shown in Table 4.1. The regression results including the values for the intercept and coefficients are shown in Table 4.2. Figure 4.1 shows the plot of predicted N_c vs. the experimental N_c values. The R-squared value for the correlation was 0.87. The coefficient values determine how well the individual variables are correlated, but it's the product of the coefficient and the variable (a_iX_i) that determines the overall impact on the predictor term. The uncertainty in the equation is accounted in the standard deviation for each parameter. The standard deviation (SD) values are normalized with respect to the coefficients, which are also shown in Table 4.2. The *t-stat* value shows whether the variable included in the correlation is statistically significant or not, which is in a way equivalent to the normalized standard deviation.

4.2.1 Sensitivity Studies

A number of plots were made to illustrate the predicted effect of different variables on the hydrophobe carbon number keeping the other variables (except the one being tested) constant.

Effect of Oil EACN and Temperature

Figure 4.2 shows the predicted optimum hydrophobe carbon number N_c vs. oil EACN. It can be seen that as the oil EACN increases, the hydrophobe size required to achieve ultra-low IFT increases. This is a classical behavior and one of the main reasons for the need of large hydrophobe surfactants. Cayias et al. (1976) were the first to coin the term EACN and they studied the microemulsion phase behavior with crude oils of varied EACN. They observed similar behavior (Figure 4.3) and concluded that as the alkyl carbon number of the oil phase increases, the equivalent weight of the surfactant

99

required to get the IFT$_{min}$ also increased. But, this definition of equivalent weight as a means to express the surfactant hydrophobicity may not hold good with these new-generation surfactants because the hydrophobicity for these surfactants also depends on several factors such as the number of PO/EO groups. Hence the effect of PO, EO, and temperature on the hydrophobe carbon number has to be studied individually. From Figure 4.2, it can also be seen that larger hydrophobes are needed with an increase in temperature, but the effect of temperature is less pronounced when compared to other variables.

Effect of PO/EO

Figure 4.4 shows the effect of PO and EO groups on the predicted optimum hydrophobe carbon number. PO is more hydrophobic than the EO moiety, which is consistent with other experimental observations. But in reality, the effect is much more complicated as they also depend on temperature. In order to account for that non-linearity, the cross terms (PO*dT and EO*dT) were added to equation (4.5), but they did not improve the correlation very much. A probable reason is that most of the formulations (used in this particular data set) involving PO and EO are part of large hydrophobe anionic surfactants. Anionic surfactants are less sensitive to temperature than the nonionic surfactants. For large hydrophobe surfactants, the contribution due to nonionic moieties (PO/EO) is small compared to that of say, C$_{9-13}$ alcohol propoxylated sulfates or alcohol ethoxylated nonionic surfactants.

Effect of Salinity

Figure 4.5 shows a marked decrease in hydrophobe size with increase in brine salinity, which can be explained by the fact that with an increase in salinity, to have an optimum condition, the surfactant hydrophilicity has to increase. Also, for a given

surfactant the optimum salinity increases with increase in temperature, which is a classical behavior for anionic surfactants.

4.2.2 Other Applications of the Correlation

Determination of Oil EACN

The equation (4.5) directly relates the optimal conditions and oil EACN. Therefore by rearranging the equation for logS*, EACN of the oil phase can be determined with the knowledge of just the optimum salinity for a given surfactant formulation. Figure 4.6 shows the plot of logS* vs. EACN. It can be seen that the optimum salinity increases as the oil EACN increases, which is consistent from previous observations. Salager et al. (1979) also observed similar behavior and their experimental observations are shown in Figure 4.7. Needless to say, the EACN determined by this method is independent of surfactant structure and temperature.

Determination of Optimum Salinity

For given oil EACN and temperature, the optimum salinity can be predicted for different surfactants with the help of equation (4.5). Figure 4.8 shows a plot of logS* as a function of PO, EO, and different hydrophobe sizes. It should be noted that the correlation predicts a slight decrease in optimum salinity with increase in EO, which does not seem consistent with other experimental observations but such observations may not always have been under consistent optimized conditions. Furthermore, this effect of PO and EO on S* depends on the hydrophobe size (ratio of nonionic to ionic moieties). For instance, C_{13}-xPO should have a more negative slope than a C_{20}-xPO hydrophobe. To study that non-linearity, the data (Table 4.1) was again regressed by having logS* as the predictor (y) and the cross terms N_c*PO and N_c*EO were added to the list of variables.

The effect due to the cross term Nc*EO was insignificant in this case, so it was not included in the final equation. The modified form of equation (4.5) was therefore:

$$\log S^* = a_1 E_O + a_2 N_{PO} + a_3 N_{EO} + a_4 (T-T_{ref}) + a_5 N_c + a_6 N_c*PO + C \qquad (4.6)$$

The regression summary for equation (4.6) is shown in Table 4.3. Using equation (4.6), the effect of S* on PO with change in hydrophobe was plotted again and is shown in Figure 4.9. It can be seen that the decrease in optimum salinity (S*) with addition of PO is less pronounced for a large hydrophobe than that of a small hydrophobe. The same trend was observed by Aoudia et al. (1995) and is shown in Figure 4.10. Even though the relationship between N_c and PO with respect to optimum salinity was captured by the model, the same dependence with respect to temperature was not observed. Generally the optimum salinity for simple anionic surfactants increases with temperature whereas for nonionic surfactants the reverse is observed. For anionic surfactants containing PO and EO the effect is complicated and is determined by the ratio of nonionic to ionic moieties. Aoudia et al. (1995) studied this effect and they observed a change in slope (in a plot of S* vs. T) from positive to negative as the ratio PO/SO_3 increased (Figure 4.11). Because of limited cross terms, the same was not predicted (Figure 4.12) by the correlation, so this is one of its limitations that needs to be removed by additional development.

4.3 Conclusions

A new correlation for predicting the optimum surfactant structure for chemical EOR has been developed. The equation for hydrophobe carbon number was developed for new-generation surfactants taking into account the effect of the formulation variables such as PON, EON, EACN of oil, temperature, and brine salinity. The correlation is independent of surfactant type and can be used for mixtures of sulfates, sulfonates, carboxylates and nonionics. It can be used as a guideline for selecting the best surfactant

structure to test and also as an aid in understanding the most important parameters affecting the optimum condition. Regression analyses show that the oil EACN and the brine salinity are key factors in determining the surfactant structure. The correlation predicts that larger hydrophobes are needed as either the temperature or oil EACN increases, which is in conformance with the experimental observations. The correlation can also be used to determine the oil EACN with the knowledge of optimal salinity for a given formulation. The complex behavior of change in optimum salinity as a function of PO, EO, and hydrophobe size was also predicted accurately in accordance with previous experimental observations. The correlation was developed only for non-active oils. Also, the parameters for co-solvent, divalent cations and hydrophobe branching were not included in the correlation, so these are additional limitations of the correlation. Additional development to include these variables is justified as data become available.

Formulation	Mole average N_C	Mole average N_{PO}	Mole average N_{EO}	$T-T_{ref = 21 C}$	Log Optimum salinity, (TDS, ppm)	Oil EACN
0.25% C32-7PO-6EO-SO4⁻, 0.25% C20-24 IOS	24.5	1.8	1.5	64	4.5485	16
1.33% C24-28 IOS, 0.67% C30 OXS	27.1	0.0	0.0	64	4.5782	16
2% C16-7PO-SO4⁻	16.0	7.0	0.0	64	4.5485	16
2% C13-13PO-SO4⁻	13.0	13.0	0.0	64	4.2395	16
0.5% C16-7PO-SO4⁻, 0.5% C14-9PO SO4-	15.1	7.9	0.0	64	4.5167	16
0.75% C16-7PO-SO4⁻, 0.25% C24-28 IOS	19.4	4.6	0.0	64	4.4894	16
1% C20-6EO-SO4⁻, 1% C20-10EO SO4⁻	20.0	0.0	7.8	64	4.5423	16
1.8% C24-10EO-SO4⁻, 0.2% C13-12EO SO4⁻	22.8	0.0	10.2	64	4.2003	16
0.5% C28-7PO-2EO-SO4⁻, 0.5% C20-24 IOS	23.8	2.0	0.6	64	4.5167	16
0.3% C28-7PO-2EO-SO4⁻, 0.3% C20-2EO SO4⁻	22.6	2.3	2.0	64	4.5167	16
1.5% C16-7PO-SO4⁻, 0.5% C15-18 IOS	16.0	4.0	0.0	4	4.5157	9.9
0.5% C28-25PO-25EO COO⁻, 0.5% C15-18 IOS	17.2	2.4	2.4	84	4.6532	11.6
0.5% C28-25PO-35EO COO⁻, 0.5% C15-18 IOS	17.0	2.2	3.0	84	4.7782	11.6
0.5% C28-25PO-45EO COO⁻, 0.5% C15-18 IOS	16.9	1.9	3.5	84	4.9085	11.6
0.25% C28-25PO-15EO-COO⁻, 0.20% C20-24 IOS, 0.05% C15-18 IOS	21.5	3.3	2.0	55	4.4771	12
0.1% C20-24 IOS, 0.1% TDA-13PO-SO4⁻, 0.1% C9-11-8EO	16.3	2.4	2.7	0	4.8451	13.6
0.25% C24-25PO-18EO COO⁻, 0.25% C13-13PO SO4-, 0.25% C12 ABS	13.3	5.2	1.6	9	4.6532	11.7
0.25% C32-7PO-14EO SO4⁻, 0.25% C20-24 IOS	24.1	1.4	2.9	79	4.4771	14
0.25% C32-7PO-18EO SO4⁻, 0.25% C20-24 IOS	23.9	1.3	3.4	79	4.4771	14
0.5% C32-7PO-6EO SO4⁻, 0.33% C16-7PO SO4⁻, 0.17% C20-24 IOS	23.1	4.7	1.9	79	4.3979	14
0.75% C16-7PO SO4⁻, 0.25% C15-18 IOS	16.0	4.0	0.0	14	4.5440	12
C13-13PO SO4⁻, 0.1% C15-18 IOS	14.3	7.2	0.0	14	4.5440	12
0.5% C24-25PO-56EO COO⁻, 0.5% C19-23 IOS	21.3	2.1	4.7	79	4.5798	15
0.5% C28-25PO-25EO COO⁻, 0.5% C15-18 IOS	17.2	2.4	2.4	79	4.8388	15
0.5% C20-24 IOS, 0.5% C13-13PO SO4⁻	19.5	3.6	0.0	17	4.3086	11
0.25% C20-24 IOS, 0.75% C13-13PO SO4⁻	17.2	7.0	0.0	0	4.3010	10
0.5% C32-7PO-32EO COO⁻, 0.5% C19-23 IOS	22.6	1.0	4.7	79	4.6021	11.4
0.5% C28-25PO-45EO COO⁻, 0.5% C15-18 IOS	16.9	1.9	3.5	79	4.5563	6.9
0.5% C24-28 IOS	26.0	0.0	0.0	79	4.2430	11.4
0.33% C32-7PO-18EO SO4⁻, 0.33% C16-7PO SO4⁻, 0.33% C15-18 IOS	18.0	2.2	2.3	79	4.6675	11.4
0.33% C32-7PO-18EO SO4⁻, 0.33% C16-7PO-2EO SO4⁻, 0.33% C15-18 IOS	17.9	2.6	2.6	79	4.7160	11.4
0.33% C32-7PO-18EO SO4⁻, 0.33% C16-7PO-6EO SO4⁻, 0.33% C15-18 IOS	18.0	2.4	3.5	79	4.7559	11.4
0.7% C28-25PO-55EO COO⁻, 0.3% C11 ABS	13.6	3.8	8.4	79	4.4150	6.9

Table 4.1: Data used in the regression study

	R-squared: 0.878			
	Standard Error: 1.4742			
	Coefficients	*Standard Error*	*Normalized Standard Error*	*t Stat*
Intercept, C	65.60251	7.543203	0.114983454	8.696903
EACN, a_1	0.47556	0.102007	0.214499497	4.662016
PO, a_2	-1.2971	0.115217	0.088827158	-11.2578
EO, a_3	-0.59155	0.122456	0.207010608	-4.83067
dT, a_4	0.030726	0.010537	0.342921504	2.916119
log Sal, a_5	-10.7535	1.586312	0.147516179	-6.77892

Table 4.2: Summary of regression coefficients and standard deviation
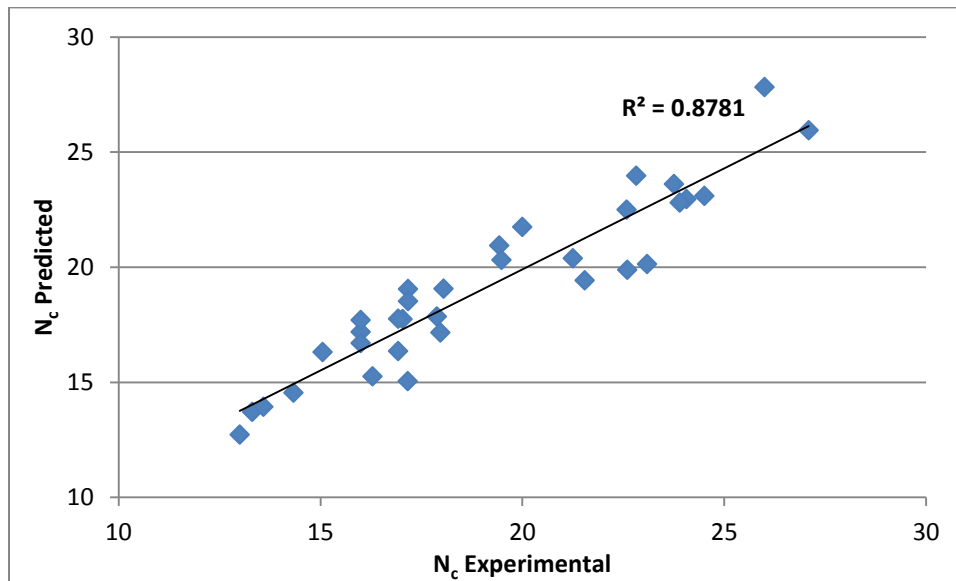
Figure 4.1: Predicted vs. experimental N_c
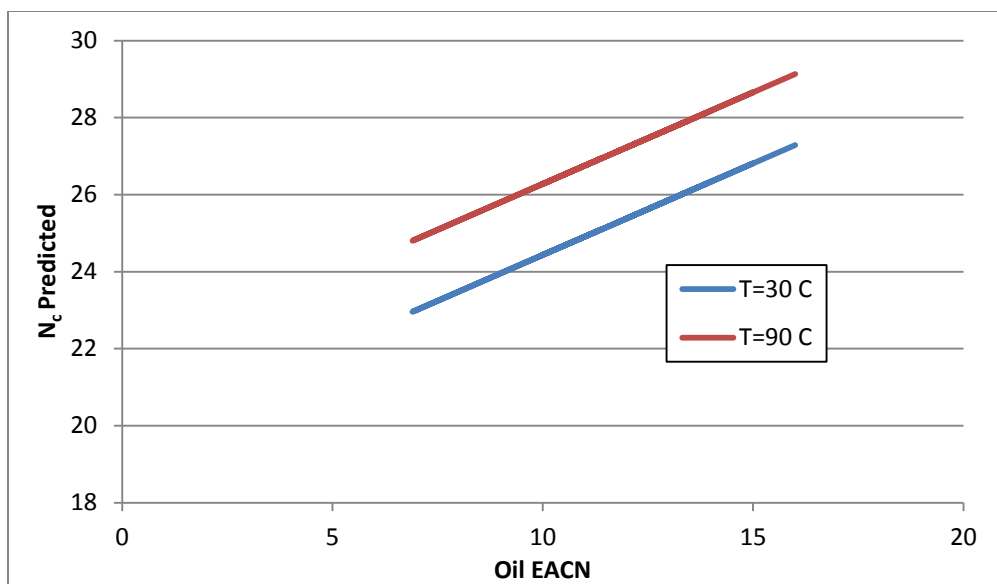
Figure 4.2: Effect oil EACN and temperature on hydrophobe size (PO-2, EO-1, S*-10000 ppm)
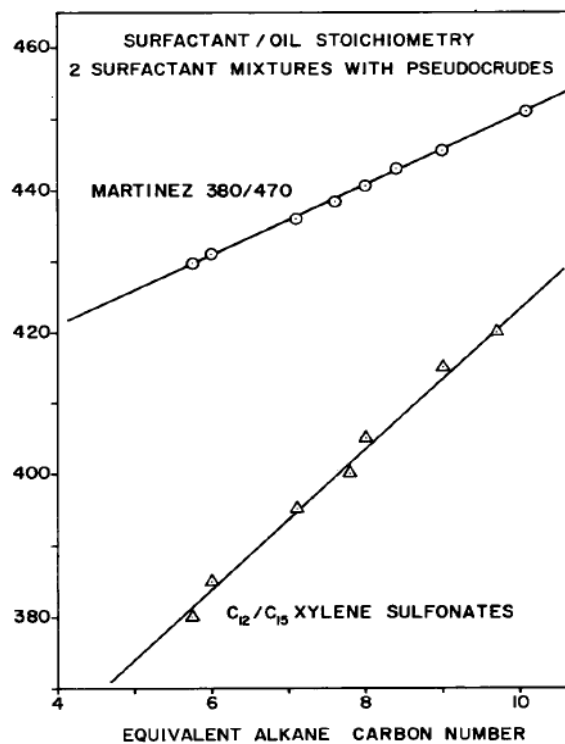
Figure 4.3: Surfactant average equivalent weight vs. EACN of oil (source: *Cayias et al., 1976*)
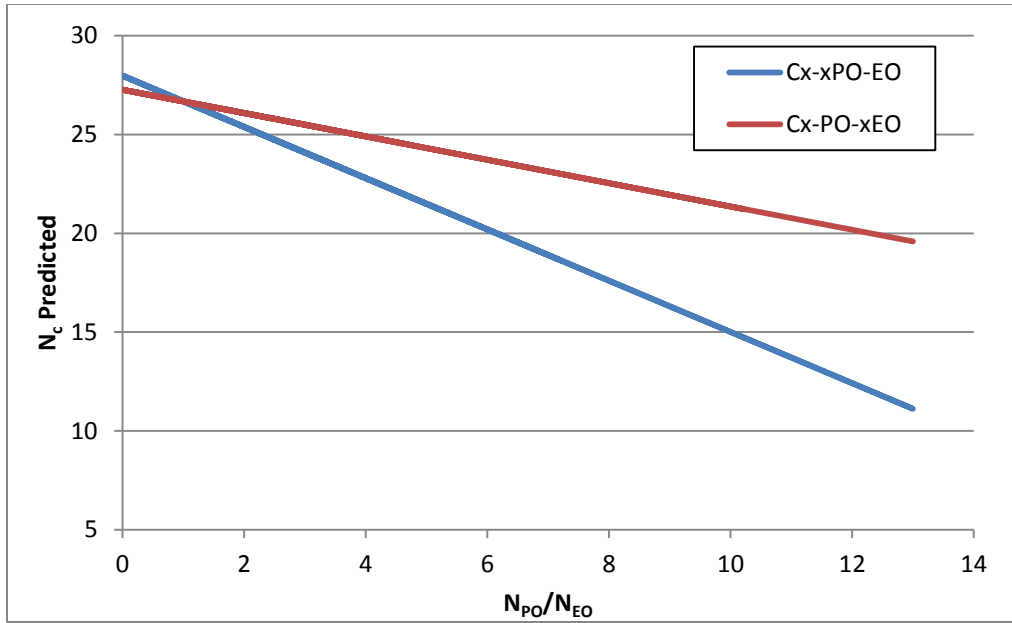
Figure 4.4: Effect of PO and EO on surfactant hydrophobe size (EACN-12, T-30 °C, S*-10000 ppm)
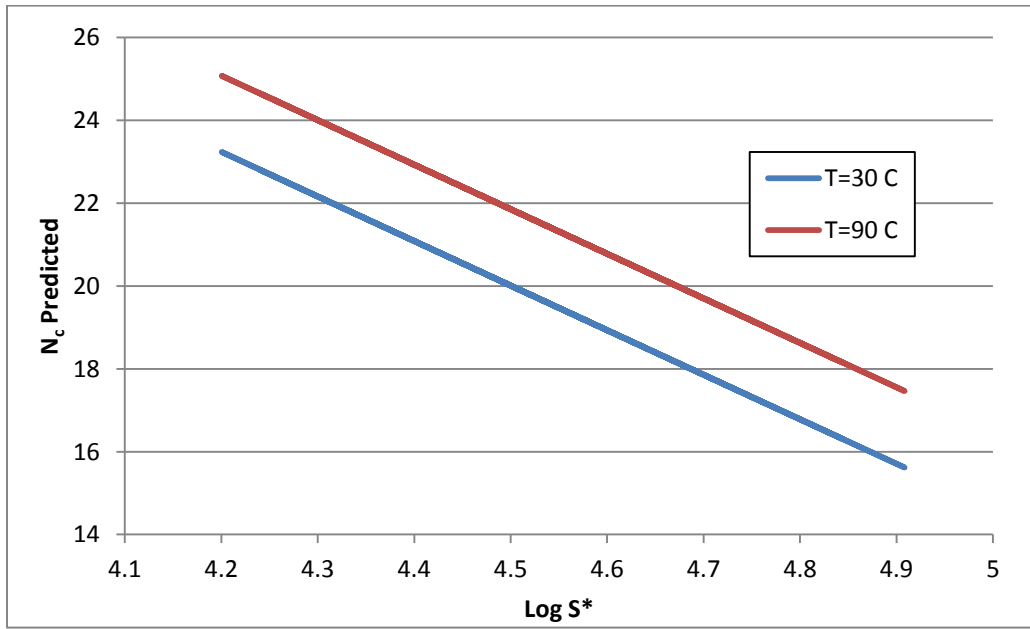
Figure 4.5: Effect of salinity on hydrophobe size (EACN-12, PO-2, EO-1)
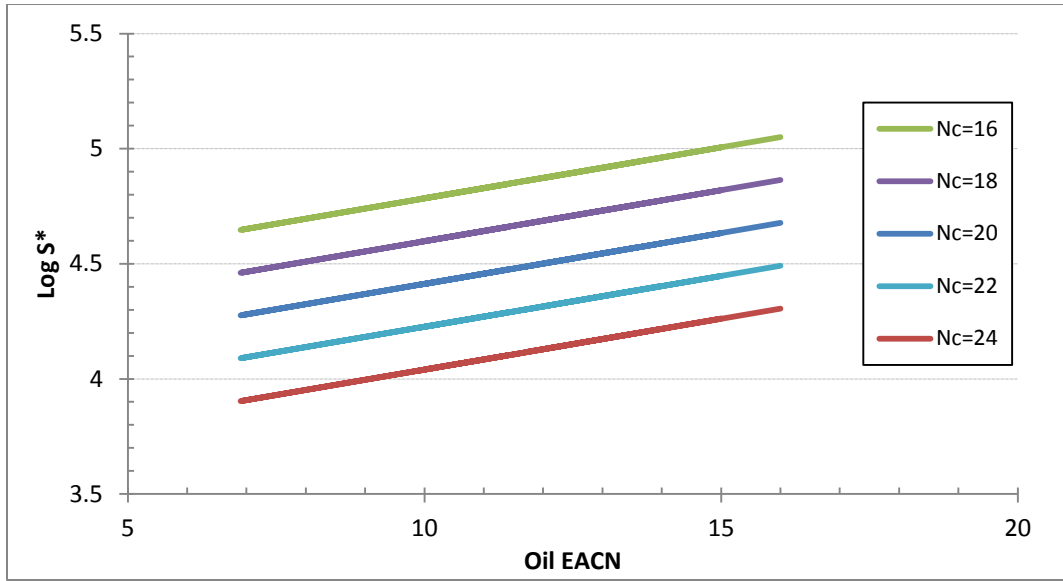
Figure 4.6: Optimum salinity shown as a function of EACN (PO-2, EO-1, T-30 °C) for different hydrophobe size
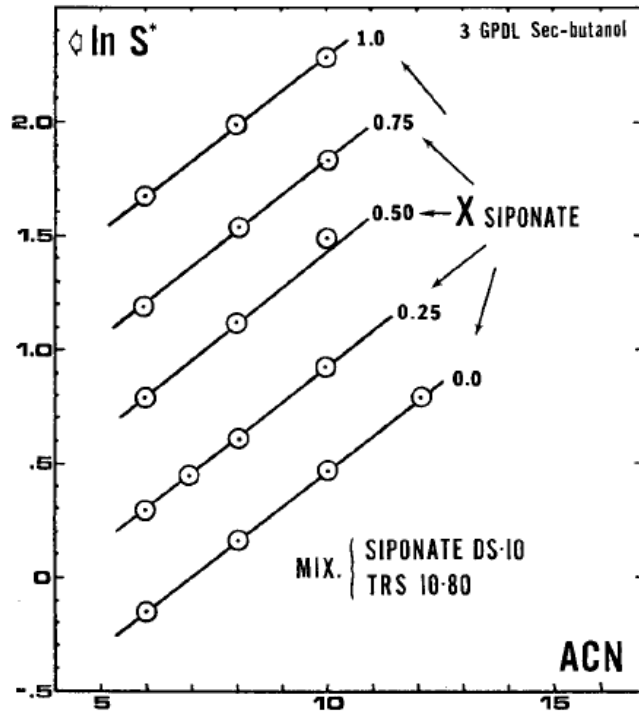
Figure 4.7: Optimum salinity vs. ACN (source: *Salager et al., 1979*)
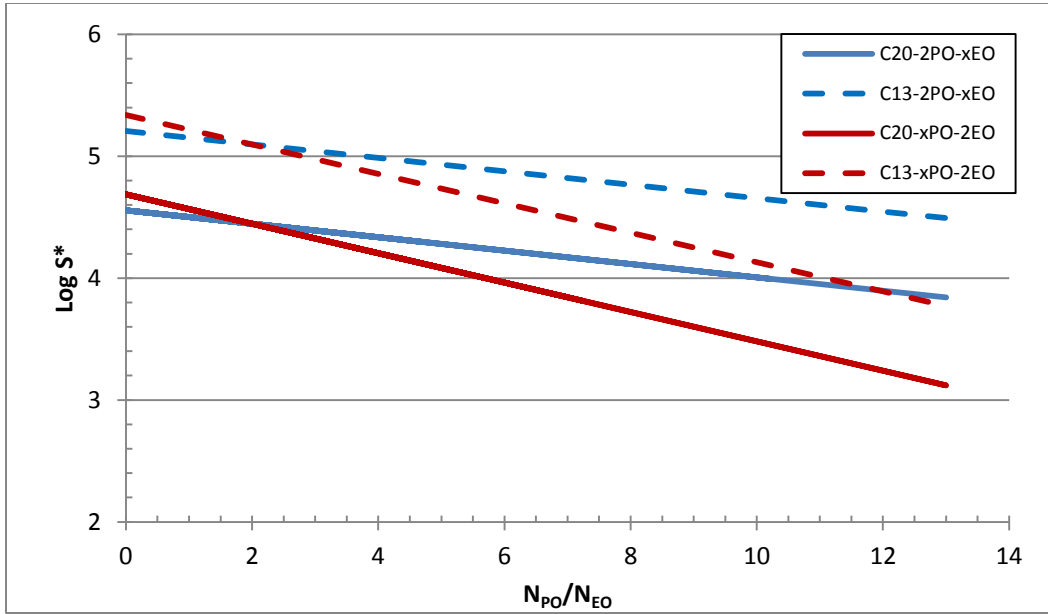
Figure 4.8: Optimum salinity as a function of PO, EO and hydrophobe size (EACN-12, T-30 °C)

	Coefficients	Standard Error	Normalized Standard Error	t Stat
R-squared: 0.702				
Standard Error: 0.105				
Intercept, C	5.625258	0.170979	0.030395	32.90032
EACN, a_1	0.027519	0.008621	0.313282	3.19202
PO, a_2	-0.134755	0.033061	0.245340	-4.07598
EO, a_3	-0.036382	0.009627	0.264599	-3.77930
dT, a_4	0.002119	0.000770	0.363587	2.75037
Nc, a_5	-0.064417	0.009066	0.140742	-7.10521
N_c*PO, a_6	0.003430	0.002051	0.597814	1.67276

Table 4.3: Summary of regression coefficients and their statistical uncertainty
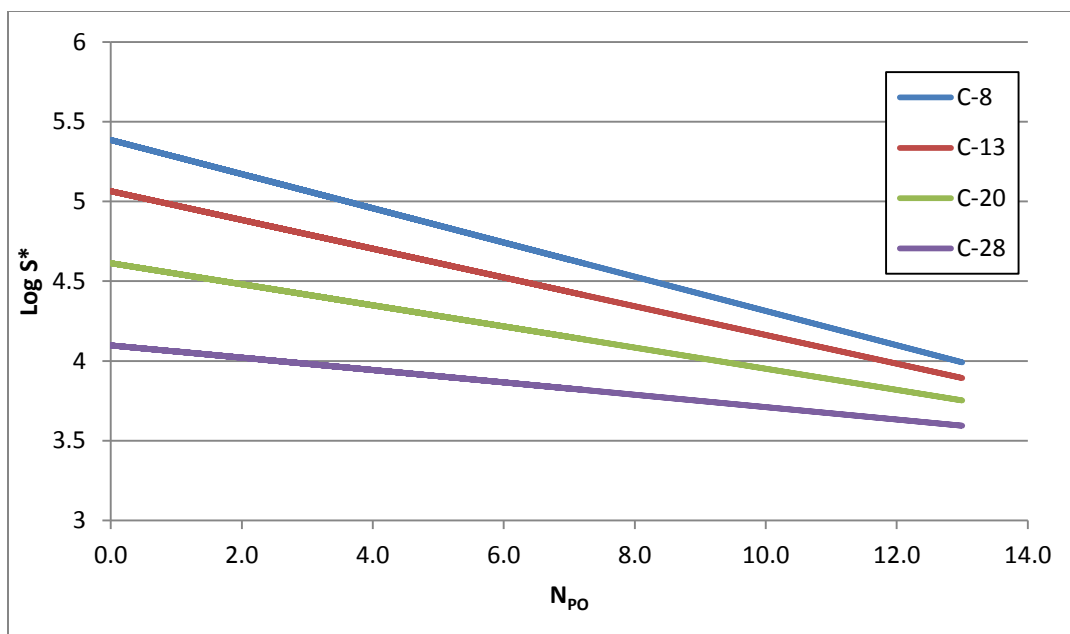
Figure 4.9: Optimum salinity as a function of PO number and hydrophobe size – notice change in slopes for different hydrophobes (EACN-12, EO-2, T-30 °C)
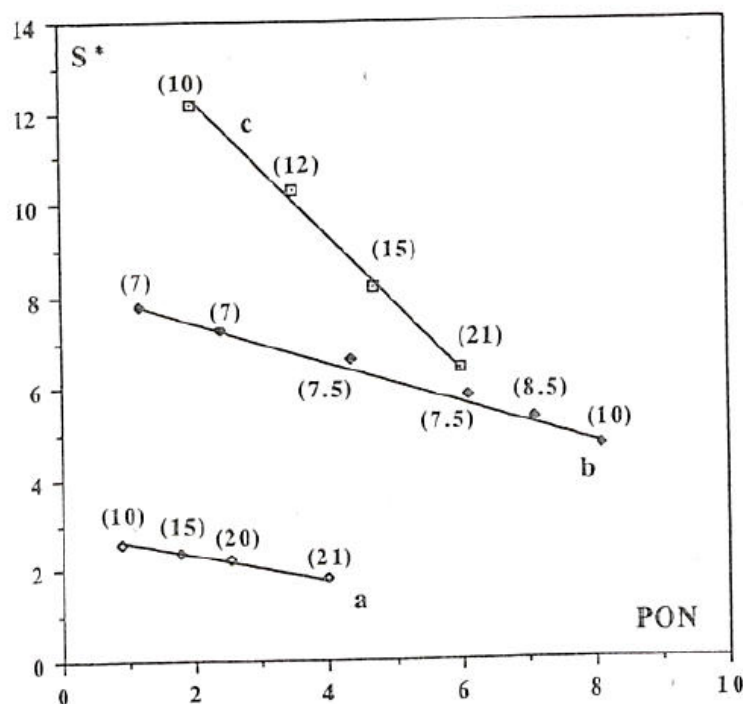
Figure 4.10: Effect of PO on S* for three series of surfactants. a: C16EX(PO)$_n$, b: C14EX(PO)$_n$, c: C13(PO)$_n$ (source: *Aoudia et al., 1995*)

110
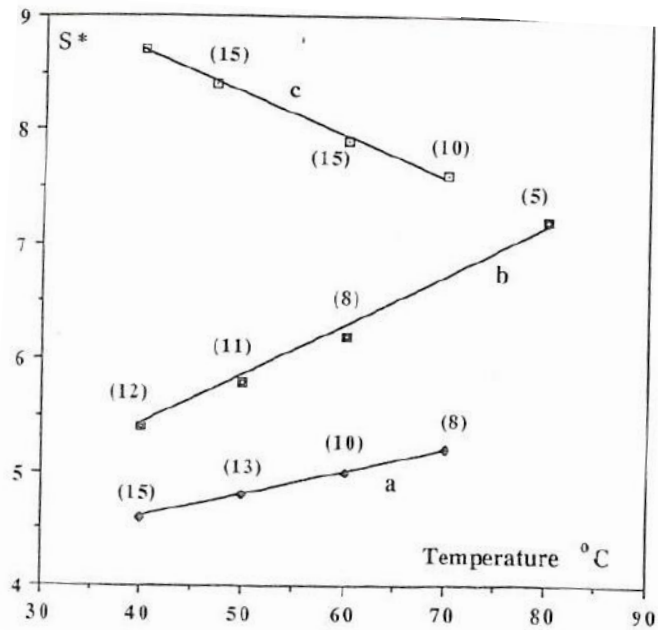
Figure 4.11: Effect of temperature on optimum salinity. a: C14EX(PO)$_{2.7}$, b: C14EX(PO)$_{1.2}$, c: C13(PO)$_{3.7}$ (source: *Aoudia et al., 1995*)
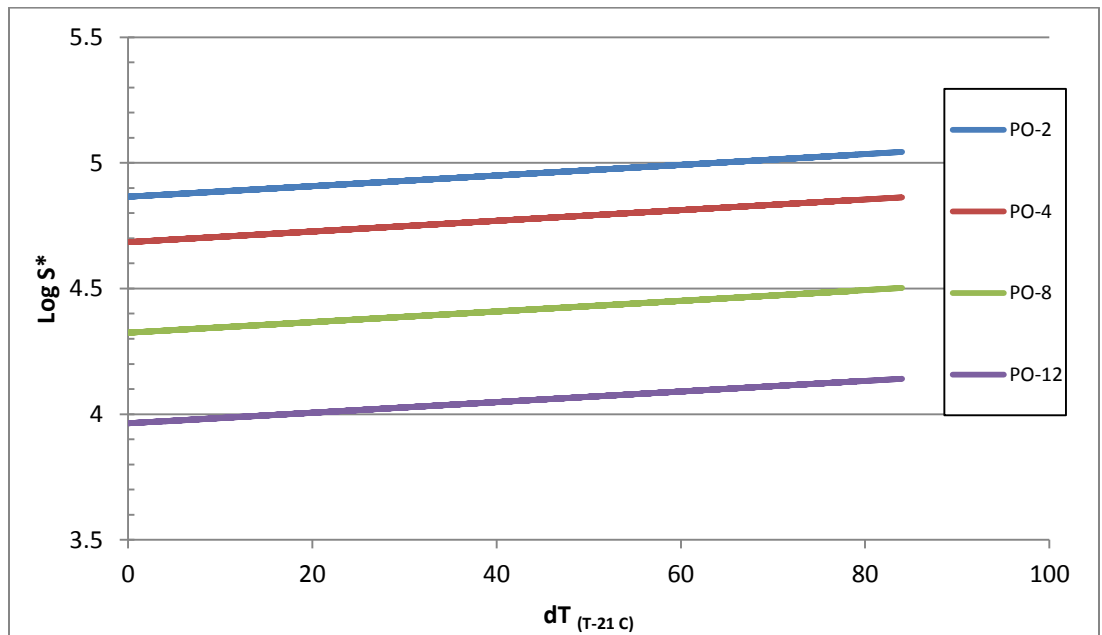
Figure 4.12: Effect of temperature on optimum salinity (EACN-12, EO-2, N$_c$-13)

Chapter 5: Measurement and Analysis of Surfactant Retention

The chemical flood success is determined mainly by the amount of oil recovered and the chemicals required to recover the same. Surfactants make up an important component in the chemical flooding process, and surfactant retention is defined as the surfactant left behind in the reservoir due to various mechanisms including adsorption on to the rock and phase trapping. Hence, surfactant retention is one of the important variables affecting the economics of chemical flooding, and varies widely depending on surfactant structure, mineralogy of the formation, salinity, pH, Eh, microemulsion viscosity, activity of the crude oil, co-solvent, mobility control and salinity gradient among other variables. This chapter will discuss the different mechanisms and factors affecting the surfactant retention. Using an extensive data set obtained from measured surfactant retention in numerous core floods conducted over the past few years by the Chemical EOR group at UT, the surfactant retention data were analyzed and a new correlation was developed.

5.1 MECHANISM AND FACTORS AFFECTING SURFACTANT RETENTION

5.1.1 Effect of Surfactant Type and pH

The type and structure of surfactant greatly determine the surfactant adsorption on the rock. Traditionally, anionic surfactants were not considered for carbonates because of high adsorption. However, increasing the pH greatly reduces the adsorption of anionic surfactants on carbonate. Zhang et al. (2006) observed that using sodium carbonate as an alkali reverses the charge of the calcite surface from positive to negative, leading to less adsorption of anionic surfactants. Interestingly, the same was not observed when sodium hydroxide was used as an alkali. They proposed that the reason could be the carbonate is a potential determining ion (for carbonate surfaces) whereas a hydroxide is not. However,

alkali cannot be used in all cases, so in such cases the most effective SP formulation must be developed and evaluated. Some anionic surfactants have also shown low surfactant retention in carbonates even without alkali that are comparable to the retention in sandstones at reservoir pH values. This surprise finding implies that the surfactant retention due to phase trapping and unfavorable phase behavior contributes as much or more than the adsorption itself.

5.1.2 Effect of Clay Content

For sandstones, surfactant adsorption depends more on the clay surfaces than on the quartz surface. Silica is negatively charged at reservoir conditions and exhibits negligible adsorption of anionic surfactants at high pH (Hirasaki et al., 2008). At neutral pH, clays have a negative charge on the faces and a positive charge at the edges. The edges exhibit pH dependent charge characteristics, and thus are expected to reverse their charge at a pH of about 9 (Somasundaran and Hanna, 1977; Hirasaki et al., 2008; Sheng, 2011). Wang (1993) also observed similar behavior and concluded that surfactant adsorption on Loudon and Berea sandstones results primarily from the presence of clays. He also showed that preserving the core in reduced conditions (by dithionite treatment) significantly reduced the surfactant adsorption.

5.1.3 Effect of Eh

Many oil reservoirs exist in anaerobic, reducing environment. However, most of the laboratory core floods are conducted in uncontrolled, aerobic, oxidizing condition. Wang (1993) observed a very significant difference in retention values between the laboratory core floods and field data. Laboratory retention values ranged from 0.5-0.9 mg/g rock, whereas in field it ranged from 0.08 to 0.35 mg/g rock. In an attempt to explain this, he conducted two sets of core floods, one in aerobic and the other in

anaerobic environment. The anaerobic, reduced condition was simulated by preflushing the core with 500 ppm sodium dithionite (a water soluble oxygen scavenger and reducing agent) and 200 ppm citric acid. The first set of core floods in aerobic environment yielded retention values between 0.55-0.82 mg/g-rock, while the second set in reduced environment yielded retention between 0.20-0.33 mg/g-rock.

5.1.4 Effect of Divalent Cation Concentration

The presence of divalent cations also influences the amount of surfactant retained. This has mainly been a problem for traditional surfactants such as petroleum sulfonates. Increased surfactant retention with an increase in divalent cation concentration was observed by several workers (Glover et al., 1979; Lawson, 1978; Novosad, 1982). The more advanced surfactants like the ones discussed in Chapter 3 show relatively high tolerance to divalent cations. In addition, the methodology for selecting the optimum surfactant formulation has also been improved with proper consideration given to aqueous stability in the salinity of interest. Sahni et al. (2010) showed that better oil recovery and less retention was observed when injecting a clear ASP solution than a cloudy ASP slug with a similar formulation (without the co-surfactant). Novosad (1981) also observed very high surfactant retention in Berea cores when surfactant solubility was affected.

5.1.5 Effect of Salinity and Microemulsion Viscosity

Glover et al. (1979) suggested that phase trapping due to immobile oil/microemulsion phase can significantly contribute to the surfactant retention. They observed that the retention increased linearly with salinity until a point where it deviates abnormally from linearity and almost all the surfactant injected was retained at that salinity. Phase behavior studies indicated type II microemulsion formed at that salinity

and was the cause of high surfactant retention since type II microemulsion is trapped in the pores of the rock unless the capillary number is extremely high or unless it is displaced by a fluid with a lower salinity to reverse the phase behavior to type I. Novosad (1982) extended the study and devised a method to quantify the surfactant retained due to adsorption and unfavorable phase behavior (entrapment of immobile oil phase and surfactant precipitation due to divalent cations). He concluded that better-performing processes are usually accompanied by lower surfactant retention (but not vice versa).

The viscosity of microemulsion plays an important role in chemical flood success, as viscous microemulsions enhance phase trapping (due to entrapment), thus increasing the surfactant retention. An interesting characteristic about microemulsion viscosity is that it's a strong function of composition. The microemulsion viscosity often exceeds the pure component viscosities (water and oil). It cannot be linearly interpolated. The viscosity is a complex function of its composition and temperature among other variables. One way to reduce the microemulsion viscosity is by adding alcohol (Sahni, 2009). Another way for reducing the microemulsion viscosity is by using highly branched surfactants, as the branching in the surfactant reduces the tendency to form ordered structures (Trogus et al. (1979); Levitt et al. (2006); and Hirasaki et al. (2008)). The authors also suggested using a blend of dissimilar surfactants to introduce heterogeneity (thus reducing the ordered structure) to reduce microemulsion viscosity as well as to improve aqueous solubility with synergistic interactions.

5.1.6 Effect of Salinity Gradient

As discussed in Chapter 3, salinity gradient has a pronounced effect on success of the chemical flood, and thereby influencing the surfactant retention also. Nelson (1982) compared the oil recovery efficiency and percentage surfactant retained for different core

floods by changing the salinity gradient (i.e. changing the salinities for water flood brine, chemical slug and polymer drive). Irrespective of the water flood and chemical slug salinities, whenever the polymer drive salinity is at the type II salinity, the surfactant retention was always 100%.When the water flood, chemical slug, and polymer drive were all in type I salinity, lower surfactant retention was observed, but the oil recovery was also low because of high IFT in type I conditions. The best oil recovery and less retention were observed during negative salinity gradient floods, i.e., transition from type II to type III to type I. The over optimum salinity ahead of the surfactant slug retards the surfactant and the low salinity (type I) behind the slug remobilizes it.

5.2 EXPERIMENTAL METHODOLOGY

Surfactant adsorption/retention studies can be either done in static tests (batch equilibrium tests on crushed core grains) or dynamic tests (core flood) in the laboratory. The static tests are conducted without the oil phase, and hence the adsorption can only be quantified. Furthermore, because of the crushed core grains the surface area is higher than the natural rock before crushing, which increases the adsorption. For this and other reasons, the adsorption from static measurements is typically higher than from dynamic measurements unless great care is taken to prevent artifacts and to match the actual process design e.g. by measuring the adsorption using the salinity of the polymer drive rather than the slug at optimum salinity. . The dynamic tests are conducted by measuring the surfactant concentration in the effluent samples from core flood experiments. By material balance, the surfactant retained in the core (adsorption, phase trapping, etc.) is calculated. All the results discussed in this chapter are dynamic tests.

The experimental methodology includes sample preparation (from core flood effluents) and analysis using HPLC (high-performance liquid chromatography). HPLC is

a chromatographic technique that can separate a mixture of compounds to identify and quantify the individual components in the mixture. The sample to be analyzed is introduced, in small volumes, in to the stream of mobile phase. The mobile phase is a solvent containing various organic liquids (acetonitrile and ammonium acetate in this study). The chemical transport through the column depends on the specific chemical or physical interactions of specific components in the solution with the stationary phase contained within the column. The time at which a specific analyte elutes is called the *retention or elution time*. The detector provides the characteristic retention time for the analyte. A refinement to the HPLC method is to vary the composition of the mobile phase during the analysis and it is called *gradient elution*. One example is to start the solvent mixture at 75% ammonium acetate and 25% acetonitrile and end with 15% ammonium acetate and 85% acetonitrile in a gradient for 30 minutes. Gradient elution decreases the retention of the later-eluting components so that they elute faster, giving narrower (and taller) peaks for most components thus increasing the resolution of the chromatogram by giving increased peak height, which helps in identifying trace components. A sample HPLC chromatogram containing three different surfactants is shown in Figure 5.1.

The more detailed procedure for sample preparation and HPLC parameters is as follows.

Sample preparation:

1. 1% sodium hypochlorite (bleach), 5% TEGBE (or other solvent) in DI water was prepared.

    a. Bleach was added only when the solution contained polymer.

2. The effluents (aqueous solution in the effluent containing A/S/P) were then diluted with the above mentioned solution to the desired concentration within the detection limit of HPLC.

117

3. It was then heated to 50-60 °C for about 24 hours or until solution was no longer viscous.

4. It was then filtered with 0.45 micron syringe filter into HPLC sample vial.

   HPLC parameters and settings:

1. Column: Dionex Acclaim Surfactant Column (4.6 x 250 mm)

2. Solvents:

   a. Acetonitrile (CH_3CN)

   b. 0.1M Ammonium Acetate in DI, pH ~5.5 (adjusted with glacial acetic acid)

3. Method:

   a. Start 75% Ammonium acetate, 25% CH_3CN

   b. Gradient to ~15% Ammonium Acetate, 85% CH_3CN, over 30 min

   c. Hold 15%/85% for 10-40 min until surfactant is eluted.

4. Parameters;

   a. Detector (ELSD from Polymer Labs/Dionex):

      i. Nebulizer – 60 °C

      ii. Evaporator – 115 °C

      iii. Gas Flow – 1.5 SLM

   b. Detection Range: ~0.005% - 0.1% surfactant for 500 μl sample loop
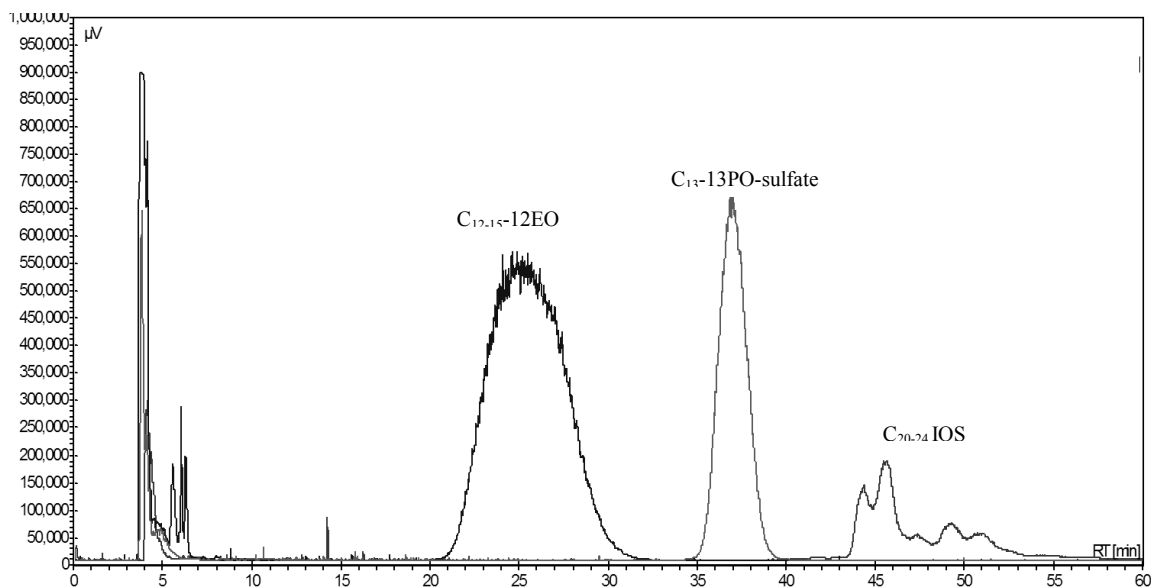
Figure 5.1: Sample chromatogram from HPLC analysis

5.3 ANALYSIS OF THE RETENTION DATA

The data used in this analysis are from the core flood experiments conducted over the past few years in the chemical EOR group of CPGE at the University of Texas at Austin. Now that we have understood the different mechanisms and factors affecting the surfactant retention during chemical floods, the purpose of this analysis is to examine whether is there any underlying trends in the surfactant retention with regards to mineralogy, surfactant structure/type, pH, Eh, oil composition and so forth. The purpose is to help identify important variables affecting retention and to use this knowledge to optimize the chemical flood parameters for low surfactant retention.

Overall the measured surfactant retention values in the data set range from 0.01 to 0.4 mg/g-rock. As shown in Figure 5.2 (Britton et al., 2011), surfactant retention decreases significantly with an increase in the activity of oil. The most reactive oils with alkali (high pH) exhibit the lowest surfactant retention and the non-reactive oil without alkali exhibit the highest retention in this data set. The non-reactive oil category without

119

alkali has surfactant retention values between 0.16 mg/g-rock and 0.37 mg/g-rock with an average value of 0.29 mg/g-rock. The highly reactive oil category with alkali has surfactant retention values between 0.01 mg/g-rock and 0.11 mg/g-rock (Table 5.1). Interestingly, there is no obvious correlation between the retention values and surface mineralogy. The carbonates also exhibit very low retention values with anionic surfactants.

Since these experiments were not conducted in a systematic way to study the effect of each variable, studying the effect of individual variables (e.g. pH - see Figure 5.3) using this data set is difficult because of huge variations in the other variables such as mineralogy, clay content, crude oil, mobility ratio, etc. Hence, it was decided to do a multi variable regression taking into account the effect of different variables. This should help in identifying key variables affecting the surfactant retention, and thus give new insights for ways to minimize the same.

Category	Observations	Surfactant retention (mg/g-rock)	
		Range	Average
Non-reactive and without alkali	11	0.16 - 0.37	0.28
Reactive and without alkali	7	0.12 - 0.31	0.25
Non-reactive with alkali	7	0.19 - 0.3	0.23
Moderately reactive with alkali	19	0.01 - 0.27	0.09
Very reactive with alkali	12	0.01 - 0.11	0.05

Table 5.1: Summary of surfactant retention values categorized under oil reactivity
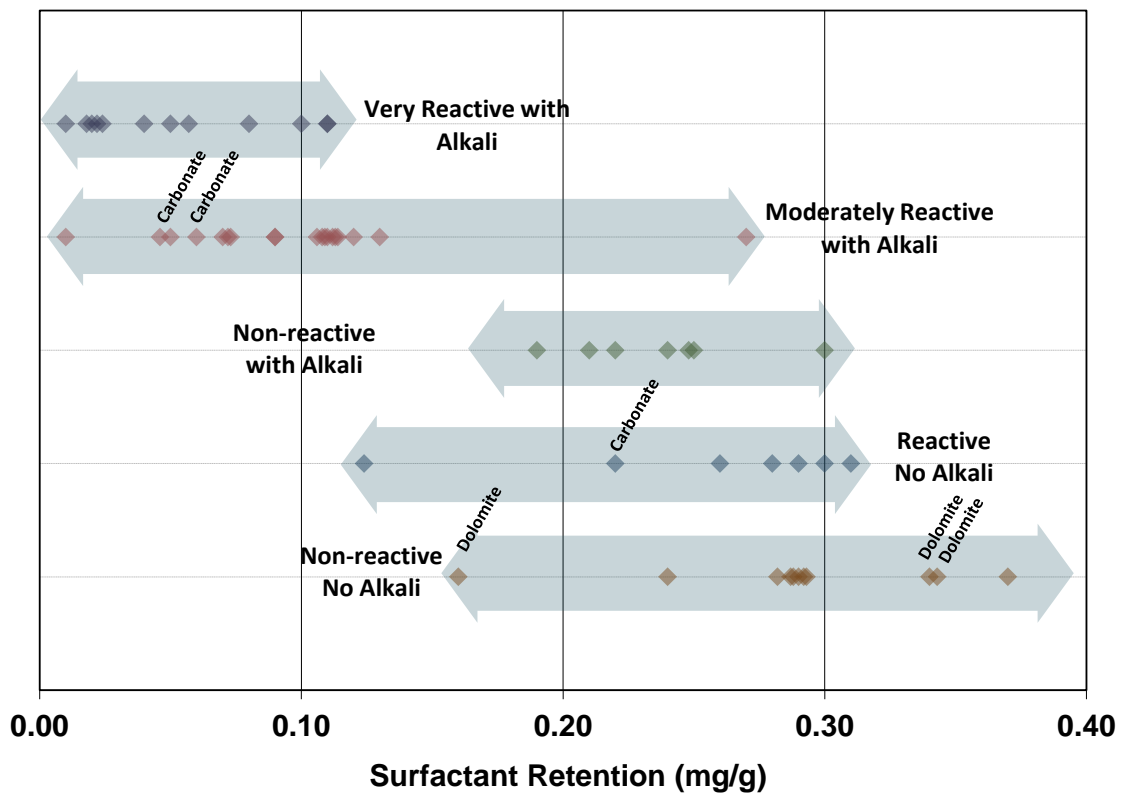
Figure 5.2: Surfactant retention values grouped under oil reactivity and pH (source: *Britton et al., 2011*)
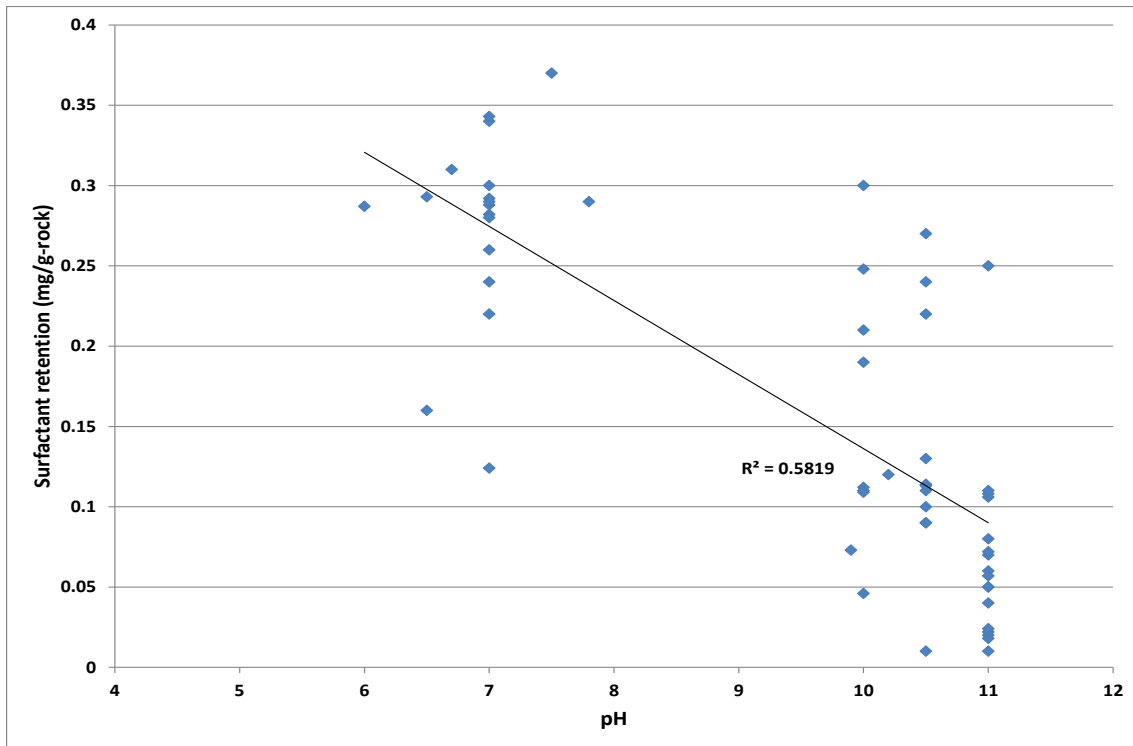
Figure 5.3: Surfactant retention vs. pH – notice poor correlation due to differences in the experimental conditions and other variables

5.4 CORRELATION TO PREDICT SURFACTANT RETENTION

As in chapter 4 (development of a surfactant structure correlation), different variables that might affect the surfactant retention in reservoir rocks were included in the regression equation. The variables were chosen based on both the current literature and our own scientific knowledge and experience. The variables that were included for this multivariable regression study are:

- pH

- Acid number of the oil (TAN)

- Temperature

- Co-solvent concentration

- Salinity of the polymer drive

- Mobility ratio

- Molecular weight of the surfactant

Some of the variables missing from this list because of inadequate data are obviously clay content (mineralogy) and Eh or oxidation-reduction potential (ORP). But, these effects have been studied in detail in the literature and are well understood. Wang (1993) concluded that the surfactant retention measured in field pilots were significantly lower than the laboratory measured retention values because of the reduced state of the reservoir.

Therefore, the equation for surfactant retention based on the variables given above will be:

$$R = a_1TAN + a_2T + a_3C_{co\text{-}solvent} + a_4S_{PD} + a_5pH + a_6M + a_7MW_{surf} + C \qquad \text{--- (5.1)}$$

where, a_1, a_2, ..., a_7 are regression coefficients and C is the intercept

R – Surfactant retention, in mg/g-rock

TAN – Acid number of the oil, in mg KOH/g-oil

T – Temperature, in °C

$C_{co\text{-}solvent}$ – Concentration of co-solvent (alcohol), in wt%

S_{PD} – Salinity of the polymer drive, in ppm

pH – pH of the chemical slug

M – Mobility ratio, given by the ratio of water flood pressure drop to polymer drive pressure drop adjusted for the same flow rate ($\Delta P_{wf}/\Delta P_{PD}|_{same\ flow\ rate}$)

MW_{surf} – mole average weighted molecular weight of the surfactant mixture ($\sum_{i=1}^{n} x_i MW_i$, x_i is mole fraction of component i and MW_i is the molecular weight of component i)

The data used in this regression study is shown in Table 5.2. The regression results (coefficients and standard error) are shown in Table 5.3. The coefficients

determine how strong the variables are affecting the overall regression, while the degree of uncertainty is accounted in the standard deviation. The correlation has an R-squared value of 0.8, implying a good fit. Figure 5.4 shows the predicted values plotted against the experimental values.

5.4.1 Sensitivity Studies

From Table 5.3, it can be seen that the variables acid number (a_1), temperature (a_2), co-solvent (a_3), and pH (a_5) have negative coefficients, while the salinity (a_4), mobility ratio (a_6), and surfactant molecular weight (a_7) have a positive coefficients. As discussed in Chapter 4, the absolute value of the coefficients should not be compared as such, because it's the product, a_iX_i that matters and not the value of a_i alone. Going by the normalized standard deviation (absolute (standard deviation/coefficient)), acid number, pH and mobility ratio have the lowest normalized standard deviation. The other variables have large normalized standard deviations. The *t* value also shows that pH, TAN, and mobility ratio are statistically significant in the equation. To better understand the effect of individual variables, the predicted values are plotted for each case by keeping the other variables (except the one being tested) constant. It should be noted that the clay content and Eh are not included in the regression due to inadequate data, which might explain the poor correlation with some of the other variables.

Effect of Acid Number

Figure 5.5 shows the surfactant retention with change in acid number. The solid lines represent the predicted value from the correlation. The parameters used in the prediction are given in Table 5.4. The predicted and the experimental values should be compared with caution as the predicted values correspond to a certain set of parameters while the experimental points are scattered because of large variation in the conditions.

124

From the figure, for a pH value of 10 and other parameters as given Table 5.4, the surfactant retention is about 0.25 mg/g-rock for a crude oil with TAN – 0 mg KOH/g and about 0.05 mg/g-rock for a TAN value of 3.0 mg KOH/g. A similar trend can be seen for neutral pH condition also, which is not very intuitive. For high pH case, it can be speculated that with increase in acid number, the in-situ generated soap decreases the active sites available for synthetic surfactant adsorption, and hence less retention. The same cannot be extended for neutral pH case as there is no soap generation. This implies that the mechanism is complex and not well understood. There were also only a few experiments conducted with high TAN oils at low pH, which makes the uncertainty large.

Effect of pH

As explained in the previous sections, the increase in pH changes the surface charge of the medium from positive to negative, which helps in repulsion of anionic surfactants. Furthermore, as explained above, with the adsorption is decreased with increase in oil reactivity also. The effect is shown in Figure 5.6. For a TAN of 0 mg KOH/g and the parameters given in Table 5.4, the retention decreases from 0.35 mg/g at pH-6 to about 0.19 mg/g at a pH of 11. For an active oil with a TAN value of 2 mg KOH/g, the retention predicted changes from 0.22 mg/g at pH-6 to about 0.08 mg/g at a pH of 11. Also, the number of observations in low or neutral pH is less (~18) compared to the high pH case, which skews the data in regression study.

Effect of Mobility Ratio

It's well known that the mobility ratio is an important parameter affecting the surfactant retention value. If the mobility ratio between the oil and the chemical slug is poor, then the surfactant will break through early, or if the mobility ratio between the chemical slug and polymer drive is poor, then the microemulsion phase trapping will be

high leading to poor oil recovery and high surfactant retention. Figure 5.7 shows the experimental and predicted values (parameters given in Table 5.4) of retention with change in mobility ratio. Even though the correlation predicts an increase in retention with increase in mobility ratio, the experimental values show large scatter probably due to variations in experimental conditions and uncertainties in the mobility ratio calculation. It should be noted that the number of observations with mobility ratio of more than 0.5 is very few and there are almost no data with mobility ratio of more than 1 in this particular data set since all of the core floods were designed to perform as well as possible using optimized formulations including polymer concentration. If sufficient retention data for mobility ratios greater than one were included, the correlation would almost certainly be stronger. Furthermore, the mobility ratio was calculated as a ratio of water flood pressure drop to polymer drive pressure drop adjusted for the same flow rate. Therefore, the calculation depends on the quality of the pressure drop data also.

Effect of Co-solvent Concentration

The change in surfactant retention with alcohol concentration is shown in Figure 5.8. It's rather surprising to see that there is almost no correlation between retention and co-solvent concentration. It's well known that an increase in alcohol concentration decreases the surfactant retention. So, why don't we see a better correlation with our experimental data? The reason could be due to the fact that the surfactant formulations used in these core floods were all optimized. In other words, the formulations containing co-solvent or no co-solvent are both equivalent in terms of aqueous solubility/stability, solubilization parameters, equilibration time, and microemulsion viscosity. Because of this optimization, the co-solvent concentration shows little or no correlation.

126

Effect of Temperature

For a given formulation at certain conditions increase in temperature should either decrease or increase surfactant retention depending on microemulsion phase behavior and aqueous stability. Novosad (1982) observed decrease in surfactant retention from 1.7 mg/g-rock to 0.65 mg/g-rock for a change in temperature from 25 °C to 70 °C. Figure 5.9 shows the experimental and predicted values for change in retention with temperature. Again, there is no correlation seen between temperature and surfactant retention. The same explanation given for co-solvent effect holds here also. The surfactants were optimized for the specific temperature, and hence there is no marked change observed with change in temperature.

Effect of Salinity

Figure 5.10 shows the plot of retention vs. salinity for experimental and the predicted values. As with co-solvent and temperature, there is no correlation observed with salinity also. Recall the observation by Glover et al. (1979) that the surfactant retention increased linearly with salinity until a critical salinity above which there was an abnormal deviation from linearity. That critical salinity corresponds to type II transition salinity. This implies that the effects of salinity gradient and phase behavior corresponding to that salinity are more important than the absolute value of salinity itself. As explained before, the surfactants were optimized for that particular salinity, and the core flood designs were made to end in type I for classical salinity gradient effect. This optimization may be a reason for poor correlation between salinity and retention.

Effect of Surfactant Molecular Weight

Conventional wisdom is that the adsorption increases as the molecular weight of the surfactant increase. Somasundaran and Hanna (1977) observed an increase in

adsorption with increase in carbon chain length of alkyl ammonium acetate and sulfonate due to increased lateral interaction between chains. However, Figure 5.11 shows that there is no correlation between surfactant retention and surfactant molecular weight (mole average). It should be noted that the molecular weight of the surfactants used in this study are several fold higher than the ones used earlier. This surprise finding implies that if the surfactants are optimized for specific conditions, the size of the surfactant has little or no impact on adsorption/retention.

5.5 CHROMATOGRAPHIC SEPARATION OF SURFACTANTS – A MYTH?

The optimum surfactant formulations often contain mixture of surfactants than just a single surfactant. Therefore, for the chemical flood to be successful, the surfactants must transport together in a mixed micelle and must not chromatographically separate. The reservoir rock can be considered as a large chromatographic column, and therefore the individual surfactants may preferentially adsorb on the rock surface or partition into the oil due to different interactions. But, why do some surfactant mixtures separate while others are not? What are the key factors in minimizing or eliminating this preferential adsorption/chromatographic separation? Graciaa et al. (1987) modeled the chromatographic separation due to partitioning of surfactants in different phases. They predicted that surfactant mixtures that resist the formation of mixed micelles are more susceptible for separation. They also concluded that mixture of anionic and nonionic surfactants show less separation than the nonionic surfactant by itself. Mannhardt and Novosad (1991) also observed similar behavior and concluded that the adsorption of surfactants depends not only on their affinity for the surface, but also on their tendency to form micelles. Austad et al. (1992) conducted static and dynamic adsorption studies for

128

polydisperse ethoxylated sulfonates, and concluded no significant preferential adsorption of the various EO-sulfonate oligomers when oil was present.

Even though a large number of papers are available on surfactant adsorption/retention, most of them discuss the overall adsorption of surfactant(s) rather than quantifying the individual surfactants in the mixture. HPLC can serve as a valuable tool in quantifying the individual surfactants in the effluent samples. As it can be seen in the results, from numerous core flood experiments conducted, no detectable chromatographic separation of surfactants has been observed.

Figures 5.12 through 5.15 (Britton et al., 2011) show retention data for surfactant mixtures without any chromatographic separation. The first three examples were conducted in Berea sandstone and the last one in a carbonate core. Figure 5.12 is a mixture of alkoxy sulfate and internal olefin sulfonate (IOS) surfactants. The surfactants broke through together, indicating no separation between the two. The y-axis is normalized to the injected concentration to account for the differences in ratio of surfactant concentrations. The overall retention was 0.05 mg/g-rock with 0.02 mg/g for the alkoxy sulfate and 0.03 mg/g for the IOS. Figure 5.13 also shows similar profile for a mixture of alkyl benzene sulfonate (ABS) and an ethoxylated alcohol with a retention value of only 0.01 mg/g-rock for each surfactant. Figure 5.14 is a three surfactant formulation containing an alkoxy sulfate, IOS, and ethoxylated alcohol. The surfactants still showed no chromatographic separation with an overall surfactant retention of 0.04 mg/g-rock. Figure 5.15 shows data for a mixture of C_{15-18} IOS and a Guerbet large hydrophobe alkoxy carboxylate (C_{28}-25PO-45EO-carboxylate). It should be noted even for this mixture having a huge variation in molecular weight (350 for IOS and about 3900 for the carboxylate), the retention is still similar (0.16 mg/g-rock for the IOS and 0.18 mg/g-rock for the carboxylate). When the molar retention (instead of mg) for the

surfactant was calculated, the value for Guerbet alkoxy carboxylate was almost an order of magnitude less than the IOS counterpart ($3*10^{-04}$ mol for IOS and $3*10^{-05}$ mol for the carboxylate).

To summarize, from hundreds of core flood effluent samples analyzed, there has not been a single case where chromatographic separation/preferential retention was observed. The data includes different mineralogy (sandstones, carbonates, clay content), different surfactant structures like ABS, IOS, alkoxy sulfates, large hydrophobe alkoxy sulfates and carboxylates, even including the nonionic surfactants. So, why don't we see chromatographic separation? The reason is mainly due to careful selection of surfactants and proper design of the core floods. The surfactants are selected systematically by conducting phase behavior and aqueous stability experiments giving proper consideration to microemulsion viscosity, equilibration time, fluidity, IFT (qualitatively observed from the emulsion test), etc. When such optimum formulations with proper design of core flood (salinity gradient, mobility control, and pH) are devised, the formation of mixed micelles is favored and hence they travel together, and are retained as a single component. When off-the-shelf surfactants are used and screened only for IFT reduction without doing these systematic studies, they will be more susceptible for preferential retention, and hence they may chromatographically separate.

5.6 CONCLUSIONS

A large number of dynamic surfactant retention measurements have been conducted over a wide range of conditions using a variety of new-generation surfactants in both sandstone and carbonate cores. Surfactant retention values for both surfactant-polymer (SP) and alkaline-surfactant-polymer (ASP) floods were between 0.01 and 0.37 mg/g-rock. Low retention of anionic surfactants has also been observed for carbonates.

This surprise finding implies that factors such as microemulsion viscosity contribute as much or more to dynamic surfactant retention than adsorption does. The analysis of core flood data suggests a strong trend between oil reactivity and pH. A new correlation has been developed for surfactant retention including the effects of acid number, pH, temperature, co-solvent concentration, salinity, mobility ratio, and surfactant molecular weight. Results suggest that for optimized surfactant formulations with good mobility control and a favorable salinity gradient, surfactant retention significantly decreases with an increase in pH or oil reactivity. HPLC measurements were used in quantifying the surfactant concentration in the core flood effluents, and results from numerous core flood data indicate no measurable chromatographic separation or preferential adsorption.

Coreflood classification	Oil TAN (mg KOH/g-oil)	Temperature (°C)	Co-solvent (wt%)	Polymer Drive Salinity (ppm)	Max Effluent pH	Mobility Ratio (dP_{wf}/dP_{PD})	Mol fraction avg. molecular weight of the mixture	Surfactant Retention (mg/g-rock)
Nonreactive, no alkali	0.0	25	1.00%	11,000	7	0.62	559.51	0.288
Nonreactive, no alkali	0.0	25	1.00%	11,000	7.5	0.95	559.51	0.37
Nonreactive, no alkali	0.0	25	1.00%	15,250	6	0.84	559.51	0.287
Nonreactive, no alkali	0.0	25	1.00%	8,000	7	0.42	559.51	0.292
Nonreactive, no alkali	0.0	25	1.00%	8,000	7	0.45	559.51	0.29
Nonreactive, no alkali	0.0	25	1.00%	20,000	6.5	0.55	559.51	0.293
Nonreactive, no alkali	0.0	30	2.00%	20,000	7	0.50	559.51	0.282
Nonreactive, no alkali	0.1	100	0.00%	25,000	7	0.93	679.91	0.34
Nonreactive, no alkali	0.1	100	0.00%	20,000	7	0.20	601.60	0.343
Reactive no alkali	0.8	44	0.25%	15,000	7	0.20	715.65	0.26
Reactive no alkali	0.8	44	0.50%	5,000	6.7	0.16	715.65	0.31
Reactive no alkali	0.8	44	0.50%	5,000	7.8	0.46	715.65	0.29
Reactive no alkali	0.5	83	1.00%	41,000	7	0.29	676.39	0.3
Reactive no alkali	1.0	46	0.50%	22,000	7	0.10	719.37	0.28
Reactive no alkali	2.4	30	0.00%	10,000	7	0.01	638.27	0.124
Reactive no alkali	0.8	83	1.00%	8,300	7	0.45	676.39	0.22
Nonreactive alkali	0.0	27	1.00%	40,000	11	0.50	559.51	0.25
Non reactive alkali	0.1	100	0.50%	2,000	10.5	0.21	650.63	0.22
Non reactive alkali	0.8	38	2.00%	14,000	10.5	0.42	588.30	0.19
Non reactive alkali	0.0	25	0.75%	17,000	10	0.37	751.76	0.248
Non reactive alkali	0.0	25	0.75%	11,000	10	0.41	751.76	0.3
Non reactive alkali	0.0	25	0.75%	16,000	10.5	1.40	751.76	0.24
Non reactive alkali	0.3	85	3.00%	3,000	10.5	0.36	580.21	0.21
Moderately reactive	1.9	62	1.00%	6,000	11	0.33	413.47	0.06
Moderately reactive	1.9	62	1.00%	6,000	10	0.17	413.47	0.112
Moderately reactive	1.9	62	1.00%	6,000	10	0.20	413.47	0.11
Moderately reactive	1.9	62	0.30%	6,500	11	0.23	588.30	0.07
Moderately reactive	1.9	62	0.30%	6,500	10.5	0.05	588.30	0.13
Moderately reactive	1.9	62	0.15%	6,500	11	0.15	1320.00	0.072
Moderately reactive	1.9	62	0.00%	6,500	11	0.10	1320.00	0.05
Moderately reactive	1.9	62	0.00%	6,500	10.5	0.08	1320.00	0.09
Moderately reactive	1.9	62	0.00%	6,500	11	0.06	1320.00	0.108
Moderately reactive	1.9	62	0.30%	6,000	10	0.17	588.30	0.109
Moderately reactive	1.9	62	0.30%	6,000	11	0.11	515.19	0.106
Moderately reactive	1.9	62	0.00%	6,000	10.5	0.06	1320.00	0.114
Moderately reactive	1.9	62	0.20%	6,000	10.5	0.04	1320.00	0.113
Moderately reactive	1.0	83	0.00%	27,000	9.9	0.40	601.36	0.073
Moderately reactive	1.0	83	0.00%	30,000	10.5	0.30	601.36	0.27
Moderately reactive	1.0	83	0.50%	28,000	10.5	0.41	601.36	0.09
Moderately reactive	1.0	55	1.00%	1,600	10.5	0.30	632.35	0.01
Moderately reactive	1.0	55	1.00%	11,600	10.2	0.07	632.35	0.12
Moderately reactive	0.5	83	0.10%	26,000	10	0.07	849.76	0.046
Very Reactive, alkali	2.0	46	0.00%	5,000	11	0.10	368.52	0.057
Very Reactive, alkali	2.0	46	1.00%	5,000	11	0.10	515.19	0.11
Very Reactive, alkali	2.0	46	1.00%	5,000	11	0.11	515.19	0.02
Very Reactive, alkali	2.0	46	1.00%	5,000	11	0.05	515.19	0.018
Very Reactive, alkali	2.0	46	1.00%	5,000	10.5	0.08	515.19	0.1
Very Reactive, alkali	2.0	46	0.40%	5,000	11	0.05	591.01	0.01
Very Reactive, alkali	3.2	55	0.00%	250	11	0.38	461.00	0.022
Very Reactive, alkali	3.2	55	0.00%	250	11	0.20	567.48	0.04
Very Reactive, alkali	3.2	55	0.00%	250	11	0.10	584.67	0.024
Very Reactive, alkali	3.2	55	0.00%	250	11	0.08	567.48	0.08
Very Reactive, alkali	2.1	85	0.00%	32,000	11	0.35	479.84	0.05
Very Reactive, alkali	2.1	55	1.00%	32,000	10.5	0.10	496.51	0.11

Table 5.2: Data used in the regression analysis

	Coefficients	Standard deviation	Normalized standard deviation	t Stat
R - squared : 0.79804				
Standard Error: 0.05311				
Intercept, C	0.4846366	0.0583338	0.1203661	8.3079854
TAN, a_1	-0.0538725	0.0132962	0.2468082	-4.05173
Temp, a_2	-0.0001459	0.0003732	2.5581479	-0.390908
Co-solvent, a_3	-0.4855773	1.5418887	3.1753725	-0.314924
Salinity, a_4	0.0000002	0.0000008	5.0571129	0.1977413
pH, a_5	-0.0275395	0.0054598	0.1982540	-5.044035
M.R, a_6	0.0383129	0.0356292	0.9299536	1.0753225
Surf MW, a_7	0.0000072	0.0000327	4.5296710	0.2207666

Table 5.3: Summary of regression coefficients and standard deviation
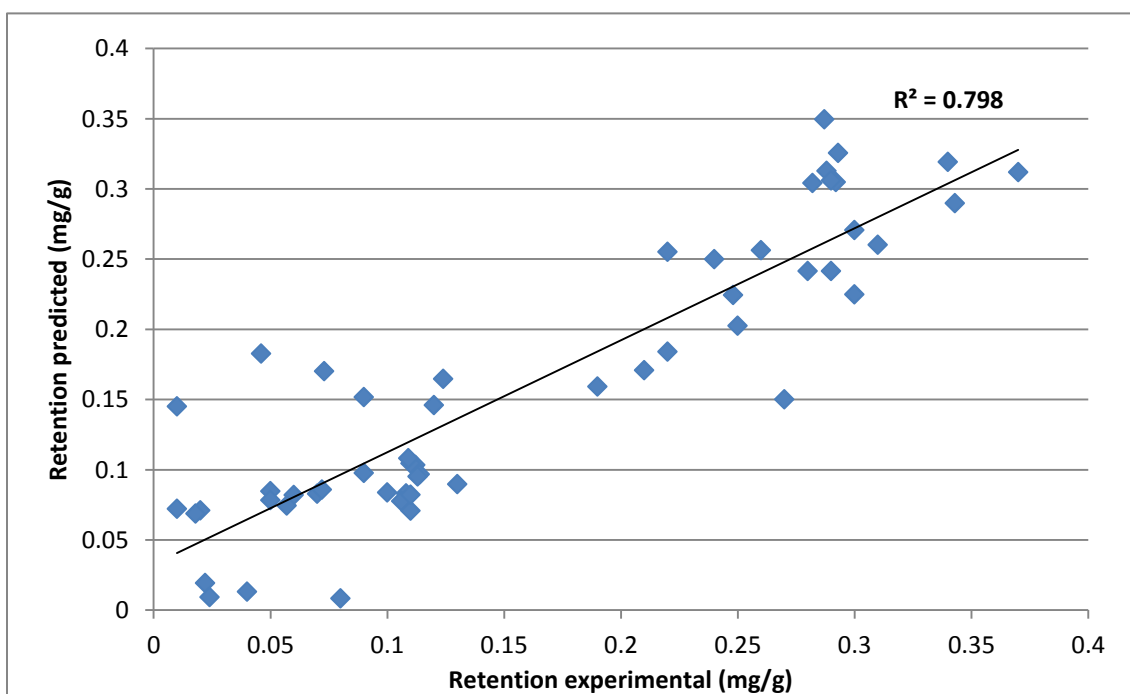
Figure 5.4: Predicted vs. experimental retention values
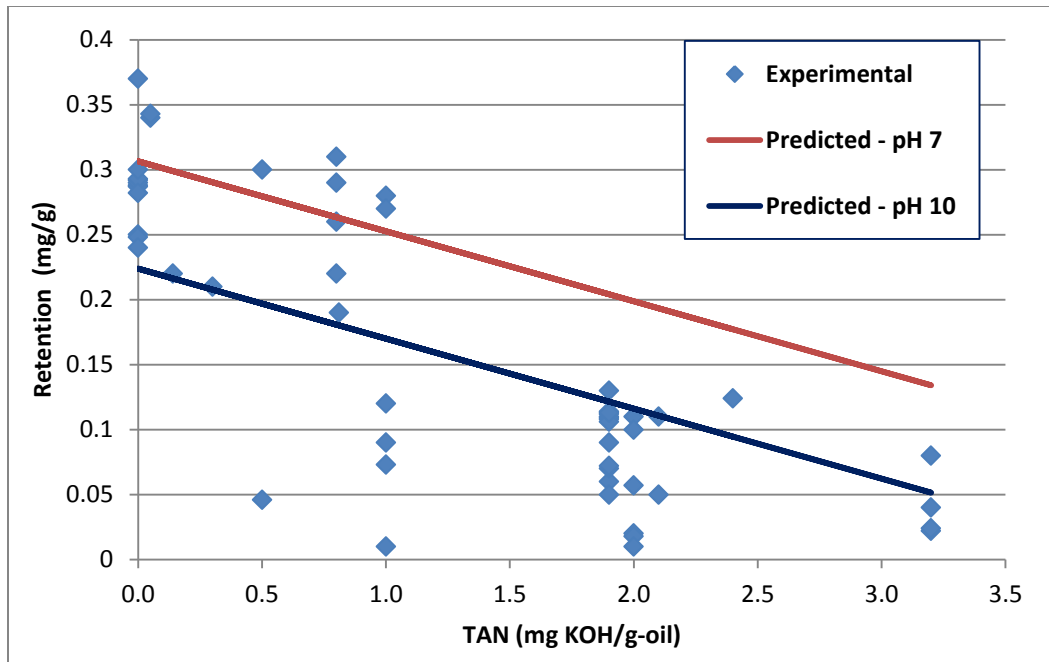
Figure 5.5: Surfactant retention vs. acid number – predicted and experimental
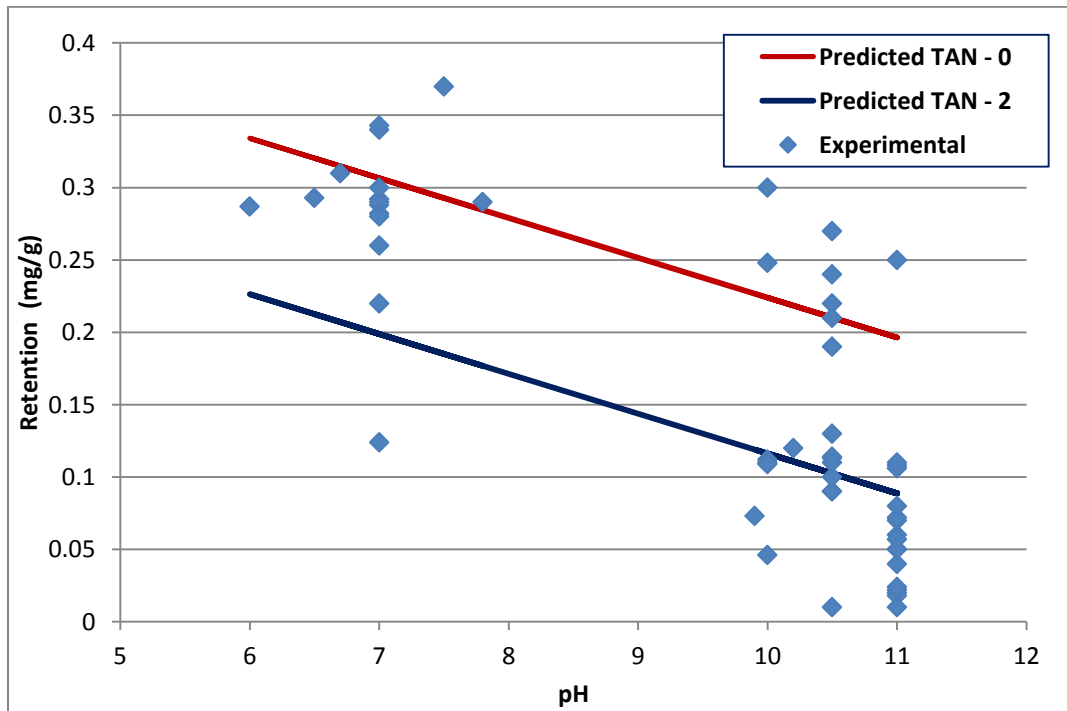
Figure 5.6: Surfactant retention vs. pH – predicted and experimental

134
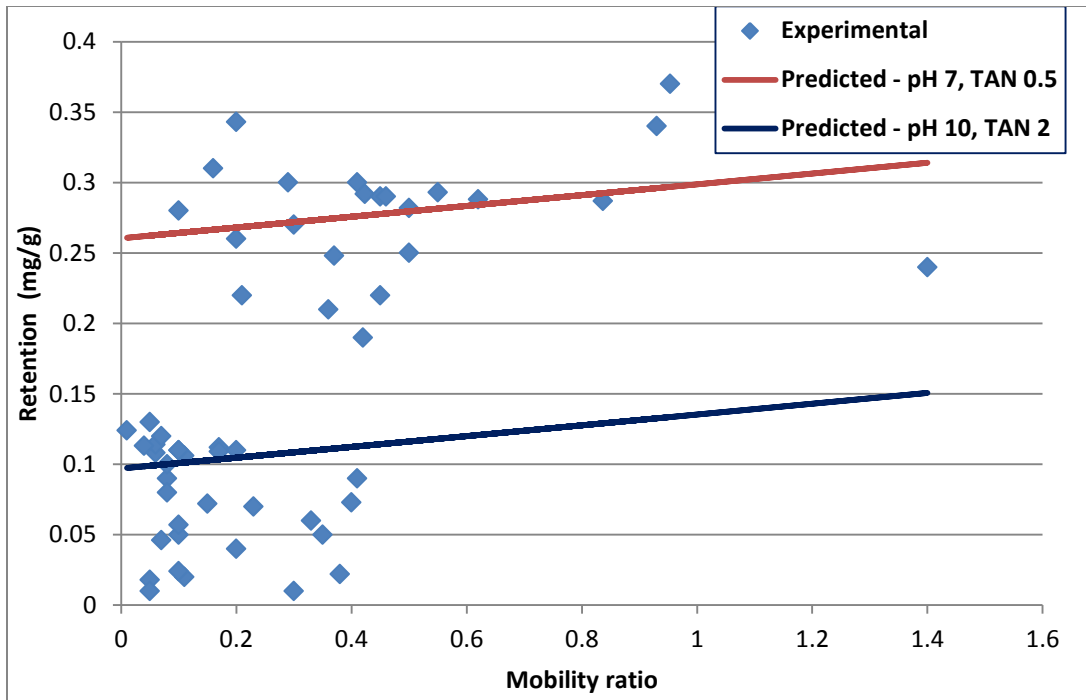
Figure 5.7: Retention vs. mobility ratio – experimental and predicted
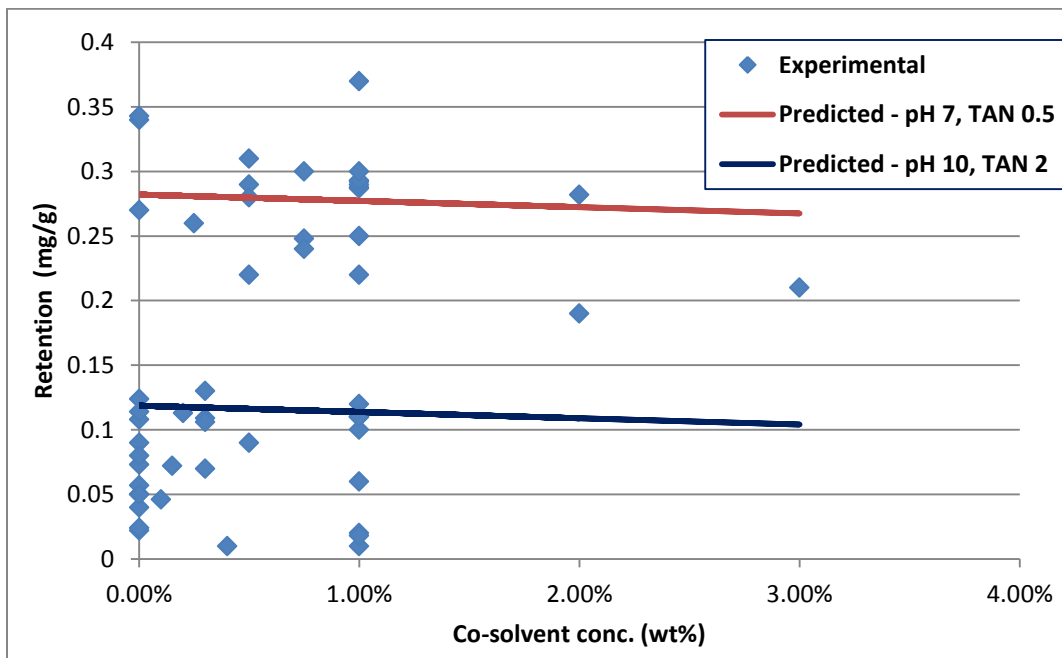
Figure 5.8: Retention vs. co-solvent concentration – experimental and predicted
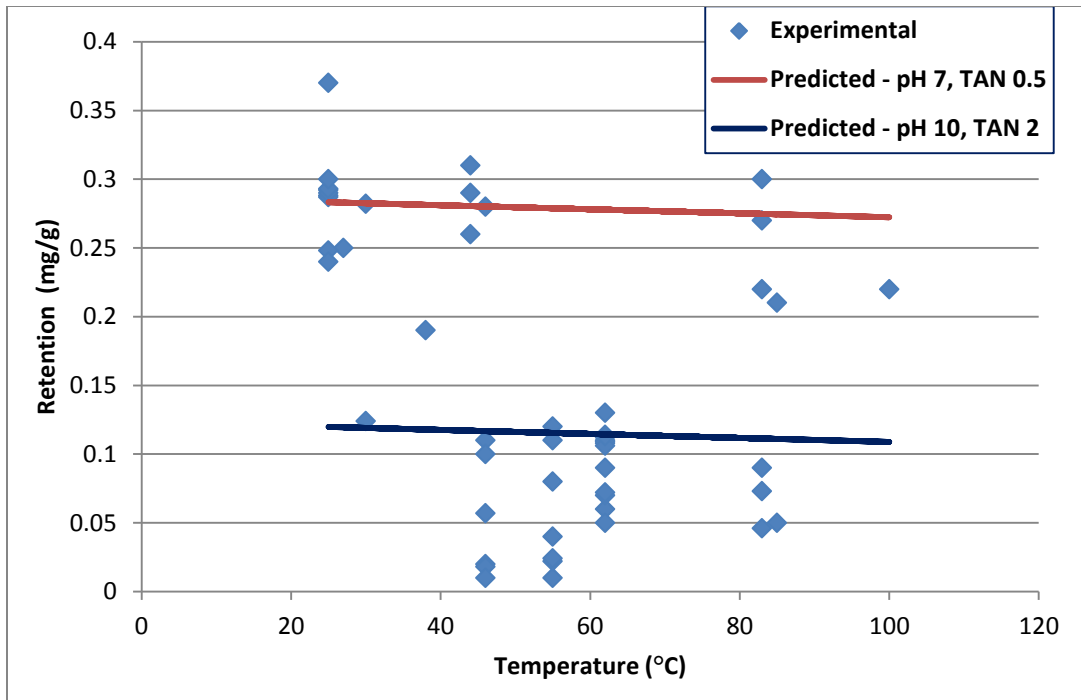
Figure 5.9: Retention vs. temperature – experimental and predicted
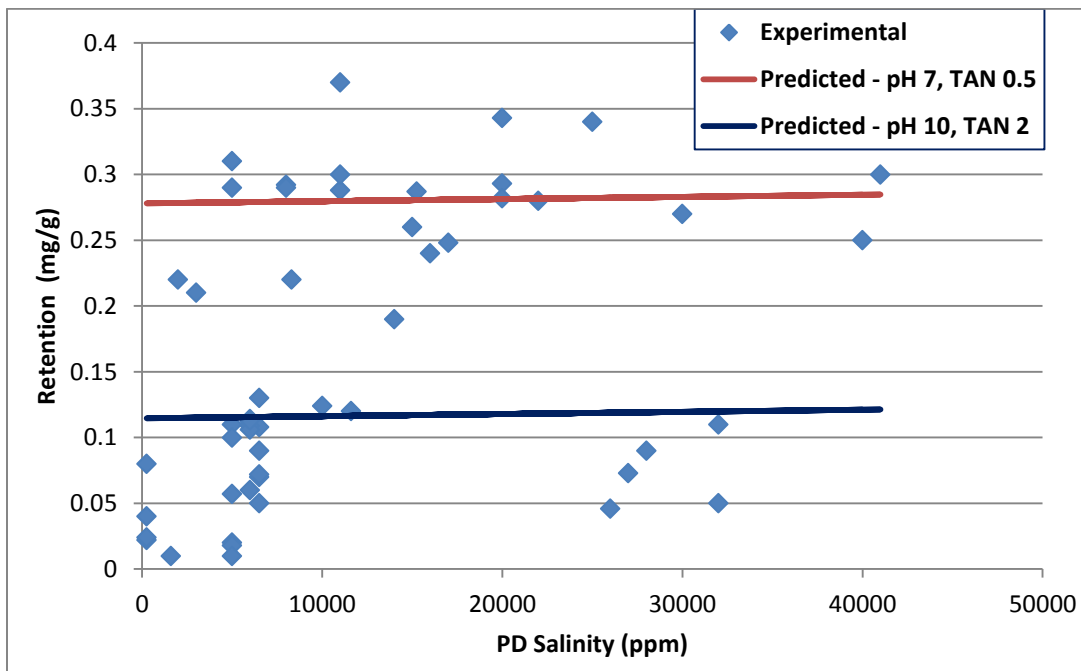
Figure 5.10: Retention vs. salinity – experimental and predicted
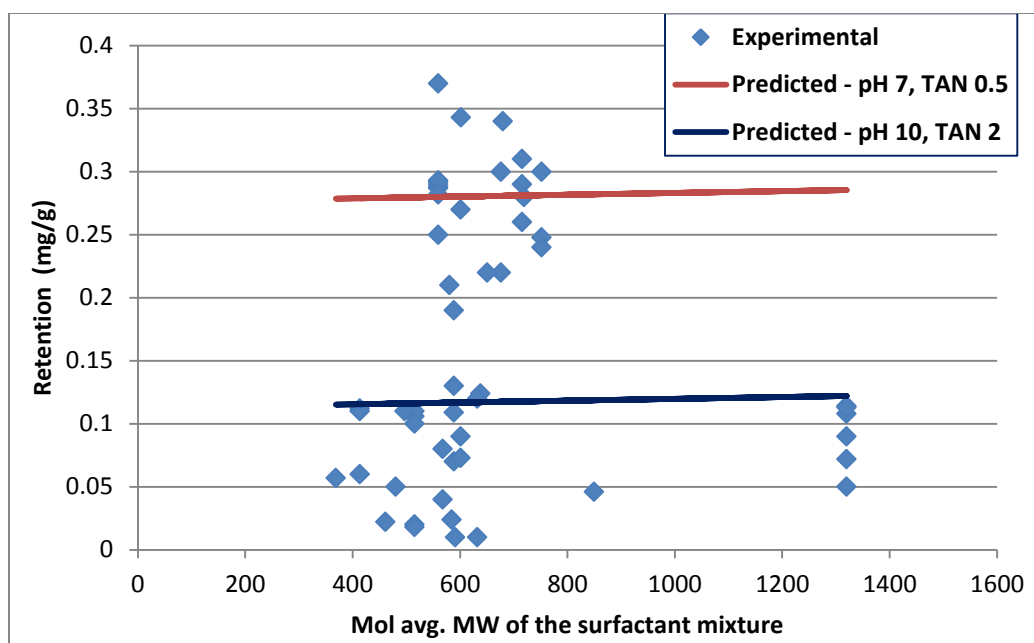
Figure 5.11: Retention vs. MW of the surfactant mixture – experimental and predicted

Parameters	Figure 5.5	Figure 5.6	Figure 5.7	Figure 5.8	Figure 5.9	Figure 5.10	Figure 5.11
TAN, mg KOH/g	varied	0 and 2	0.5 and 2	0.5 and 2	0.5 and 2	0.5 and 2	0.5 and 2
pH	7 and 10	varied	7 and 10	7 and 10	7 and 10	7 and 10	7 and 10
Mobility ratio	0.5	0.5	varied	0.5	0.5	0.5	0.5
Co-solvent, wt %	0.50%	0.50%	0.50%	varied	0.50%	0.50%	0.50%
Temp, C	50	50	50	50	varied	50	50
PD Salinity, ppm	10,000	10,000	10,000	10,000	10,000	varied	10,000
Surf MW wt.	500	500	500	500	500	500	varied

Table 5.4: Parameters used for prediction
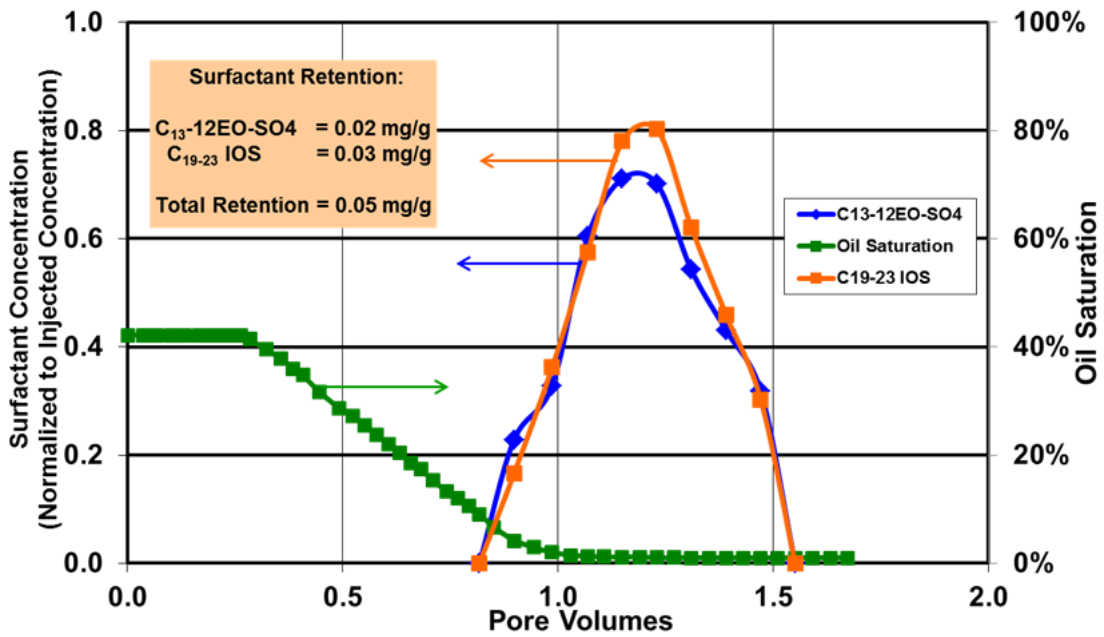
Figure 5.12: Mixture of IOS and ether sulfate showing no separation (source: *Britton et al., 2011*)
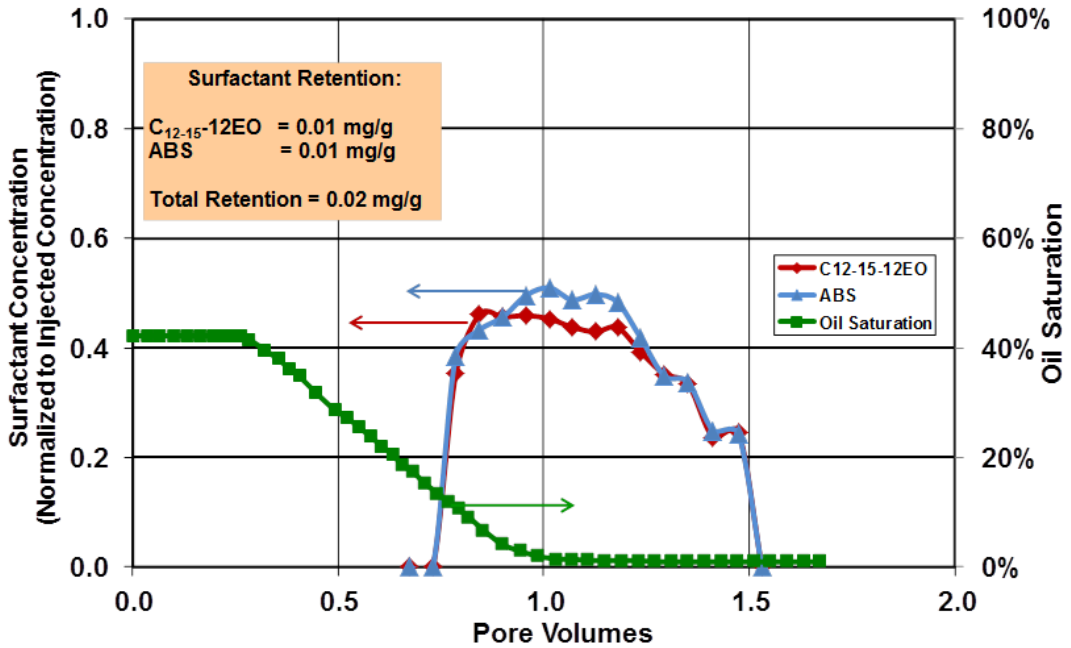
Figure 5.13: Mixture of alkyl benzene sulfonate (ABS) and alcohol ethoxylated showing no separation (*source: Britton et al., 2011*)
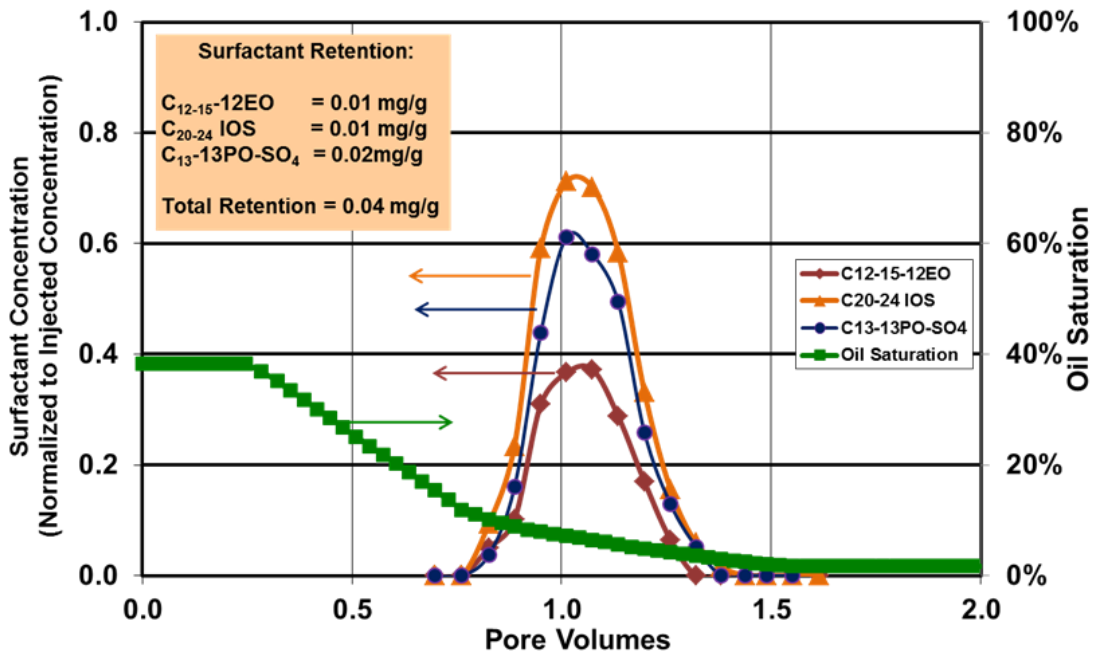
Figure 5.14: Mixture of IOS, alcohol ethoxylated and alcohol propoxy sulfate showing no separation (*source: Britton et al., 2011*)
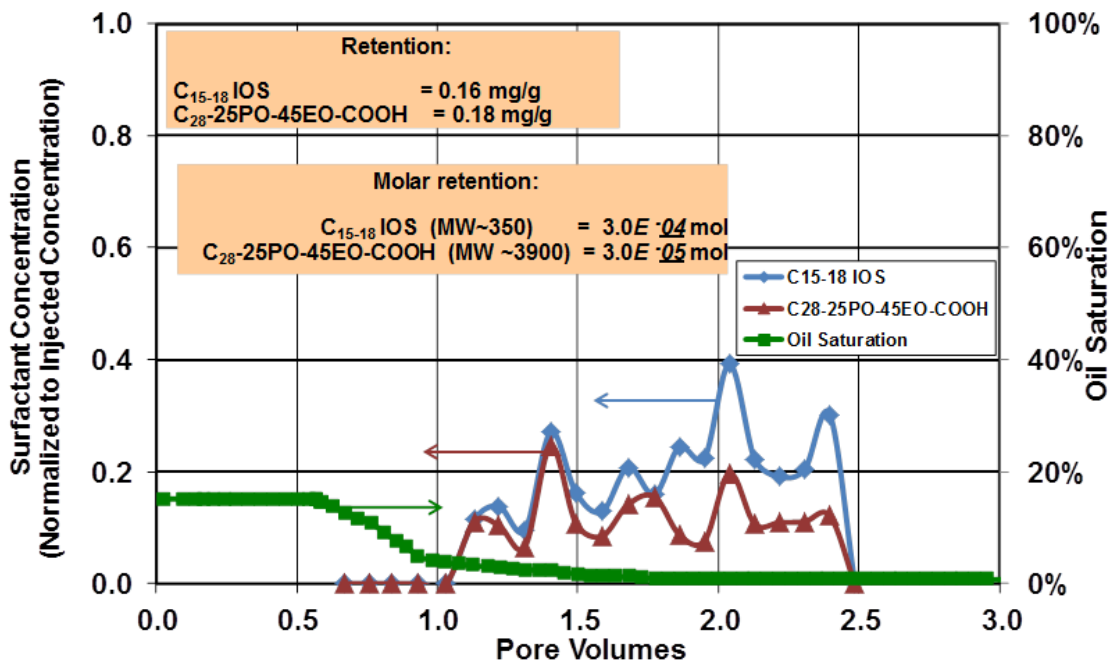
Figure 5.15: Mixture of IOS and Guerbet alkoxy carboxylate showing no separation (*source: Britton et al., 2011*)

Chapter 6: Summary and Conclusions

The summary of key findings and conclusions of the research are discussed in this chapter. Significant progress was made in terms of both developing and testing new surfactants and how to determine the optimum structure of surfactants under different conditions, particularly harsh reservoir conditions.

The need for large hydrophobe surfactants is ever increasing with chemical enhanced oil recovery being tested for more new candidates with varied oils and reservoir conditions. The advent of stabilizing ether sulfate surfactants at elevated temperatures was a significant invention, and it greatly increased the surfactant options that can be tested for a particular candidate. Guerbet alkoxy sulfates (GAS) satisfy the requirement for large hydrophobes, and have given a chance to explore new candidates for chemical EOR, which would have otherwise not been considered. Formulations containing GAS surfactants produced ultra-low interfacial tensions and core flood experiments produced high oil recoveries with low residual oil saturation.

GAS surfactants, however needed high pH for thermal stability at elevated temperatures. In cases where usage of alkali is prohibitive, an alternative would be to find an effective formulation at neutral pH. Guerbet alkoxy carboxylates (GAC) surfactants satisfy this requirement. They are thermally and chemically stable at all values of reservoir pH up to at least 120 C (250 F). Formulations containing mixture of GAC and IOS surfactants produced ultra-low interfacial tensions and core flood experiments produced high oil recoveries with residual oil saturation as low as 1%. Analysis of core flood effluent samples also showed that the GAC-IOS mixture had transported together (no chromatographic separation). Additional benefits have been observed when GAC surfactants were tested with reactive oils. For the first time, synergistic interactions of a

surfactant and an active oil have been observed at neutral pH conditions that appear to be similar to the formation of soap when alkali reacts with organic acids contained in active oils.. Low-cost alkyl benzene sulfonate (ABS) surfactant has been re-tested as an alternative co-surfactant showing enhanced calcium tolerance, due to the synergy between the carboxylate and ABS components. Thus, the advent of this new class of cost-effective surfactants greatly broadens the application of chemical EOR.

Also, a new class of alternative petrochemical-based large hydrophobe surfactants (TSP) was successfully developed and tested and is expected to be competitive in cost with other high performance surfactants. A high-pressure (1700 psi) live oil core flood using a waxy crude and reservoir core was conducted with this new surfactant and produced high oil recovery and very low final oil saturation of about 1%. The new structure (4 benzene rings) is expected to be effective in solubilizing heavy crude oils with high paraffin and asphaltene content.

Surfactant technology has improved dramatically in the last 5 years, both in terms of efficiency and reduction in cost relative to the price of crude oil. Highly branched surfactants with much larger hydrophobes and chemical structures are now available or soon will be available for field use. The challenge often lies in choosing the optimum surfactant for a particular candidate reservoir. In an attempt to simplify that process, a new correlation for predicting the optimum surfactant structure for chemical EOR has been developed. It can be used as a guideline for selecting the best surfactant formulation and also the parameters such as the number of EOs and POs affecting the optimum condition can be better understood. The correlation predicts that larger hydrophobes are needed as either the temperature or oil EACN increases, which is in conformance with recent experimental observations including this study. The correlation can also be used to determine the oil EACN with the knowledge of optimal salinity for a given formulation.

Surfactant retention is a major factor determining the success of a chemical flood and it has to be studied and estimated carefully. A large number of dynamic surfactant retention measurements have been conducted over a wide range of conditions using a variety of new-generation surfactants in both sandstone and carbonate cores. Overall, the surfactant retention values for both surfactant-polymer (SP) and alkaline-surfactant-polymer (ASP) floods were low and ranges between 0.01 and 0.37 mg/g-rock. Low retention of anionic surfactants has also been observed for carbonates. This surprise finding implies that factors such as microemulsion viscosity contribute as much or more to dynamic surfactant retention than adsorption does. The analyses of data suggest a strong trend between oil reactivity and pH. A new correlation has also been developed for surfactant retention including the effects of acid number, pH, temperature, co-solvent concentration, salinity, mobility ratio, and surfactant molecular weight. HPLC measurements were used in quantifying the surfactant concentration in the core flood effluent samples, and results from numerous core flood data indicate no measurable chromatographic separation or preferential adsorption when using the optimized formulations developed as part of this and similar studies at UT.

6.1 RECOMMENDATIONS FOR FUTURE WORK

The interaction of Guerbet alkoxy carboxylate surfactants with reactive oils at neutral pH is worthy of a separate study. The acid number approach to quantify the mobilization of acids in crude oil was not conclusive and hence a different analytical method should be explored. For example, the electrospray ionization mass spectroscopy (ES-MS) is a technique that has been widely used in the industry for identifying individual acids in crude oil. The inconclusiveness in TAN data could also be due to problems in the sampling procedure that was used in this very preliminary attempt.

Therefore, a stringent sampling method/procedure should be followed for any future studies.

As with any new class of surfactants, additional lab testing is needed to further establish their performance and limitations under a wide range of conditions followed by appropriate field tests under promising conditions. The best formulations are equally dependent on the other components including co-solvents, co-surfactants, alkali and in some cases chelating agents. The alkoxy carboxylates (GAC) were used in this study primarily under non-alkaline (neutral) pH conditions. However, they should perform equally well under alkaline conditions. For these reasons, many more tests will be needed over the next few years to fully realize the potential of the GAC surfactants, but the initial results show great promise.

The correlation for predicting surfactant structure discussed in Chapter 4 was developed only for non-active oils. Also, the limitations of the correlation such as not including the effects of co-solvent, divalent cations, and hydrophobe branching should be addressed in future extensions. The correlation should be tested on new formulations as they become available. In fact, it should be used to predict specific outcomes and then the measurements made to evaluate its predictive value over a wide range of conditions followed by improvements and extensions as needed.

A more systematic study of surfactant retention under dynamic conditions would be useful. Although some progress was made in understanding and correlating surfactant retention in cores based on available data taken under different conditions as part of unrelated field studies, a systematic study with each variable studied one at a time is needed to create a data set more suitable for this purpose.

Appendix: Microemulsion Phase Behavior Summary

Exp. #	Surfactant (A) Structure	lot#	wt%	Surfactant (B) & (C) Structure	lot#	wt%	Solvent Co-Solvent	wt%	Oil	Scan	Alkali	Sol. Ratio (cc/cc)	Opt. Sal. wt% (Sca	Max Sol. Clear	Brine	Comments
U-01	C15-18 IOS	18239-5A	1.00%	-	-	-	TEGBE	0.50%	U # 1 Dead	SUTIB	none	~4 @ 8.5% TDS	>8.5%	-	SUTIB	All Type 1 Very dark low viscocity emultion
U-02	C12-15 AOS	7258054-BN2	1.00%	-	-	-	TEGBE	0.50%	U # 1 Dead	2X SUTIB	none	~4	>7.5%	n/a	SUTIB	No good emulsion is observed
U-03	C15-18 ABS	18098-062007	1.00%	-	-	-	TEGBE	0.50%	U # 1 Dead	2X SUTIB	none	~8	0.02	n/a	SUTIB	Possible type III observed but viscous
U-04	C20-24 IOS	18239-091907	1.00%	-	-	-	TEGBE	0.50%	U # 1 Dead	2X SUTIB	none	~6	~6%	n/a	SUTIB	Viscous gels near optimum salinity
U-05	C20-24 IOS	18239-091907	0.50%	C15-18 ABS	18098-062007	0.50%	TEGBE	1.00%	U # 1 Dead	2X SUTIB	none	-	-	n/a	SUTIB	All Type 2 behavior
U-06	C15-18 IOS	18239-5A	0.50%	C15-18 ABS	18098-062007	0.50%	TEGBE	1.00%	U # 1 Dead	2X SUTIB	none	-	-	n/a	SUTIB	Predominantly Type 2 With gel formation
U-07	C15-18 ABS	18098-062007	0.75%	C12-15 15EO Sulfonate	102287789C	0.25%	TEGBE	1.00%	U # 1 Dead	2X SUTIB	none	-	-	n/a	SUTIB	All Type 2 behavior
U-08	C15-18 IOS	18239-5A	0.75%	C14-30 ABS	8697-038-A	0.25%	TEGBE	1.00%	U # 1 Dead	2X SUTIB	none	6	5.70%	n/a	SUTIB	Possible type III observed but viscous
U-09	C15-18 IOS	18239-5A	0.75%	C14-24 ABS	8697-038-C	0.25%	TEGBE	1.00%	U # 1 Dead	2X SUTIB	none	~10	5.80%	n/a	SUTIB	No good type III is formed
U-10	C16-18-4PO-2EO-COOH	1297-176	0.50%	C20-24 IOS	18239-091907	0.50%	TEGBE	1.00%	U # 1 Dead	2X SUTIB	none	-	-	n/a	SUTIB	Formation of gel
U-11	C16-18-4PO-2EO-COOH	1297-176	1.00%	-	-	-	TEGBE	1.00%	U # 1 Dead	2X SUTIB	none	-	-	n/a	SUTIB	All type 2 Behavaior
U-12	TDA 7EO-COOH	Av07A0432	0.50%	C20-24 IOS	18239-091907	0.50%	TEGBE	1.00%	U # 1 Dead	2X SUTIB	none	-	-	n/a	SUTIB	All type 2 Behavaior
U-13	C20-24 IOS	18239-091907	0.25%	C15-18 ABS	18098-062007	0.25%	TEGBE	0.50%	U # 1 Dead	2X SUTIB	none	-	-	n/a	SUTIB	All type 2 Behavaior
U-14	C15-18 IOS	18239-5A	0.25%	C15-18 ABS	18098-062007	0.25%	TEGBE	0.50%	U # 1 Dead	2X SUTIB	none	-	-	n/a	SUTIB	No emulsion is formed
U-15	C15-18 ABS	18098-062007	1.00%	-	-	-	Butanol 2.77 Ethoxylate (8697-023-C)	1.00%	U # 1 Dead	2X SUTIB	none	-	-	n/a	SUTIB	All type 2 Behavior
U-16	C20-24 IOS	18239-091907	0.50%	C15-18 ABS	18098-062007	0.50%	Butanol 2.77 Ethoxylate (8697-023-C)	1.00%	U # 1 Dead	2X SUTIB	none	-	-	n/a	SUTIB	Formation of gel
U-17	C15-18 IOS	18239-5A	0.50%	C15-18 ABS	18098-062007	0.50%	-	-	U # 1 Dead	2X SUTIB	none	-	>8.5 %	n/a	SUTIB	All Type 1
U-18	C15-18 IOS	18239-5A	0.75%	C14-30 ABS	8697-038-A	0.25%	-	-	U # 1 Dead	2X SUTIB	none	-	-	n/a	SUTIB	No good emulsion is observed
U-19	ORS 27HF(C21.4SO3)	CCPhC14.8CSO3Na	1.00%	-	-	-	TEGBE	1.00%	U # 1 Dead	2X SUTIB	none	-	-	n/a	SUTIB	All Type II
U-20	ORS 41HF (C18.9S03)	15-29	0.50%	C24-28 IOS	26956-36	0.50%	TEGBE	1.00%	U # 1 Dead	2X SUTIB	none	-	-	n/a	SUTIB	All Type II

144

U-21	C14-30 ABS	8697-038-D	0.50%	C24-28 IOS	26956-36	0.50%	TEGBE	1.00%	U # 1 Dead	2X SUTIB	none	-	-	n/a	SUTIB	All Type II
U-22	C20-24 LAOS	3153-027	0.50%	C20-24 IOS	18239-091907	0.50%	TEGBE	1.00%	U # 1 Dead	2X SUTIB	none	-	-	n/a	SUTIB	All Type II
U-23	C14-30 ABS	8697-038-A	0.50%	C20-24 IOS	18239-091907	0.50%	TEGBE	1.00%	U # 1 Dead	2X SUTIB	none	-	-	n/a	SUTIB	All Type II
U-24	ORS 41HF (C18.9S03)	15-29	0.50%	C24-28 IOS	26956-36	0.50%	Neodol (N-25-12)	0.20%	U # 1 Dead	2X SUTIB	none	-	-	n/a	SUTIB	All Type II wit gel
U-25	C14-30 ABS	8697-038-D	0.50%	C24-28 IOS	26956-36	0.50%	Neodol (N-25-12)	0.20%	U # 1 Dead	2X SUTIB	none	-	-	n/a	SUTIB	All Type II
U-26	C20-24 LAOS	3153-027	0.50%	C20-24 IOS	18239-091907	0.50%	Neodol (N-25-12)	0.20%	U # 1 Dead	2X SUTIB	none	-	-	n/a	SUTIB	All Type II
U-27	C14-30 ABS	8697-038-A	0.50%	C20-24 IOS	18239-091907	0.50%	Neodol (N-25-12)	0.20%	U # 1 Dead	2X SUTIB	none	-	-	n/a	SUTIB	All Type II
UNTM N-28	ORS 41HF (C18.9S03)	15-29	0.50%	C15-18 IOS	18239-5A	0.50%	TDA 30EO	0.30	U # 1 Dead	2X SUTIB	none	-	-	n/a	SUTIB	Changes from Type I to II at around 49000 TDS but very low solubility
U-29	C15-18 IOS	18239-5A	0.50%	C14-24 ABS	8697-038-C	0.25%	TDA 30EO	0.30	U # 1 Dead	2X SUTIB	none	-	-	n/a	SUTIB	Possible type III observed but viscous
U-30	Isofol C20-18EO Sulfate		1.00%	-	-	-	-	-	U # 1 Dead	2X SUTIB	1-10%					-
U-31	C15-18 IOS	18239-5A	0.50%	-	-	-	-	-	U # 1 Dead	2X SUTIB	none	-	-	n/a	SUTIB	All type I but the oil solubilization is not high
U-32	C15-18 IOS	18239-5A	1.00%	-	-	-	-	-	U # 1 Dead	2X SUTIB	none	-	-	n/a	SUTIB	All type I but the oil solubilization is not high
U-33	C20-24 IOS	18239-091907	0.50%	-	-	-	-	-	U # 1 Dead	2X SUTIB	none	-	-	n/a	SUTIB	All type II with gel
U-34	C20-24 IOS	18239-091907	1.00%	-	-	-	-	-	U # 1 Dead	2X SUTIB	none	-	-	n/a	SUTIB	All type II with gel
U-35	C12-15 AOS	7258054-BN2	0.50%	-	-	-	-	-	U # 1 Dead	2X SUTIB	none	-	-	n/a	SUTIB	All type II
U-36	C12-15 AOS	7258054-BN2	1.00%	-	-	-	-	-	U # 1 Dead	2X SUTIB	none	-	-	n/a	SUTIB	All type II with gel
U-37	C12-15 15EO Sulfonate	102287789C	0.50%	-	-	-	-	-	U # 1 Dead	2X SUTIB	none	-	-	n/a	SUTIB	All type II
U-38	C12-15 15EO Sulfonate	102287789C	1.00%	-	-	-	-	-	U # 1 Dead	2X SUTIB	none	-	-	n/a	SUTIB	All type II
U-39	Alfoterra 63 Branched Alchohol Propoxylate sulfate	V 1191-164-15	0.50%	-	-	-	-	-	U # 1 Dead	2X SUTIB	none	-	-	n/a	SUTIB	All type II
U-40	C15-18 IOS	18239-5A	0.50%	C14-30 ABS	8697-083-B	0.50%	TDA 30EO	0.30%	U # 1 Dead	2X SUTIB	none	-	-	n/a	SUTIB	Possible type III observed but viscous
U-41	RD 2027 ASO	-	0.50%	-	-	-	-	-	U # 1 Dead	2X SUTIB	none	-	-	n/a	SUTIB	All type II
U-42	RD 2027 ASO	-	0.50%	-	-	-	TDA 30EO	0.30%	U # 1 Dead	2X SUTIB	none	-	-	n/a	SUTIB	All type II
U-43	C15-18 IOS	18239-5A	0.50%	RD 2027 ASO	-	0.50%	TDA 30EO	0.30%	U # 1 Dead	2X SUTIB	none	-	-	n/a	SUTIB	All type II with trapped Oil blobs
U-44	C15-18 IOS	18239-5A	0.50%	C20-24 IOS	18239-091907	0.50%	TDA 30EO	0.30%	U # 1 Dead	2X SUTIB	none	<10	4.70%	n/a	SUTIB	Shift from Type I to II at around 49000 TDS but the oil solubization is not high

U-45	C15-18 IOS	18239-5A	0.50%	C24-28 IOS	26956-36	0.50%	TDA 30EO	0.30%	U # 1 Dead	2X SUTIB	none	<10	4.90%	n/a	SUTIB	Sizeable type III microemulsion is observed but at lower salinity around 3.7%to 4.9%
U-46	C15-18 IOS	18239-5A	0.50%	C24-28 IOS	26956-36	0.50%	TDA 30EO	0.50%	U # 1 Dead	2X SUTIB	none	~7	5.80%	n/a	SUTIB	Possible type III observed but the solubilization is low
U-47	C15-18 IOS	18239-5A	0.50%	C24-28 IOS	26956-36	0.50%	TDA 30EO	1.00%	U # 1 Dead	2X SUTIB	none	-	-	n/a	SUTIB	High co-solvent concentration has decreased the solubilization pretty much. No microemulsion is formed.
U-48	C24-28 IOS	26956-36	1.00%	-	-	-	TDA 30EO	1.00%	U # 1 Dead	2X SUTIB	none	-	-	n/a	SUTIB	Big middle phase is formed. Since it is having 1%surfactant, it is difficult to get the aqueous stability for this system.
U-49	C15-18 IOS	18239-5A	0.80%	C24-28 IOS	B 20	0.20%	TDA 30EO	0.30%	U # 1 Dead	2X SUTIB	none	-	-	n/a	SUTIB	Low oil is solubilized at around 40000 TDS but no micremulsion is formed
U-50	C15-18 IOS	18239-5A	0.50%	C 15-18 ABS	18098-062007	0.50%	TDA 30EO	0.30%	U # 1 Dead	2X SUTIB	none	-	-	n/a	SUTIB	Negligible oil is solubilized at low salinities (<45000 TDS)
U-51	C15-18 IOS	18239-5A	0..5%	C20-24 IOS	26862-104-6	0.50%	TDA 30EO	0.30%	U # 1 Dead	2X SUTIB	none	-	-	n/a	SUTIB	Shift from Type I to II at around 49000 TDS but the oil solubization is not high
U-52	C15-18 IOS	18239-5A	0.50%	C24-28 IOS	B 20	0.50%	-	-	U # 1 Dead	2X SUTIB	none	~12.5	4.50%	n/a	SUTIB	The interfaces are not clear and moreover the optimum is too low and the solubilization has decreased with time.
U-53	C24-28 IOS	B 20	0.50%	C 15-18 IOS	18239-5A	0.20%	TDA 30EO	0.30%	U # 1 Dead	2X SUTIB	none	~9	>8	n/a	SUTIB	Forms big middle phase at very high salinities.
U-54	C24-28 IOS	B 20	0.50%	C 15-18 IOS	18239-5A	0.20%	-	-	U # 1 Dead	2X SUTIB	none	-	-	n/a	SUTIB	Possible type III but very viscous (might be gel also)
U-55	C24-28 IOS	B 20	0.50%	-	-	-	DA 30EO SO4	0.50%	U # 1 Dead	2X SUTIB	none	-	-	n/a	SUTIB	All type II with some trapped oil blobs in the aqueous phase
U-56	C24-28 IOS	B 20	0.50%	-	-	-	-	-	U # 1 Dead	2X SUTIB	none	-	-	n/a	SUTIB	Under equilibration
U-57	C24-28 IOS	B 20	0.50%	-	-	-	TDA 30EO	0.30%	U # 1 Dead	2X SUTIB	none	-	-	n/a	SUTIB	-
U-57 (repeat)	C24-28 IOS	B 20	0.50%	-	-	-	TDA 30EO	0.30%	U # 1 Dead	2X SUTIB						Seems to have the optimum at 17000 TDS but the microemulsion is not free flowing
U-58	C24-28 IOS	B 20	1.00%	-	-	-	-	-	U # 1 Dead	2X SUTIB	none	-	-	n/a	SUTIB	Upper phase me with gel
U-59	C24-28 IOS	B 20	1.00%	-	-	-	TDA 30EO	0.50%	U # 1 Dead	2X SUTIB	none		-	n/a	SUTIB	Same as U-57
U-60	C24-28 IOS	B 20	0.20%	-	-	-	TDA 30EO	0.10%	U # 1 Dead	2X SUTIB	none		-	n/a	SUTIB	No charecteristic behavior (all type II)
U-61	C24-28 IOS	B 20	0.50%	-	-	-	TDA 30EO, Aerosol M A-80	0.3% 0.5%	U # 1 Dead	2X SUTIB	none			n/a	SUTIB	Very viscous upper phase microemulsion
U-62	C24-28 IOS	B 13	0.50%	-	-	-	TDA 30EO	0.30%	U # 1 Dead	2X SUTIB	none			n/a	SUTIB	Same upper phase me but initially the trend was slightly different from the other batch

146

U-63	C24-28 IOS	B 20	0.50%	-	-	-	Aerosol MA-80	0.50%	U # 1 Dead	2X SUTIB	none			n/a	SUTIB	
U-64	Alkyl xylene sulfonate	3358-058	1%	-	-	-	TEGBE	1.00%	U # 1 Dead	2X SUTIB	none			n/a	SUTIB	All type II with gel
U-65	Alkyl xylene sulfonate	3358-058	1%	-	-	-	TDA 30 EO	0.30%	U # 1 Dead	2X SUTIB	none			n/a	SUTIB	All type II with gel
U-66	C16-18 ABS	3678-096	1%	-	-	-	TEGBE	1.00%	U # 1 Dead	2X SUTIB	none			n/a	SUTIB	All type II with gel
U-67	C16-18 ABS	3678-096	1%	-	-	-	TDA 30 EO	0.30%	U # 1 Dead	2X SUTIB	none			n/a	SUTIB	All type II with gel
U-68 (Refined scan of 53)	C24-28 IOS	B 20	0.50%	C15-18 IOS	18239-5A	0.20%	TDA 30EO	0.30%	U # 1 Dead	2X SUTIB	none	10.5	4%	4 wt%(0% MA) 5 wt%(0.2% MA)	SUTIB	
U-69	C24-28 IOS	B 20	0.50%	C15-18 IOS	18239-5A	0.20%	eodol (N-25-1	0.20%	U # 1 Dead	2X SUTIB	none	-	-	-	-	long macroemulsion
U-70	C24-28 IOS	B 20	0.50%	C15-18 IOS	18239-5A	0.20%	eodol (N-25-1	0.40%	U # 1 Dead	2X SUTIB	none	-	-	-	-	long macroemulsion
U-71	C24-28 IOS	B 20	0.50%	C15-18 IOS	18239-5A	0.20%	MA-80	0.20%	U # 1 Dead	2X SUTIB	none	-	-	-	-	similar to U 68 but the system is still under equilibration
U-72	C24-28 IOS	B 20	0.50%	C15-18 IOS	18239-5A	0.20%	MA-80	0.40%	U # 1 Dead	2X SUTIB	none	-	-	-	-	similar to U 68 but the system is still under equilibration
U-73 to 79							EDTA Na4	varied	U # 1 Dead	EDTA scan		-	-	-	-	EDTA scan to find the min. EDTA required to seq. Ca, Mg
U-80	Isofol C32-7 PO-32 EO So4-	6/12/2009	0.50%	C20-24 IOS	18239-091907	0.50%	TEGBE MA-80	1.0% 1.0%	U # 1 Dead	2X SUTIB	EDTA Na4 3.5%	-	-	-	-	Type II(+) behavior
U-81	Isofol C32-7 PO-32 EO So4-	6/12/2009	0.50%	C20-24 IOS	18239-091907	0.50%	TDA 30 EO	0.30%	U # 1 Dead	2X SUTIB	EDTA Na4 3.5%	-	-	-	-	Type II(+) behavior
U-82	Isofol C32-7 PO-32 EO So4-	6/12/2009	0.50%	C24-22 EO	U 24 - 005	0.50%	TEGBE	1.00%	U # 1 Dead	2X SUTIB	EDTA Na4 3.5%	-	-	-	-	Type II(+) behavior
U-83	C16-17-7PO-Sulfate	18102-7A	0.50%	C15-18 IOS	18239-5A	0.50%	-	-	U # 1 Dead	2X SUTIB	EDTA Na4 3.5%					Sizeable middle phase was observed intially but after mixing those sasmples they are still in Type I stage.
U-84	Isofol C32-7 PO-32 EO So4-	6/12/2009	0.50%	C24-28 IOS	B20	0.50%	TDA 30 EO	0.30%	U # 1 Dead	2X SUTIB	EDTA Na4 3.5%	-	-	-	-	Type II(+) behavior
U-85									U # 1 Dead	Sodium Carbonate scan		-	-	-	-	Oil activity test
U-86	C16-7PO-SO4		0.50%	C15-18 IOS	18239-5A	0.50%	-	-	U # 1 Dead	2X SUTIB	EDTA Na4 3.5%					Somewhat similar to the system U-83, but a clear middle phase is not formed (seems like emulsion at the higher salinity)
U-87	C16-17-7PO-Sulfate	18102-7A	0.50%	C20-24 IOS	18239-101707	0.50%	-	-	U # 1 Dead	2X SUTIB	EDTA Na4 3.5%					
U-88	Isofol C32-7 PO-40 EO So4-	6/25/2009	0.50%	C15-18 IOS	18239-5A	0.50%	TEGBE	1.00%	U # 1 Dead	2X SUTIB	EDTA Na4 3.5%	-	-	-	-	Type II(+) behavior

147

U-89	C16-7PO-SO4		0.50%	C20-24 IOS	LR-26862-104-6	0.50%	TEGBE	1.00%	U # 1 Dead	2X SUTIB	EDTA Na4 3.5%	-	-	-	-	-
U-90	C16-7PO-2EO-SO4		0.50%	C20-24 IOS	LR-26862-104-6	0.50%	TEGBE	1.00%	U # 1 Dead	2X SUTIB	EDTA Na4 3.5%	-	-	-	-	-
U-91	C20-7PO-2EO-SO4		0.50%	C20-24 IOS	LR-26862-104-6	0.50%	TEGBE	1.00%	U # 1 Dead	2X SUTIB	EDTA Na4 3.5%	-	-	-	-	-
U-92	C16-7PO-SO4		0.50%	C20-24 IOS	LR-26862-104-6	0.50%	Basasol RD 1734	0.30%	U # 1 Dead	2X SUTIB	EDTA Na4 3.5%	-	-	-	-	-
U-93	C16-7PO-2EO-SO4		0.50%	C20-24 IOS	LR-26862-104-6	0.50%	Basasol RD 1735	100.30%	U # 1 Dead	2X SUTIB	EDTA Na4 3.5%	-	-	-	-	-
U-94	C20-7PO-2EO-SO4	6/25/2009	0.50%	C15-18 IOS	18239-5A	0.50%			U # 1 Dead	2X SUTIB	EDTA Na4 3.5%	-	-	-	-	-
U-95	C20-7PO-2EO-SO4	6/25/2009	0.50%	C15-18 IOS	18239-5A	0.50%	Basasol RD 1734	0.30%	U # 1 Dead	2X SUTIB	EDTA Na4 3.5%	-	-	-	-	-
U-96	J771	27130-31	0.50%	C15-18 IOS	18239-5A	0.50%			U # 1 Dead	2X SUTIB	EDTA Na4 3.5%	-	-	-	-	-
U-97	C16-17-7PO-Sulfate	18102-7A	0.50%	C15-18 IOS	18239-5A	0.50%	TEGBE	1.00%	U # 1 Dead	2X SUTIB	EDTA Na4 3.5%	-	-	-	-	-
U-98	C16-17-7PO-Sulfate	18102-7A	0.80%	C15-18 IOS	18239-5A	0.20%	-	-	U # 1 Dead	2X SUTIB	EDTA Na4 3.5%	-	-	-	-	-
U-99	C16-17-7PO-Sulfate	18102-7A	0.80%	C15-18 IOS	18239-5A	0.20%	TEGBE	1.00%	U # 1 Dead	2X SUTIB	EDTA Na4 3.5%	-	-	-	-	-
U-100	C16-17-7PO-Sulfate	18102-7A	0.50%	C15-18 IOS + C32-7PO-18EO-SO4	18239-5A	0.5% 0.5%			U # 1 Dead	2X SUTIB	EDTA Na4 3.5%	-	-	-	-	-
U-101	C16-17-7PO-Sulfate	18102-7A	0.50%	C15-18 IOS + C32-7PO-18EO-SO4	18239-5A	0.5% 0.5%	TDA 30 EO	0.30%	U # 1 Dead	2X SUTIB	EDTA Na4 3.5%	-	-	-	-	-
U-102	C16-17-7PO-Sulfate	18102-7A	0.50%	C15-18 IOS + C32-7PO-18EO-SO4	18239-5A	0.5% 0.5%	TEGBE	0.50%	U # 1 Dead	2X SUTIB	EDTA Na4 3.5%	-	-	-	-	-
U-103	C16-17-7PO-Sulfate	18102-7A	0.33%	C15-18 IOS + C32-7PO-18EO-SO4	18239-5A	0.33% 0.33%			U # 1 Dead	2X SUTIB	EDTA Na4 3.5%	-	-	-	-	-
U-104	C16-17-7PO-Sulfate	18102-7A	0.33%	C15-18 IOS + C32-7PO-18EO-SO4	18239-5A	0.33% 0.33%	TEGBE	0.25%	U # 1 Dead	2X SUTIB	EDTA Na4 3.5%	-	-	-	-	-
U-105	C16-17-7PO-Sulfate	18102-7A	0.33%	C15-18 IOS + C32-7PO-18EO-SO4	18239-5A	0.33% 0.33%	TEGBE	0.50%	U # 1 Dead	2X SUTIB	EDTA Na4 3.5%	-	-	-	-	-
U-106	C16-7PO-2EO-SO4		0.33%	C15-18 IOS + C32-7PO-18EO-SO4	18239-5A	0.33% 0.33%	TEGBE	0.50%	U # 1 Dead	2X SUTIB	EDTA Na4 3.5%	-	-	-	-	-
U-107	C16-7PO-6EO-SO4	7/12/2009	0.33%	C15-18 IOS + C32-7PO-18EO-SO4	18239-5A	0.33% 0.33%	TEGBE	0.50%	U # 1 Dead	2X SUTIB	EDTA Na4 3.5%	-	-	-	-	-
U-108	C16-7PO-6EO-SO4	7/12/2009	0.33%	C15-18 IOS + C32-7PO-18EO-SO4	18239-5A	0.33% 0.33%			U # 1 Dead	2X SUTIB	EDTA Na4 3.5%	-	-	-	-	-
U-109	C16-7PO-6EO-SO4	7/12/2009	0.33%	C15-18 IOS + C32-7PO-18EO-SO4	18239-5A	0.33% 0.33%	TEGBE	0.25%	U # 1 Dead	2X SUTIB	EDTA Na4 3.5%	-	-	-	-	-
U-110	C16-7PO-6EO-SO4	7/12/2009	0.33%	C20-24 IOS + C32-7PO-18EO-SO4	18239-101707	0.33% 0.33%			U # 1 Dead	2X SUTIB	EDTA Na4 3.5%	-	-	-	-	-
U-111	C16-7PO-6EO-SO4	7/12/2009	0.33%	C20-24 IOS + C32-7PO-18EO-SO4	18239-101707	0.33% 0.33%	TEGBE	0.50%	U # 1 Dead	2X SUTIB	EDTA Na4 3.5%					

U-112	C16-7PO-6EO-SO4	7/12/2009	0.33%	C20-24 IOS + C32-7PO-14EO-SO4	18239-101707	0.33% 0.33%	TEGBE	0.50%	U # 1 Dead	2X SUTIB	EDTA Na4 3.5%	-	-	-	-	-
U-113	C24-28 IOS	B 20	0.70%	C15-18 IOS	18239-5A	0.30%	TEGBE	1.00%	U # 1 Dead	2X SUTIB	none	-	-	-	-	-
U-114	C15-18 IOS	18239-5A	1.00%						U # 1 Dead	Calcium	none	-	-	-	-	Cacium tolerance test for IOS
U-115	C16-7PO-6EO-SO4	7/12/2009	0.33%	C15-18 IOS + C32-7PO-18EO-SO4	18239-5A	0.33% 0.33%	Huntsman Butanol Ethoxylate (2.2 EO)	0.50%	U # 1 Dead	2X SUTIB	EDTA Na4 3.5%	-	-	-	-	-
U-116	C16-7PO-6EO-sulfate	7/13/2009	0.33%	C15-18 IOS + C32-7PO-18EO-sulfate	18239-5A -	0.33% 0.33%	M A-80	0.50%	U Dead	SUTIB	EDTA Na4 3.5%	-	-	-	SUTIB	M A-80 Aq. Stab test
U-117	C16-7PO-6EO-sulfate	7/13/2009	0.33%	C15-18 IOS + C32-7PO-18EO-sulfate	18239-5A -	0.33% 0.33%	M A-80	0.25%	U Dead	SUTIB	EDTA Na4 3.5%	-	-	-	SUTIB	M A-80 Aq. Stab test
U-118	C16-7PO-6EO-sulfate	7/13/2009	0.17%	C15-18 IOS + C32-7PO-18EO-sulfate	18239-5A -	0.17% 0.17%	TEGBE	0.25%	U Dead	SUTIB	EDTA Na4 3.5%	-	-	-	SUTIB	
U-119	C16-7PO-6EO-sulfate	7/13/2009	0.17%	C15-18 IOS + C32-7PO-18EO-sulfate	18239-5A -	0.17% 0.17%	TEGBE	0.50%	U Dead	SUTIB	EDTA Na4 3.5%	-	-	-	SUTIB	-
U-120	C16-7PO-6EO-sulfate	7/13/2009	0.33%	C15-18 IOS + C32-7PO-18EO-sulfate	18239-5A -	0.33% 0.33%	M A-80	0.15%	U Dead	SUTIB	EDTA Na4 3.5%	-	-	-	SUTIB	M A-80 Aq. Stab test
U-121	C16-7PO-6EO-sulfate	7/13/2009	0.33%	C15-18 IOS + C32-7PO-18EO-sulfate	18239-5A -	0.33% 0.33%	TEGBE	0.50%	U Dead	SUTIB	EDTA Na4 3.75%	9	6%	-	SUTIB	Starting expt with 3.75% EDTA.4Na
U-122	C16-7PO-10EO-sulfate	8/15/2009	0.33%	C15-18 IOS + C32-7PO-18EO-sulfate	18239-5A -	0.33% 0.33%	TEGBE	0.50%	U Dead	SUTIB	EDTA Na4 3.75%	-	-	-	SUTIB	
U-123	C16-7PO-10EO-sulfate	8/15/2009	0.33%	C15-18 IOS + C32-7PO-18EO-sulfate	18239-5A -	0.33% 0.33%	TEGBE	0.25%	U Dead	SUTIB	EDTA Na4 3.75%	-	-	-	SUTIB	Change in TEGBE conc from U-122
U-124	C16-7PO-10EO-sulfate	8/15/2009	0.33%	C15-18 IOS + C32-7BO-7PO-25EO-sulfate	18239-5A -	0.33% 0.33%	TEGBE	0.25%	U Dead	SUTIB	EDTA Na4 3.75%	10	6.90%	-	SUTIB	Starting expts with C32-7BO-xPO-xEO-sulfate
U-125	C20-7PO-10EO-sulfate	7/2/2009	0.33%	C15-18 IOS + C32-7BO-7PO-25EO-sulfate	18239-5A -	0.33% 0.33%	TEGBE	0.25%	U Dead	SUTIB	EDTA Na4 3.75%	12	6.80%	-	SUTIB	-
U-126	C20-7PO-10EO-sulfate	7/2/2009	0.33%	C20-24 IOS (E) + C32-7BO-7PO-25EO-sulfate	27131-1413; 118 73 13 -	0.33% 0.33%	TEGBE	0.25%	U Dead	SUTIB	EDTA Na4 3.75%	-	-	-	SUTIB	-
U-127	C20-7PO-10EO-sulfate	7/2/2009	0.33%	C24-28 IOS (E) + C32-7BO-7PO-25EO-sulfate	27131-14A; 07880-83 -	0.33% 0.33%	TEGBE	0.25%	U Dead	SUTIB	EDTA Na4 3.75%	-	-	-	SUTIB	-
U-128	C32-7BO-7PO-25EO-sulfate	-	1.00%	-	-	-	TEGBE	0.25%	U Dead	SUTIB	EDTA Na4 3.75%	-	-	-	SUTIB	-
U-129	C28-7PO-6EO-Sulfate	8/4/2009	0.33%	C15-18 IOS + C32-7BO-7PO-25EO-sulfate	18239-5A -	0.33% 0.33%	TEGBE	0.25%	U Dead	SUTIB	EDTA Na4 3.75%	12	5.70%	-	SUTIB	-
U-130	C32-7BO-7PO-55EO-sulfate	-	1.00%	-	-	-	TEGBE	0.25%	U Dead	SUTIB	EDTA Na4 3.75%	-	-	-	SUTIB	-
U-131	C32-7PO-10EO-Sulfate		0.33%	C15-18 IOS + C32-7BO-7PO-25EO-sulfate	18239-5A -	0.33% 0.33%	TEGBE	0.50%	U Dead	SUTIB	EDTA Na4 3.75%	12.5	5.70%	-	SUTIB	-
U-132	C28-7PO-10EO-Sulfate		0.33%	C15-18 IOS + C32-7BO-7PO-25EO-sulfate	18239-5A -	0.33% 0.33%	TEGBE	0.50%	U Dead	SUTIB	EDTA Na4 3.75%	8	6.80%	-	SUTIB	-

U-133	C28-7PO-6EO-Sulfate	8/4/2009	0.33%	C15-18 IOS + C32-7BO-7PO-25EO-sulfate	18239-5A -	0.33% 0.33%	TEGBE	0.50%	U Dead	SUTIB	EDTA Na4 3.75%	10	5.70%	-	SUTIB	Increased TEGBE than U-129
U-134	C32-7BO-7PO-25EO-sulfate	-	0.50%	C15-18 IOS	18239-5A	0.50%	TEGBE	0.50%	U Dead	SUTIB	EDTA Na4 3.75%	-	-	-	SUTIB	-
U-135	C32-7PO-10EO-Sulfate	-	0.40%	C15-18 IOS + C32-7BO-7PO-25EO-sulfate	18239-5A	0.20% 0.40%	TEGBE	0.50%	U Dead	SUTIB	EDTA Na4 3.75%	-	-	-	SUTIB	Changing the ratio of surf keeping the total at 1%
U-136	C32-7PO-10EO-Sulfate	-	0.40%	C15-18 IOS + C32-7BO-7PO-25EO-sulfate	18239-5A	0.40% 0.20%	TEGBE	0.50%	U Dead	SUTIB	EDTA Na4 3.75%	9	6.30%	-	SUTIB	Changing the ratio of surf keeping the total at 1%
U-137	C32-7PO-10EO-Sulfate	-	0.33%	C15-18 IOS + C32-7BO-7PO-25EO-sulfate	18239-5A	0.33% 0.58%	TEGBE	0.50%	U Dead	SUTIB	EDTA Na4 3.75%	23	4.30%	-	SUTIB	Increased %of C32-7BO molecule
U-138	C28-7PO-6EO-Sulfate	8/4/2009	0.33%	C15-18 IOS + C32-7BO-7PO-40EO-sulfate	18239-5A	0.33% 0.33%	-	-	U Dead	SUTIB	EDTA Na4 3.75%	12	6.00%	-	SUTIB	-
U-139	C32-7PO-10EO-Sulfate	-	0.17%	C15-18 IOS + C32-7BO-7PO-25EO-sulfate	18239-5A	0.17% 0.29%	TEGBE	0.50%	U Dead	SUTIB	EDTA Na4 3.75%	-	-	-	SUTIB	Decreased surf conc. of U-137
U-140	C32-7PO-10EO-Sulfate	-	0.33%	C15-18 IOS + C32-7BO-7PO-25EO-sulfate	18239-5A	0.33% 0.83%	TEGBE	0.75%	U Dead	SUTIB	EDTA Na4 3.75%	-	-	-	SUTIB	Varied surf conc. of U-137
U-141	C32-7PO-10EO-Sulfate	-	0.33%	C15-18 IOS + C32-7BO-7PO-25EO-sulfate	18239-5A	0.33% 1.08%	TEGBE	1.00%	U Dead	SUTIB	EDTA Na4 3.75%	-	-	-	SUTIB	Varied surf conc. of U-137
U-142	C32-7PO-10EO-Sulfate	-	0.33%	C15-18 IOS + C32-7BO-7PO-25EO-sulfate	18239-5A	0.33% 1.33%	TEGBE	1.00%	U Dead	SUTIB	EDTA Na4 3.75%	-	-	-	SUTIB	Varied surf conc. of U-137
U-143	C32-7PO-10EO-Sulfate	-	0.33%	C15-18 IOS + C32-7BO-7PO-40EO-sulfate	18239-5A	0.33% 0.58%	TEGBE	0.50%	U Dead	SUTIB	EDTA Na4 3.75%	9	5.70%	-	SUTIB	Increased EO from U-137
U-144	C32-7PO-10EO-Sulfate	-	0.33%	C15-18 IOS + C32-7BO-7PO-40EO-sulfate	18239-5A	0.33% 0.91%	TEGBE	0.75%	U Dead	SUTIB	EDTA Na4 3.75%	9	4.60%	-	SUTIB	Increased %of C32-7BO molecule from U-143
U-145	C32-7PO-14EO-Sulfate	5/28/2009	0.33%	C15-18 IOS + C32-7BO-7PO-25EO-sulfate	18239-5A	0.33% 0.58%	TEGBE	0.50%	U Dead	SUTIB	EDTA Na4 3.75%	-	-	-	SUTIB	Very good PB, but interfaces not clear at this surf conc
U-146	C32-7PO-18EO-Sulfate	-	0.33%	C15-18 IOS + C32-7BO-7PO-25EO-sulfate	18239-5A	0.33% 0.58%	TEGBE	0.50%	U Dead	SUTIB	EDTA Na4 3.75%	10	5.20%	-	SUTIB	Increased EO from U-145
U-147	C32-7PO-14EO-Sulfate	5/28/2009	0.17%	C15-18 IOS + C32-7BO-7PO-25EO-sulfate	18239-5A	0.17% 0.29%	TEGBE	0.25%	U Dead	SUTIB	EDTA Na4 3.75%	22	4.00%	-	SUTIB	Decreased surf conc. of U-145
U-147 (F)	C32-7PO-14EO-Sulfate	5/28/2009	0.17%	C15-18 IOS + C32-7BO-7PO-25EO-sulfate	18239-5A	0.17% 0.29%	TEGBE	0.25%	U Dead	SUTIB	EDTA Na4 3.75%	19	4.60%	5.20%	SUTIB	Fine scan of U-147
U-148	C28-7PO-10EO-Sulfate	-	0.33%	C15-18 IOS + C32-7BO-7PO-25EO-sulfate	18239-5A	0.33% 0.58%	TEGBE	0.50%	U Dead	SUTIB	EDTA Na4 3.75%	14	5.20%	-	SUTIB	-
U-149	C32-7PO-14EO-Sulfate	5/28/2009	0.08%	C15-18 IOS + C32-7BO-7PO-25EO-sulfate	18239-5A	0.08% 0.14%	TEGBE	0.25%	U Dead	SUTIB	EDTA Na4 3.75%	19	3.90%	-	SUTIB	Decreased surf conc. of U-147
U-150	C32-7PO-14EO-Sulfate	5/28/2009	0.08%	C15-18 IOS + C32-7BO-7PO-25EO-sulfate	18239-5A	0.08% 0.14%	TEGBE	0.13%	U Dead	SUTIB	EDTA Na4 3.75%	-	-	-	SUTIB	Decreased surf conc. of U-147
U-151	C32-7PO-14EO-Sulfate	5/28/2009	0.08%	C15-18 IOS + C32-7BO-7PO-25EO-sulfate	18239-5A	0.08% 0.14%	-	-	U Dead	SUTIB	EDTA Na4 3.75%	-	-	-	SUTIB	Decreased surf conc. of U-147

150

ID	Surfactant	Date	Conc	Co-surfactant	Batch	Conc	Co-solvent	Conc	Oil	Brine	Alkali	#	%		Brine2	Notes
U-152	C32-7PO-14EO-Sulfate	5/28/2009	0.04%	C15-18 IOS + C32-7BO-7PO-25EO-sulfate	18239-5A -	0.04% 0.07%	TEGBE	0.13%	U Dead	SUTIB	EDTA Na4 3.75%	-	-	-	SUTIB	Decreased surf conc. of U-147
U-153	C32-7PO-14EO-Sulfate	5/28/2009	0.04%	C15-18 IOS + C32-7BO-7PO-25EO-sulfate	18239-5A -	0.04% 0.07%	-	-	U Dead	SUTIB	EDTA Na4 3.75%	-	-	-	SUTIB	Decreased surf conc. of U-147
U-154	C32-7PO-18EO-Sulfate	-	0.04%	C15-18 IOS + C32-7BO-7PO-25EO-sulfate	18239-5A -	0.04% 0.07%	TEGBE	0.13%	U Dead	SUTIB	EDTA Na4 3.75%	-	-	-	SUTIB	Increased EO from U-152
U-155	C32-7PO-18EO-Sulfate C28-7PO-10EO-sulfate	-	0.17% 0.17%	C15-18 IOS + C32-7BO-7PO-25EO-sulfate	18239-5A -	0.33% 0.58%	TEGBE	0.50%	U Dead	SUTIB	EDTA Na4 3.75%	-	-	-	SUTIB	Four surfactant trial
U-156	C32-7PO-24EO-Sulfate C28-7PO-10EO-sulfate	-	0.17% 0.17%	C15-18 IOS + C32-7BO-7PO-25EO-sulfate	18239-5A -	0.33% 0.58%	TEGBE	0.50%	U Dead	SUTIB	EDTA Na4 3.75%	-	-	-	SUTIB	Four surfactant trial
U-157	C32-7PO-14EO-Sulfate	5/28/2009	0.17%	C15-18 IOS + C32-7BO-7PO-25EO-sulfate	18239-5A -	0.17% 0.29%	-	-	U Dead	SSUTIB	Na2CO3 0.5%	-	-	-	SSUTIB	Softened sea brine w/o EDTA
U-158	C32-7PO-14EO-Sulfate	5/28/2009	0.17%	C15-18 IOS + C32-7BO-7PO-25EO-sulfate	18239-5A -	0.17% 0.29%	-	-	U Dead	Na2CO3	Na2CO3	23	3.00%	-	SSUTIB	Softened sea brine w/o EDTA
U-158 (ii)	C32-7PO-14EO-Sulfate	5/28/2009	0.17%	C15-18 IOS + C32-7BO-7PO-25EO-sulfate	18239-5A -	0.17% 0.29%	TEGBE	0.25%	U Dead	Na2CO3	Na2CO3			-	SSUTIB	TEGBE scan for U-158
U-158 (iii)	C32-7PO-14EO-Sulfate	5/28/2009	0.17%	C15-18 IOS + C32-7BO-7PO-25EO-sulfate	18239-5A -	0.17% 0.29%	TEGBE	0.50%	U Dead	Na2CO3	Na2CO3			-	SSUTIB	TEGBE scan for U-158
U-158 (iv)	C32-7PO-14EO-Sulfate	5/28/2009	0.17%	C15-18 IOS + C32-7BO-7PO-25EO-sulfate	18239-5A -	0.17% 0.29%	TEGBE	0.75%	U Dead	Na2CO3	Na2CO3			-	SSUTIB	TEGBE scan for U-158
U-158 (v)	C32-7PO-14EO-Sulfate	5/28/2009	0.17%	C15-18 IOS + C32-7BO-7PO-25EO-sulfate	18239-5A -	0.17% 0.29%	TEGBE	1.00%	U Dead	Na2CO3	Na2CO3			-	SSUTIB	TEGBE scan for U-158
U-159	C32-7PO-10EO-Sulfate	-	0.17%	C20-24 IOS (E) + C32-7BO-7PO-25EO-sulfate	27131-14 I3 -	0.17% 0.29%	-	-	U Dead	SSUTIB	Na2CO3 0.5%	-	-	-	SSUTIB	-
U-160	C32-7PO-10EO-Sulfate	-	0.17%	C32-7BO-7PO-25EO-sulfate	27131-14 I3	0.29%	-	-	U Dead	SSUTIB	Na2CO3 0.5%	-	-	-	SSUTIB	-
U-161	C32-15PO-10EO-Sulfate	8/14/2009	0.33%	C15-18 IOS + C32-7BO-7PO-25EO-sulfate	18239-5A -	0.33% 0.33%	-	-	U Dead	SSUTIB	Na2CO3 0.5%	-	-	-	SSUTIB	-
U-162	C32-15PO-10EO-Sulfate	8/14/2009	0.33%	C15-18 IOS + C32-7BO-7PO-40EO-sulfate	18239-5A 11/4/09	0.33% 0.33%	-	-	U Dead	SSUTIB	Na2CO3 0.5%	-	-	-	SSUTIB	-
U-163	C32-15PO-10EO-Sulfate	8/14/2009	0.33%	C15-18 IOS + C32-7BO-7PO-25EO-sulfate	18239-5A -	0.33% 0.33%	-	-	U Dead	Na2CO3	Na2CO3	15	4.50%	-	SSUTIB	-
U-164	C32-15PO-10EO-Sulfate	8/14/2009	0.33%	C15-18 IOS + C32-15BO-7PO-25EO-sulfate	18239-5A 10/27/09	0.33% 0.33%	-	-	U Dead	Na2CO3	Na2CO3	15	4.20%	-	SSUTIB	-
U-165	C32-15PO-10EO-Sulfate	8/14/2009	0.33%	C15-18 IOS + C32-15BO-7PO-25EO-sulfate	18239-5A 10/27/09	0.33% 0.88%	-	-	U Dead	Na2CO3	Na2CO3	-	-	-	SSUTIB	Increased % of C32-15BO surf
U-166	C32-15PO-10EO-Sulfate	8/14/2009	0.33%	C15-18 IOS + C32-15BO-7PO-25EO-sulfate	18239-5A 10/27/09	0.33% 1.33%	-	-	U Dead	Na2CO3	Na2CO3	-	-	-	SSUTIB	Increased % of C32-15BO surf
U-167	C32-7PO-18EO-Sulfate	9/30/2009	0.17%	C15-18 IOS + C32-7BO-7PO-25EO-sulfate	18239-5A -	0.17% 0.29%	-	-	U Dead	Na2CO3	Na2CO3	28	4.00%	-	SSUTIB	-

ID	Surfactant 1	Date	Conc 1	Surfactant 2	Code	Conc 2	Co-solvent	Co-solvent Conc	Oil	Brine/Alkali	Alkali 2		#	%	%	Cell	Notes
U-168	C32-7PO-24EO-Sulfate	-	0.17%	C15-18 IOS + C32-7BO-7PO-25EO-sulfate	18239-5A -	0.17% 0.29%	-	-	U Dead	Na2CO3	Na2CO3	-	-	-		SSUTIB	-
U-169	C32-7PO-14EO-Sulfate	5/28/2009	0.08%	C15-18 IOS + C32-7BO-7PO-25EO-sulfate	18239-5A -	0.08% 0.14%	-	-	U Dead	Na2CO3	Na2CO3	-	-	-		SSUTIB	Decreased surf conc. from U-158
U-170	C32-7PO-14EO-Sulfate	5/28/2009	0.05%	C15-18 IOS + C32-7BO-7PO-25EO-sulfate	18239-5A -	0.05% 0.10%	-	-	U Dead	Na2CO3	Na2CO3	-	-	-		SSUTIB	Decreased surf conc. from U-158
U-171	TSP-7PO-10EO-sulfate	-	1.00%	-	-	-	-	-	U Dead	Na2CO3	Na2CO3	-	-	-		SSUTIB	-
U-172	TSP-7PO-30EO-sulfate	-	1.00%	-	-	-	-	-	U Dead	Na2CO3	Na2CO3	-	-	-		SSUTIB	-
U-173	C32-7PO-14EO-Sulfate	5/28/2009	0.33%	TSP-7PO-10EO-sulfate + C32-7BO-7PO-25EO-sulfate		0.33% 0.33%	-	-	U Dead	Na2CO3	Na2CO3	-	-	-		SSUTIB	-
U-174	C32-15PO-14EO-Sulfate	-	0.17%	C15-18 IOS + C32-7BO-7PO-25EO-sulfate	18239-5A -	0.17% 0.29%	-	-	U Dead	Na2CO3	Na2CO3	-	-	-		SSUTIB	-
U-216	TSP-15PO-65EO-carboxylate	-	1.00%	-	-	-	-	-	U Dead	SUTIB	-	-	-	-		SUTIB	-
U-217	C32-15BO-7PO-65EO-carboxylate	-	0.33%	C12-15-7EO-sulfonate C15-18 IOS	101132461C 7376946	0.33% 0.33%	-	-	U Dead	SUTIB	-	-	-	-		SUTIB	-
U-218	C32-7PO-60EO-carboxylate	-	1.00%	-	-	-	-	-	U Dead	SUTIB	-	-	-	-		SUTIB	-
U-219	C32-7PO-60EO-carboxylate	-	0.33%	C12-15-7EO-sulfonate C15-18 IOS	101132461C 7376946	0.33% 0.33%	-	-	U Dead	SUTIB	-	-	-	-		SUTIB	-
U-220	C32-7PO-60EO-carboxylate	-	0.33%	C12-15-7EO-sulfonate C19-23 IOS (E)	101132461C -	0.33% 0.33%	-	-	U Dead	SUTIB	-	-	-	-		SUTIB	-
U-221	C32-7PO-60EO-carboxylate	-	0.33%	C12-15-7EO-sulfonate C19-23 IOS (E)	101132461C -	0.33% 0.33%	TEGBE	0.50%	U Dead	SUTIB	-	-	-	-		SUTIB	-
U-222	C24-26EO-carboxylate	-	1.00%	-	-	-	-	-	-	SUTIB	-	-	-	-		SUTIB	-
U-223	C32-7PO-60EO-carboxylate	-	0.50%	C19-23 IOS (E)	-	0.50%	-	-	U Dead	SUTIB	-	-	-	-		SUTIB	-
U-224	C12-15-7EO-sulfonate	101132461C	0.50%	C19-23 IOS (E)	-	0.50%	-	-	U Dead	SUTIB	-	-	-	-		SUTIB	-
U-225	C32-7PO-60EO-carboxylate	-	-	C19-23 IOS (E)	-	-	-	-	-	-	-	-	-	-		SUTIB	Surf scan in SUTIB
U-226	C32-7PO-60EO-carboxylate	-	0.33%	C15-18 IOS C19-23 IOS	7376946 -	0.33% 0.33%	-	-	U Dead	SUTIB	-	-	-	-		SUTIB	-
U-227	C32-7PO-60EO-carboxylate	-	0.50%	TSP-15PO-22EO-sulfonate		0.50%	-	-	U Dead	SUTIB	-	-	-	-		SUTIB	-
U-228	C32-7PO-60EO-carboxylate	-	0.50%	C19-23 IOS (E)	-	0.50%	TEGBE	varied	U Dead	TEGBE	-	-	-	-		SUTIB	TEGBE scan for U-223
U-229	C32-7PO-60EO-carboxylate	-	0.50%	C24-28 IOS (E)	-	0.50%	-	-	U Dead	SUTIB	-	-	-	-		SUTIB	-
U-230	C32-7PO-32EO-carboxylate	-	0.50%	C19-23 IOS (E)	-	0.50%	-	-	U Dead	SUTIB	-	15	3.50%	-		SUTIB	Very good PB
U-230 (R)	C32-7PO-32EO-carboxylate	-	0.50%	C19-23 IOS (E)	-	0.50%	-	-	U Dead	SUTIB	-	19	4.00%	4.20%		SUTIB	U-230 (adjusted pH ~7.5)
U-231	C19-23 IOS (E)	-	1.00%	-	-	-	-	-	U Dead	SUTIB	-	18	2.80%	-		SUTIB	-
U-232	C32-7PO-32EO-carboxylate	-	1.00%	-	-	-	-	-	U Dead	SUTIB	-	-	-	-		SUTIB	-

ID	Surf 1		Conc	Surf 2	Number	Conc	Co-solvent	Conc	Status							Notes
U-233	C32-7PO-32EO-carboxylate	-	1.00%	-	-	-	TEGBE	1.00%	U Dead	SUTIB	-	-	-	-	SUTIB	-
U-234	C32-7PO-32EO-carboxylate	-	0.50%	C15-18 IOS	7376946	0.50%	-	-	U Dead	SUTIB	-	-	-	-	SUTIB	-
U-235-239	-	-	-	-	-	-	-	-	U Dead	-	-	-	-	-	-	SSUTIB scan no good formulation
U-240	C24-26EO-carboxylate	-	0.50%	C19-23 IOS (E)	-	0.50%	-	-	U Dead	SUTIB	-	-	-	-	SUTIB	-
U-241	C24-26EO-carboxylate	-	0.50%	C15-18 IOS	7376946	0.50%	-	-	U Dead	SUTIB	-	-	-	-	SUTIB	-
U-242	C32-50EO-carboxylate	-	0.50%	C19-23 IOS (E)	-	0.50%	-	-	U Dead	SUTIB	-	-	-	-	SUTIB	-
U-243	C32-50EO-carboxylate	-	0.50%	C15-18 IOS	7376946	0.50%	-	-	U Dead	SUTIB	-	-	-	-	SUTIB	-
U-244	C24-26EO-carboxylate	-	0.33%	C32-50EO C19-23 IOS		0.33% 0.33%	-	-	U Dead	SUTIB	-	-	-	-	SUTIB	Starting expts with large hydrophobe anionic and large hydrophobe nonionic
U-245	C32-7BO-7PO-55EO-carboxylate	-	1.00%	-	-	-	-	-	U Dead	SUTIB	-	-	-	-	SUTIB	-
U-246	C24-26EO-carboxylate	-	0.33%	C32-50EO-carboxylate C19-23 IOS	-	0.33% 0.33%	-	-	U Dead	SUTIB	-	-	-	-	SUTIB	-
U-247	C32-70EO	-	1.00%	-	-	-	-	-	U Dead	SUTIB	-	-	-	-	SUTIB	-
U-248	C24-26EO-carboxylate	-	0.50%	TDA-30EO C19-23 IOS	-	0.30% 0.50%	-	-	U Dead	SUTIB	-	-	-	-	SUTIB	-
U-249	C24-26EO	-	1.00%	-	-	-	-	-	U Dead	SUTIB	-	-	-	-	SUTIB	-
U-250	C24-26EO-carboxylate	-	0.50%	C19-23 IOS (E)	-	0.50%	TEGBE	1.00%	U Dead	SUTIB	-	-	-	-	SUTIB	-
U-251	C32-7PO-60EO	-	1.00%	-	-	-	-	-	U Dead	SUTIB	-	-	-	-	SUTIB	-
U-252	TSP-7PO-45EO	-	1.00%	-	-	-	-	-	U Dead	SUTIB	-	-	-	-	SUTIB	-
U-253	TSP-7PO-45EO	-	0.50%	C19-23 IOS (E)	-	0.50%	-	-	U Dead	SUTIB	-	-	-	-	SUTIB	-
U-254-265	-	-	-	-	-	-	-	-	U Dead	-	-	-	-	-	-	Partially softened brine expts - not related
U-266	C32-7PO-32EO-carboxylate	-	0.25%	C19-23 IOS (E)	-	0.25%	-	-	U Dead	SUTIB	-	20	4.00%	-	SUTIB	U-230 (lower conc.)
U-267	C19-23 IOS (E)	-	0.50%	C15-18 IOS	18239-5A	0.50%	-	-	U Dead	SUTIB	-	-	-	-	SUTIB	-
U-268	C19-23 IOS (E)	-	0.50%	C15-18 IOS	18239-5A	0.20%	TDA-30EO	0.30%	U Dead	SUTIB	-	-	-	-	SUTIB	-
U-269	C32-7PO-32EO-carboxylate	-	0.10%	C19-23 IOS (E)	-	0.10%	-	-	U Dead	SUTIB	-	-	~4%	-	SUTIB	U-230 (lower conc) (269 (a) to (e) - oil scan)
U-270	C32-7PO-32EO-carboxylate	-	0.35%	C19-23 IOS (E)	-	0.15%	-	-	U Dead	SUTIB	-	~13	~4%	-	SUTIB	-
U-271	C32-7PO-32EO-carboxylate	-	0.15%	C19-23 IOS (E)	-	0.35%	-	-	U Dead	SUTIB	-	-	-	-	SUTIB	-
U-272	C32-7PO-32EO-carboxylate	-	0.18%	C19-23 IOS (E)	-	0.08%	-	-	U Dead	SUTIB	-	-	-	-	SUTIB	-
U-272 (a) to (e)	C32-7PO-32EO-carboxylate	-	0.14%	C19-23 IOS (E)	-	0.06%	-	-	U Dead	SUTIB	-	-	-	-	SUTIB	Oil Scan
U-273	C32-7BO-7PO-55EO-carboxylate	-	0.50%	C19-23 IOS (E)	-	0.20%	-	-	U Dead	SUTIB	-	-	-	-	SUTIB	
U-274	C32-7BO-7PO-55EO-carboxylate	-	0.50%	C19-23 IOS (E)	-	0.50%	-	-	U Dead	SUTIB	-	-	-	-	SUTIB	-
U-275	C32-7BO-7PO-55EO-carboxylate	-	0.25%	C19-23 IOS (E)	-	0.25%	-	-	U Dead	SUTIB	-	-	-	-	SUTIB	-

153

U-276	C32-7BO-7PO-55EO-carboxylate	-	0.10%	C19-23 IOS (E)	-	0.10%	-	-	U Dead	SUTIB	-	-	-	-	SUTIB	U-275 (low conc) (276 (a) to (e) - oil scan)
U-277	C24-25PO-56EO-carboxylate	-	1.00%	-	-	-	-	-	U Dead	SUTIB	-	-	-	-	SUTIB	Starting expt with C24 and C28 carboxylate
U-278	C24-25PO-56EO-carboxylate	-	0.50%	C19-23 IOS (E)	-	0.50%	-	-	U Dead	SUTIB	-	-	-	-	SUTIB	Good PB
U-278 (R)	C24-25PO-56EO-carboxylate	-	0.50%	C19-23 IOS (E)	-	0.50%	-	-	U Dead	SUTIB	-	-	-	-	SUTIB	UTM-278 (adjusted pH ~7)
U-279	C28-25PO-55EO-carboxylate	-	0.50%	C19-23 IOS (E)	-	0.50%	-	-	U Dead	SUTIB	-	-	-	-	SUTIB	Good PB
U-279 (R)	C28-25PO-55EO-carboxylate	-	0.50%	C19-23 IOS (E)	-	0.50%	-	-	U Dead	SUTIB	-	15	~4.3%	-	SUTIB	UTM-279 (adjusted pH ~7)
U-280	C28-25PO-55EO-carboxylate	-	1.00%	C19-23 IOS (E)	-	1.00%	-	-	U Dead	SUTIB	-	-	-	-	SUTIB	pH-7
U-281	C28-25PO-55EO-carboxylate	-	1.00%	-	-	-	-	-	U Dead	SUTIB	-	-	-	-	SUTIB	-
U-282	C15-18 IOS	18239-5A	0.20%	-	-	-	-	-	U Dead	SUTIB	-	-	-	-	SUTIB	pH-7
U-282	C19-23 IOS (E)	-	0.20%	-	-	-	-	-	U Dead	SUTIB	-	-	-	-	SUTIB	pH-7
U-283	C32-7PO-32EO-carboxylate	-	1.00%	C19-23 IOS (E)	-	1.00%	-	-	U Dead	SUTIB	-	-	-	-	SUTIB	pH-7
U-284	C28-25PO-55EO-carboxylate	-	1.00%	C19-23 IOS (E)	-	1.00%	-	-	U Dead	SUTIB	-	-	-	-	SUTIB	pH-7
U-285	C28-25PO-55EO-carboxylate	-	0.50%	C15-18 IOS	18239-5A	0.50%	-	-	U Dead	SUTIB	-	-	-	-	SUTIB	pH-7
U-286	C28-25PO-55EO-carboxylate	-	0.25%	C15-18 IOS	18239-5A	0.25%	-	-	U Dead	SUTIB	-	-	-	-	SUTIB	pH-7
U-287	C28-25PO-55EO-carboxylate	-	0.10%	C15-18 IOS	18239-5A	0.10%	-	-	U Dead	SUTIB	-	-	-	-	SUTIB	pH-7
U-288	C32-7PO-32EO-carboxylate	-	0.10%	C19-23 IOS (E)		0.10%	-	-	U Dead	SUTIB	-	-	~4%	-	SUTIB	U-269 (pH~7) (269 (a) to (c) - oil scan)
U-289	C28-25PO-55EO-carboxylate	-	0.10%	C19-23 IOS (E)	-	0.10%	-	-	U Dead	SUTIB	-	-	-	-	SUTIB	pH-7 (a) to (c) oil scan
U-290	C32-7PO-32EO-carboxylate	-	0.10%	C19-23 IOS (E)	-	0.10%	-	-	U Dead	SUTIB	-	-	~4%	-	SUTIB	U-288 repeat with C19-23 IOS (lot BJ)
U-291-293	-	-	-	-	-	-	-	-	U Dead	-	-	-	-	-	-	softened brine expts - not related
U-294	C28-25PO-25EO-carboxylate	-	0.50%	C15-18 IOS	18239-5A	0,5%	-	-	U surrogate	SUTIB	-	-	-	-	SUTIB	pH-7 (50%cyclohexane diluted oil)
U-294 (a)	C28-25PO-25EO-carboxylate	-	0.50%	C15-18 IOS	18239-5A	0,5%	-	-	U surrogate	SUTIB	-	-	-	-	SUTIB	pH-7 (30%cyclohexane diluted oil)
U-295 (a)	C28-25PO-45EO-carboxylate	-	0.50%	C15-18 IOS	7376946	0,5%	-	-	U surrogate	SUTIB	-	-	-	-	SUTIB	pH-7 (30%cyclohexane diluted oil)
U-295 (b)	C28-25PO-45EO-carboxylate	-	0.50%	C15-18 IOS	7376946	0,5%	-	-	U surrogate	SUTIB	-	~20	~4%	6.00%	SUTIB	pH-7 (50%cyclohexane diluted oil)
U-296 (a)	C32-7PO-32EO-carboxylate	-	0.10%	C19-23 IOS (E)	-	0.10%	-	-	U surrogate	SSUTIB	-	-	-	-	SSUTIB	pH-7 (50%cyclohexane diluted oil)
U-296 (b)	C32-7PO-32EO-carboxylate	-	0.10%	C19-23 IOS (E)	-	0.10%	-	-	U surrogate	SSUTIB	-	-	-	-	SSUTIB	pH-7 (30%cyclohexane diluted oil)
U-297 (a)	C28-25PO-45EO-carboxylate	-	0.10%	C15-18 IOS	7376946	0.10%	-	-	U surrogate	SUTIB	-	-	-	-	SUTIB	pH-7 (50%cyclohexane diluted oil)
U-297 (b)	C28-25PO-45EO-carboxylate	-	0.10%	C15-18 IOS	7376946	0.10%	-	-	U surrogate	SUTIB	-	-	-	-	SUTIB	pH-7 (30%cyclohexane diluted oil)
U-298 (a) to (	C28-25PO-45EO-carboxylate	-	0.10%	C15-18 IOS	7376946	0.10%	-	-	U surrogate	SUTIB	-	-	-	-	SUTIB	pH-7 (50%cyclohexane diluted oil) Oil scan
U-299 (a) to (	C28-25PO-85EO-carboxylate	-	0.10%	C15-18 IOS	7376946	0.10%	-	-	U surrogate	SUTIB	-	-	-	-	SUTIB	pH-7 (50%cyclohexane diluted oil) Oil scan

ID																
-300 (a) to (	C28-25PO-55EO-carboxylate	-	0.10%	C15-18 IOS	7376946	0.10%	-	-	U surrogate	SUTIB	-	-	-	-	SUTIB	pH-7 (50%cyclohexane diluted oil) Oil scan
-301 (a) to (	C28-25PO-65EO-carboxylate	-	0.10%	C15-18 IOS	7376946	0.10%	-	-	U surrogate	SUTIB	-	-	-	-	SUTIB	pH-7 (50%cyclohexane diluted oil) Oil scan
U-302	C28-25PO-45EO-carboxylate	-	0.50%	C11-ABS	A225	0.50%	-	-	U surrogate	SUTIB	-	-	-	-	SUTIB	pH-7 (50%cyclohexane diluted oil) Starting expt with Carb+ABS
U-303	C28-25PO-55EO-carboxylate	-	0.50%	C11-ABS	A225	0.50%	-	-	U surrogate	SUTIB	-	-	-	-	SUTIB	pH-7 (50%cyclohexane diluted oil)
U-304	C28-25PO-55EO-carboxylate	-	0.60%	C11-ABS	A225	0.40%	-	-	U surrogate	SUTIB	-	-	-	-	SUTIB	pH-7 (50%cyclohexane diluted oil) Only aq. Stab
U-305	C28-25PO-55EO-carboxylate	-	0.70%	C11-ABS	A225	0.30%	-	-	U surrogate	SUTIB	-	-	-	-	SUTIB	pH-7 (50%cyclohexane diluted oil) Only aq. Stab
U-306	C28-25PO-75EO-carboxylate	-	0.70%	C11-ABS	A225	0.30%	-	-	U surrogate	SUTIB	-	-	-	-	SUTIB	pH-7 (50%cyclohexane diluted oil)
U-307	C28-25PO-85EO-carboxylate	-	0.70%	C11-ABS	A225	0.30%	-	-	U surrogate	SUTIB	-	-	-	-	SUTIB	pH-7 (50%cyclohexane diluted oil)
U-308	C28-25PO-55EO-carboxylate	-	0.80%	C11-ABS	A225	0.20%	-	-	U surrogate	SUTIB	-	-	-	-	SUTIB	pH-7 (50%cyclohexane diluted oil)
U-309	C28-25PO-55EO-carboxylate	-	0.50%	Isocarb 12 acid	-	0.50%	-	-	U surrogate	SUTIB	-	-	-	-	SUTIB	pH-7 (50%cyclohexane diluted oil)
-310 (a) to (	C28-25PO-45EO-carboxylate	-	0.15%	C15-18 IOS	7376946	0.15%	-	-	U surrogate	SUTIB	-	-	-	-	SUTIB	pH-7 (50%cyclohexane diluted oil) Oil scan
U-311	C28-25PO-55EO-carboxylate	-	0.70%	C11-ABS	A225	0.30%	-	-	U surrogate	SUTIB	-	20	2.30%	2.30%	SUTIB	pH-7 (50%cyclohexane diluted oil)
U-312	C28-25PO-55EO-carboxylate	-	0.21%	C11-ABS	A225	0.09%	-	-	U surrogate	SUTIB	-	20	2.30%	2.30%	SUTIB	pH-7 (50%cyclohexane diluted oil) Only aq. Stab
U-313	C28-25PO-55EO-carboxylate	-	0.21%	C11-ABS	A225	0.09%	-	-	U surrogate	SUTIB	-	20	2.30%	2.30%	SUTIB	pH-7 (50%cyclohexane diluted oil)
U-314	C28-25PO-45EO-carboxylate	-	0.30%	C15-18 IOS	7376946	0.70%	-	-	U surrogate	SUTIB	-	-	-	-	SUTIB	pH-7 (50%cyclohexane diluted oil)
U-315	C28-25PO-45EO-carboxylate	-	0.70%	C15-18 IOS	7376946	0.30%	-	-	U surrogate	SUTIB	-	-	-	-	SUTIB	pH-7 (50%cyclohexane diluted oil)
U-316	C28-25PO-45EO-carboxylate	-	0.50%	2-ethylhexanoic acid	-	0.50%	-	-	U surrogate	SUTIB	-	-	-	-	SUTIB	pH-7 (50%cyclohexane diluted oil)
U-317	C28-25PO-45EO-carboxylate	-	0.75%	2-ethylhexanoic acid	-	0.25%	-	-	U surrogate	SUTIB	-	-	-	-	SUTIB	pH-7 (50%cyclohexane diluted oil)

155

References

Adkins, S., Liyanage, P. J., Arachchilage, G. W. P., Mudiyanselage, T., Weerasooriya, U., and Pope, G. A. "A New Process for Manufacturing and Stablizing High-Performance EOR Surfactants at Low Cost for High Temperature, High Salinity Oil Reservoirs", SPE 129923, SPE IOR Symposium, Tulsa, OK, 25-28 April 2010.

Anton, R.E., Anderez, J.M., Bracho, C., Vejar, F., and Salager, J.L. "Practical Surfactant Mixing Rules Based on the Attainment of Microemulsion-Oil-Water Three-Phase Behavior Systems", *Adv Polymer Science* 218, 83-113, 2008.

Aoudia, M., Wade, W.H., and Weerasooriya, V. "Optimum Microemulsions Formulated with Propoxylated Guerbet Alcohol and Propoxylated Tridecyl Alcohol Sodium Sulfates", *Journal of Dispersion Science and Technology 16(2)*, 115-135, 1995.

Austad, Tor and Milter, Jess. "Surfactant Flooding in Enhanced Oil Recovery", Surfactants: Fundamentals and Applications in the Petroleum Industry, Cambridge University Press, October 1998.

Barnes, J. R., Dirkzwager, H., Smit, J. R., Smit, J. P., On, An., Navarette, R.C., Ellison, B.H., and Buijse, M.A. "Application of Internal Olefin Sulfonates and Other Surfactants to EOR. Part 1: Structure - Performance Relationships for Selection at Different Reservoir Conditions", SPE 129766, presented at SPE IOR Symposium, Tulsa, OK, 2010.

Britton, C, Pope, G.A., Kim, D.H., Walker, D.L., Solairaj, S. "Surfactant Retention and Chromatographic Separation", presented at the Chemical EOR JIP Annual Workshop, Austin, TX, April, 2011.

Bourrel, M. and Schechter, R. S. "Microemulsions and Related Systems", Marcel Dekker, Inc., New York, NY, 1988.

Buijse, M.A., Prelicz, R.M., and Barnes, J. R. "Application of Internal Olefin Sulfonates and Other Surfactants to EOR. Part 2: The Design and Execution of an ASP Field Test", SPE 129769, presented at SPE IOR Symposium, Tulsa, OK, 2010.

Cayias, J.L., Schechter, R.S., Wade, W.H., "Modeling Crude Oils for Low Interfacial Tension", SPE 5813, presented at SPE-AIME IOR Symposium, Tulsa, OK, 22-24 March 1976.

Dean, R. M. "Selection and Evaluation of Surfactants for Field Pilots", M.S. Thesis, University of Texas at Austin, May 2011.

Falls, A.H., Thigpen, D.R., Nelson, R.C., Ciaston, J.W., Lawson, J.B., Good, P.A., Ueber, R.C., and Shahin, G.T. "A Field Test of Co-surfactant Enhanced Alkaline Flooding", SPE 24117, August 1994.

Flaaten, A.K. "Experimental Study of Microemulsion Characterization and Optimization in Enhanced Oil Recovery: A Design Approach for Reservoirs with High Salinity and Hardness", M.S. Thesis, The University of Texas at Austin, December 2007.

Graciaa, A., Lachaise, J., Bourrel, M., Osborne-Lee, I, Schechter, R.S., and Wade, W.H. "Partitioning of Nonionic and Anionic Surfactant Mixtures Between Oil/Microemulsion/Water Phases", SPE 13030, *SPE Reservoir Engineering* 2(3), 305-314, 1987.

Glinsmann, G.R., "Surfactant Flooding with Microemulsions Formed In-situ – Effect of Oil Characteristics", SPE 8326, presented at SPE-AIME ATCE Symposium, Dallas, TX, 1979.

Glover, C.J, Puerto, M.C., Maerker, J.M., and Sandvik, E.L. "Surfactant Phase Behavior and Retention in Porous Media", SPE 7053, *SPEJ* 19(3), 183-193, 1979.

Green, D. W. and Willhite, G. P. "Enhanced Oil Recovery", SPE Textbook Series, Henry L. Doherty Memorial Fund of AIME, Society of Petroleum Engineers, Richardson, Texas, Volume 6, 1998.

Gogarty, W. B. and Tosch, W. C. "Miscible-Type Waterflooding: Oil Recovery with Micellar Solutions", *Journal of Petroleum Technology*, December 1968, 1407-1414.

Hirasaki, G.J., van Domselaar, H.R., and Nelson, R.C. "Evaluation of the Salinity Gradient Concept in Surfactant Flooding", SPE 8825, *SPEJ*, 486-500, June 1983.

Hirasaki, G.J., Miller, C.A., and Puerto, M. "Recent Advances in Surfactant EOR", SPE 115386, presented at SPE ATCE, Denver, CO, September 2008.

Huh, C., and Pope, G.A. "Residual Oil Saturations from Polymer Floods", SPE 113417, presented at SPE IOR Symposium, Tulsa, OK, 2008.

Huh, C. "Interfacial Tensions and Solubilization Ability of a Microemulsion Phase that Coexist with Oil and Brine", *Journal of Colloid and Interface Science*, September 1979.

Jackson, A.C. "Experimental Study of the Benefits of Sodium Carbonate on Surfactants for Enhanced Oil Recovery", M.S. Thesis, The University of Texas, December 2006.

Jayanti, S., Britton, L.N., Dwarakanath V., and Pope, G.A. "Laboratory Evaluation of Custom Designed Surfactants to Remediate NAPL Source Zones", *Environmental Science and Technology*, 5491-5497, 2002.

Levitt, D. B. "Experimental Evaluation of High Performance EOR Surfactants for a Dolomite Oil Reservoir", M.S. Thesis, The University of Texas, December 2006.

Levitt, D. B., Jackson, A. C., Heinsen, C. Britton, L. N., Malik, T., Dwarakanath, V., and Pope, G. A. "Identification and Evaluation of High-Performance EOR Surfactants", SPE 100089, SPE/DOE Symposium, Tulsa, OK, April 2006.

Levitt, D. B., Jackson, A. C., Heinsen, C. Britton, L. N., Malik, T., Dwarakanath, V., and Pope, G. A. "Identification and Evaluation of High-Performance EOR Surfactants", SPE 100089, *SPE Reservoir Evaluation and Engineering* 12(2), 243-253, 2009.

Lake, L.W. "Enhanced Oil Recovery", Prentice-Hall, Upper Saddle River, NJ, 1989.

Lawson, J.B. "The Adsorption of Nonionic and anionic Surfactants on Sandstone and Carbonate", SPE 7052, SPE IOR Symposium, Tulsa, OK, April 1978.

Maerker, J.M and Gale, W.W. "Surfactant Flood Process Design for Loudon", *SPERE*, 36-44, 1992.

Mannhardt, K. and Novosad, J. "Chromatographic Effects in Flow of a Surfactant Mixture in a Porous Sandstone", *Journal of Petroleum Science and Engineering* 5(2), 89-103, 1991.

Meredith, W., Kelland, S.J., Jones, D.M. "Influence of Biodegradation on Crude Oil Acidity and Carboxylic Acid Composition", *Organic Chemistry 31*, 1059-1073, 2000.

Nelson, R.C. "The Salinity-Requirement Diagram – A Useful Tool in Chemical Flooding Research and Development", SPE 8824, *SPEJ* 22(2), 259-270, 1982.

Nelson, R.C., Lawson, J.B., Thigpen, D.R., Stegemeier, G.L. "Cosurfactant-Enhanced Alkaline Flooding", SPE/DOE 12672, presented at SPE IOR Symposium, Tulsa, OK, 1984.

Nelson, R.C., and Pope, G.A. "Phase Relationships in Chemical Flooding", SPE 6773, presented in ATCE, Denver, CO, October 1977.

Novosad, J. "Surfactant Retention in Berea Sandstone – Effects of Phase Behavior and Temperature", SPE 10064, *SPEJ* 22(6), 962-970, 1982.

O'Lenick Jr., A.J. "Guerbet Chemistry", *Journal of Surfactants and Detergents 4(3)*, 311-315, 2001.

Pinnawala-Arachchilage, G.W. "Part I: Design and Synthesis of Organic Materials for Dye Synthesized Solar Cells. Part II: Qualitative and Semi-quantitative Study of the Behavior of Surfactant on Crude Oil Recovery Processes", M.S. Thesis, Bowling Green State University, 2010.

Pope, G.A. "The Application of Fractional Flow Theory to Enhanced Oil Recovery", SPE 7660, *SPEJ 20(3)*, 191-205, June 1980.

Poprawski, J., Catte, M., Marquez, L., Marti, M.J., Salager, J.L., and Aubry, J.M. "Application of Hydrophilic-Lipophilic Deviation Formulation Concept to

Microemulsions Containing Pine Oil and Nonionic Surfactant", *Polymer International* 52, 629-632, 2003.

Puerto, M.C., and Reed, R.L. "A Three Parameter Representation of Surfactant/Oil/Brine Interactions", *SPE Journal 23(4)*, 669-682, 1983.

Queste, S., Salager, J.L., Strey, R., and Aubry, J.M. "The EACN Scale for Oil Classification Revisited − Thanks to Fish Diagrams", *Journal of Colloid and Interface Science* 312, 98-107, 2007.

Roshanfekr, M. "Effect of Pressure and Methane on Microemulsion Phase Behavior and its Impact on Surfactant-Polymer Flood Oil Recovery", PhD Dissertation, The University of Texas at Austin, December 2010.

Sahni, V., Dean, R. M., Britton, C., Kim, D. H., Weerasooriya, U., and Pope, G. A. "The Role of Co-solvents and Co-surfactants in Making Chemical Floods Robust", SPE 130007, presented at SPE IOR Symposium, Tulsa, OK, 25-28 April 2010.

Sahni, V. "Experimental Evaluation of Co-solvents in Development of High Performance Alkali/Surfactant/Polymer Formulations for Enhanced Oil Recovery", M.S. Thesis, The University of Texas at Austin, December 2009.

Salager, J.L. "Surfactant Types and Uses", Laboratory of Formulation, Interfaces, Rheology and Processes, 2002.

Salager, J.L., Bourrel, M.U., Schechter, R.S., and Wade, W.H. "Mixing Rules for Optimum Phase-Behavior Formulations of Surfactant/Oil/Water Systems", *SPEJ* 19(5), 271-278, 1979.

Salager, J.L. "Microemulsions", en *Handbook of Detergents – part A: Properties*, G. Broze Ed., Surfactant Science Series vol. 82, Chapter 8, 253-302, Marcel Dekker New York (1999).

Sanz, C.A., and Pope, G.A. "Alcohol-Free Chemical Flooding: From Surfactant Screening to Coreflood Design", SPE 28956, SPE Symposium on Oilfield Chemistry, San Antonio, TX, February 1995.

Sheng, J. J. "Modern Chemical Enhanced Oil Recovery: Theory and Practice", Elsevier, Burlington, MA, 2011.

Shepherd, A.G. "A Mechanistic Analysis of Naphthenate and Carboxylate Soap-Forming Systems in Oilfield Exploration and Production", PhD Dissertation, Heriot-Watt University, December 2008.

Shinoda, K., Arai, H. *Journal of Physical Chemistry 68*, 3485, 1964.

Somasundaran, P. and Hanna, H.S. "Physico-Chemical Aspects of Adsorption at Solid-Liquid Interfaces", *Improved Oil Recovery by Surfactant and Polymer Flooding*, 253, Academic Press, New York, 1977.

Talley, L.D. "Hydrolytic Stability of Alkylethoxy sulfates", SPE 14912, 1988.

159

Trogus, F.J., Pope, G.A., Schechter, R.S., and Wade, W.H. "Adsorption of Mixed Surfactant Systems", *Journal of Petroleum Technology*, 31, June 1979.

Walker, D.L. "Experimental Investigation of the Effect of Increasing the Temperature of ASP Flooding", M.S. Thesis, The University of Texas at Austin, December 2011.

Wang, F.H.L. "Effects of Reservoir Anaerobic, Reducing Conditions on Surfactant Retention in Chemical Flooding", SPE 22648, *SPE Reservoir Engineering* 8(2), 108-116, 1993.

Winsor, P.A. "Solvent Properties of Amphiphilic Compounds", Butterworths, London, 1954.

Yang, H. "Development of Improved ASP Formulations for Reactive and Non-reactive Crudes", M.S. Thesis, The University of Texas, December 2010.

Yang, H., Britton, C., Liyanage, P.J., Solairaj, S., Kim, D., Nguyen, Q., Weerasooriya, U., and Pope, G.A. "Low-cost, High-performance Chemicals for Enhanced Oil Recovery", SPE 129978, presented at the SPE IOR Symposium, Tulsa, OK, April 2010.

Zhang, L.D., and Hirasaki, G.J. "Surface Chemistry of Oil Recovery from Fractured Oil-wet, Carbonate Formations", *SPEJ*, 2004.

Zhang, L.D., and Hirasaki, G.J. "Favorable Attributes of Alkali-Surfactant-Polymer Flooding",SPE 99744, presented at SPE IOR Symposium, Tulsa, OK, 2006.